Copyright

By

Jarkko Tuomas Simonen

2004

Development of an Embedded Wireless Corrosion Sensor for Monitoring Corrosion in Reinforced Concrete Members

by

Jarkko Tuomas Simonen, B.S.C.E.

Thesis

Presented to the Faculty of the Graduate School of

The University of Texas at Austin

in Partial Fulfillment

of the Requirements

for the Degree of

Master of Science in Engineering

The University of Texas at Austin

May 2004

Development of an Embedded Wireless Corrosion Sensor for Monitoring Corrosion in Reinforced Concrete Members

APPROVED BY
SUPERVISING COMMITTEE:

Sharon L. Wood

Dean P. Neikirk

Dedication

To anyone who helped along the way

Acknowledgements

I gratefully acknowledge the Texas Higher Education Coordinating Board for funding this project (#003658-0201-2001).

I want to thank my advisor, Dr. Sharon L. Wood, for her unmatched dedication to her students. Without her this thesis could not have been possible.

I want to thank Dr. Dean Neikirk, Dr. Harovel Wheat and Dave Whitney for taking the time to come up with creative ways to solve different problems that were encountered along the way.

I want to thank the staffs and students at both the Ferguson Structural Engineering Lab and at the Construction Material Research Group, especially: Blake Stasney, Mike Brown, Nate Dickerson, and Taichro Okazaki.

I also want to thank Matthew Andringa for helping me with all electrical aspects of the project.

May 2004

Development of an Embedded Wireless Corrosion Sensor for Monitoring Corrosion in Reinforced Concrete Members

Jarkko Simonen, M.S.E

The University of Texas at Austin, 2004

SUPERVISOR: Sharon L. Wood

The objective of this thesis is to discuss the development and testing of two wireless sensors that are designed to detect corrosion in reinforced concrete structures. These sensors are intended to be placed inside the concrete structure adjacent to the steel reinforcement before concrete is placed. Although not connected electrically to the embedded reinforcement, the sensor is surrounded by concrete and exposed to the same environmental conditions as the reinforcement. The sensors, therefore, experience the same levels of oxygen, water, and chloride ions as the adjacent layer of reinforcement within the structural member. Two types of sensors have been developed and have been tested in representative applications. The sensors are inexpensive to fabricate, sufficiently durable to survive the construction process and can be interrogated through concrete.

Table of Contents

CHAPTER 1 INTRODUCTION 1

1.1 Introduction 1

1.2 Scope of work 2

CHAPTER 2 CONCEPTUAL DESIGN OF SENSORS 4

2.1 Introduction 4

2.2 Technology 4

2.2.1 Data transmission 4

2.2.2 Corrosion detection 6

2.3 Sensor description 7

2.3.1 Basic sensor 7

2.3.2 Improved sensor 9

2.4 External switch behavior 11

CHAPTER 3 ACCELERATED CORROSION TESTS 12

3.1 Test Setup 12

3.2 Results from Accelerated Corrosion Tests 14

3.2.1 Wire Performance 16

3.2.2 Reinforcement Performance 18

3.3 Summary of acclerated corrosion tests 19

CHAPTER 4 FULL SCALE SLAB TESTS 20

4.1 Introduction 20

4.2 Slab Description 20

4.3 Test Setup 21

4.3.1 Salt Water Ponds 22

4.4 Sensor Placement 23

4.5 Durability 24

4.6 Interrogation of the Slabs 25

4.6.1 Visual Inspection 30

4.6.2 Half cell measurements 32

4.6.3 Chloride penetration 33

4.7 Summary 34

CHAPTER 5 SENSOR TESTING AND BEHAVIOR 36

5.1 Introduction 36

5.2 Internal Corrosion 36

5.2.1 Causes 36

5.2.2 Protecting Against Internal Corrosion Using a Potting Compound 37

5.2.3 Testing Potting Compounds 38

5.3 Behavior / Performance 40

5.3.1 Response with Time 40

5.3.1.1 Effect of corrosion of the external switch 40

5.3.1.2 Effect of moisture and chlorides 43

5.3.2 Embedment depth 45
5.3.2.1 Read depths in air 45
5.3.2.1.1 Results 46
5.3.2.2 Influence of moisture and chloride ions on transmission range 47
5.3.2.2.1 Experiment setup 47
5.3.2.2.2 Results 48
5.4 Summary 50

CHAPTER 6 CONCLUSION 52
6.1 Summary 52
6.2 Future recommendations 53

APPENDIX A FULL SCALE SLAB TEST RESULTS 55
A.1 Interrogation of the slabs 55
A.1.1 Slab 2 results 55
A.1.2 Slab 3 results 60
A.1.3 Slab 4 results 64
A.1.4 Slab 1 results 69

APPENDIX B RESULTS OF CHLORIDE PENETRATION TESTS 74
B.1 Chloride penetrtation 74

APPENDIX C EFFECT OF CORROSION ON SENSOR RESPONSE 77

C.1 Results of daily sensor interogations 77

APPENDIX D INFLUENCE OF DISTANCE BETWEEN THE INTERROGATION COIL AND THE SENSOR 114

D.1 Results of Transmission range 114

APPENDIX E INFLUENCE OF MOISTURE AND CHLORIDES ON TRANSMISSION RANGE 124

E.1 Concrete discs submersed ininto fresh water 124

E.2 Concrete discs submersed in salt water 127

REFERENCES 131

VITA 134

List of Tables

Table 3-1. Data from first set of accelerated corrosion test 15
Table 3-2. Data from second accelerated corrosion test 16

Table 4-1. Response of sensors by date 28
Table 4-2. Sensor response at the time of autopsy 29
Table 4-3. Chloride penetration results 34

Table 5-1. Weights of discs exposed to fresh water 48
Table 5-2. Weights of discs exposed to salt water 48

Table B-1. Chloride concentration 74

List of Figures

Figure 2-1. Typical LC circuit 5
Figure 2-2. Typical phase angle response 5
Figure 2-3. Typical LC circuit with added state switch and capacitor 7
Figure 2-4. Phase angle response corresponding to state of switch 7
Figure 2-5. Basic sensor 8
Figure 2-6. Improved sensor 10

Figure 3-1. Accelerated corrosion test setup 12
Figure 3-2. Time to wire break for accelerated corrosion test 1 17
Figure 3-3. Time to wire break for accelerated corrosion test 2 17
Figure 3-4. Average time to wire break for accelerated corrosion tests 1 and 2 .. 18
Figure 3-5. Cross-sectional area reduction of accelerated corrosion Test 1 19
Figure 3-6. Cross-sectional area reduction for accelerated corrosion test 2 19

Figure 4-1. Slab layout 21
Figure 4-2. Slab layout 22
Figure 4-3. Typical sensor placement 23
Figure 4-4. Switch configurations 24
Figure 4-5. Basic sensor response 26
Figure 4-6. Improved sensor response 26
Figure 4-7. Characteristic frequency with time 27
Figure 4-8. Concrete removal 30
Figure 4-9. Corrosion around reinforcement 31
Figure 4-10. Heavy reinforcement degradation caused by corrosion 32
Figure 4-11. Section of reinforcement in the cracked region 32
Figure 4-12. Half cell potential measurements 33

Figure 5-1. Different types of potting compounds 39
Figure 5-2. Sensors after being exposed to accelerated corrosion tests 41
Figure 5-3. Time response of basic sensors 42
Figure 5-4. Time response of improved sensors 42
Figure 5-5. Sensor response in different environments 44
Figure 5-6. Variation of sensor response with distance to interrogation coil in air 46
Figure 5-7. Basic sensor: variation in phase angle response after salt water exposure 49
Figure 5-8. Improved sensor: variation in phase angle response after salt water exposure 49

Figure 5-9. Basic sensor: variation in phase angle response after fresh water exposure 50
Figure 5-10. Improved sensor: variation in phase angle response after fresh water exposure 50

Figure A-1 Sensor 2 response 56
Figure A-2. Sensor 3 response 56
Figure A-3. Sensor 14 response 57
Figure A-4. Sensor 20 response 57
Figure A-5. Sensor 21 response 58
Figure A-6. Sensor 23 response 58
Figure A-7. Sensor 24 response 59
Figure A-8. Sensor 25 response 59
Figure A-9. Sensor 7 response 60
Figure A-10. Sensor 8 response 61
Figure A-11. Sensor 9 response 61
Figure A-12. Sensor 11 response 62
Figure A-13. Sensor 16 response 62
Figure A-14. Sensor 28 response 63
Figure A-15. Sensor 29 response 63
Figure A-16. Sensor 31 response 64
Figure A-17. Sensor 1 response 65
Figure A-18. Sensor 5 response 65
Figure A-19. Sensor 6 response 66
Figure A-20. Sensor 10 response 66
Figure A-21. Sensor 12 response 67
Figure A-22. Sensor 19 response 67
Figure A-23. Sensor 22 response 68
Figure A-24. Sensor 32 response 68
Figure A-25. Sensor 4 response 69
Figure A-26. Sensor 13 response 70
Figure A-27. Sensor 15 response 70
Figure A-28. Sensor 17 response 71
Figure A-29. Sensor 18 response 71
Figure A-30. Sensor 26 response 72
Figure A-31. Sensor 27 response 72
Figure A-32. Sensor 30 response 73

Figure B-1. Chloride concentration at the surface 75
Figure B-2. Chloride concentration at level of reinforcement 75
Figure B-3. Chloride concentration at level of reinforcement 76

Figure C-1. 05 March 04: Basic sensor 1a 77
Figure C-2. 08 March 04: Basic sensor 1a 78
Figure C-3. 09 March 04: Basic sensor 1a 78
Figure C-4. 11 March 04: Basic sensor 1a 79
Figure C-5. 12 March 04: Basic sensor 1a 79
Figure C-6. 22 March 04: Basic sensor 1a 80
Figure C-7. 23 March 04: Basic sensor 1a 80
Figure C-8. 24 March 04: Basic sensor 1a 81
Figure C-9. 25 March 04: Basic sensor 1a 81
Figure C-10. 26 March 04: Basic sensor 1a 82
Figure C-11. 30 March 04: Basic sensor 1a 82
Figure C-12. 01 April 04: Basic sensor 1a 83
Figure C-13. 06 April 04: Basic sensor 1a 83
Figure C-14. 07 April 04: Basic sensor 1a 84
Figure C-15. 15 April 04: Basic sensor 1a 84
Figure C-16. 20 April 04: Basic sensor 1a 85
Figure C-17. 22 April 04: Basic sensor 1a 85
Figure C-18. 27 April 04: Basic sensor 1a 86
Figure C-19. 05 March 04: Basic sensor 2a 86
Figure C-20. 08 March 04: Basic sensor 2a 87
Figure C-21. 09 March 04: Basic sensor 2a 87
Figure C-22. 11 March 04: Basic sensor 2a 88
Figure C-23. 12 March 04: Basic sensor 2a 88
Figure C-24. 22 March 04: Basic sensor 2a 89
Figure C-25. 23 March 04: Basic sensor 2a 89
Figure C-26. 24 March 04: Basic sensor 2a 90
Figure C-27. 25 March 04: Basic sensor 2a 90
Figure C-28. 26 March 04: Basic sensor 2a 91
Figure C-29. 30 March 04: Basic sensor 2a 91
Figure C-30. 01 April 04: Basic sensor 2a 92
Figure C-31. 06 April 04: Basic sensor 2a 92
Figure C-32. 07 April 04: Basic sensor 2a 93
Figure C-33. 15 April 04: Basic sensor 2a 93
Figure C-34. 20 April 04: Basic sensor 2a 94
Figure C-35. 22 April 04: Basic sensor 2a 94
Figure C-36. 27 April 04: Basic sensor 2a 95
Figure C-37. 05 March 04: Improved sensor 1b 95
Figure C-38. 08 March 04: Improved sensor 1b 96
Figure C-39. 09 March 04: improved sensor 1b 96
Figure C-40. 11 March 04: Improved sensor 1b 97
Figure C-41. 12 March 04: Improved sensor 1b 97
Figure C-42. 22 March 04: Improved sensor 1b 98

Figure C-43. 23 March 04: Improved sensor 1b 98
Figure C-44. 24 March 04: Improved sensor 1b 99
Figure C-45. 25 March 04: Improved sensor 1b 99
Figure C-46. 26 March 04: Improved sensor 1b 100
Figure C-47. 30 March 04: Improved sensor 1b 100
Figure C-48. 01 April 04: Improved sensor 1b 101
Figure C-49. 06 April 04: Improved sensor 1b 101
Figure C-50. 07 April 04: Improved sensor 1b 102
Figure C-51. 15 April 04: Improved sensor 1b 102
Figure C-52. 20 April 04: Improved sensor 1b 103
Figure C-53. 22 April 04: Improved sensor 1b 103
Figure C-54. 27 April 04: Improved sensor 1b 104
Figure C-55. 05 March 04: Improved sensor 4b 104
Figure C-56. 08 March 04: Improved sensor 4b 105
Figure C-57. 09 March 04: improved sensor 4b 105
Figure C-58. 11 March 04: Improved sensor 4b 106
Figure C-59. 12 March 04: Improved sensor 4b 106
Figure C-60. 22 March 04: Improved sensor 4b 107
Figure C-61. 23 March 04: Improved sensor 4b 107
Figure C-62. 24 March 04: Improved sensor 4b 108
Figure C-63. 25 March 04: Improved sensor 4b 108
Figure C-64. 26 March 04: Improved sensor 4b 109
Figure C-65. 30 March 04: Improved sensor 4b 109
Figure C-66. 01 April 04: Improved sensor 4b 110
Figure C-67. 06 April 04: Improved sensor 4b 110
Figure C-68. 07 April 04: Improved sensor 4b 111
Figure C-69. 15 April 04: Improved sensor 4b 111
Figure C-70. 20 April 04: Improved sensor 4b 112
Figure C-71. 22 April 04: Improved sensor 4b 112
Figure C-72. 27 April 04: Improved sensor 4b 113

Figure D-1. Basic sensor phase angle response: Gap distance 0.0 in. 114
Figure D-2. Basic sensor phase angle response: Gap distance 0.25 in. 115
Figure D-3. Basic sensor phase angle response: Gap distance 0.5 in. 115
Figure D-4. Basic sensor phase angle response: Gap distance 0.75 in. 116
Figure D-5. Basic sensor phase angle response: Gap distance 1.0 in. 116
Figure D-6. Basic sensor phase angle response: Gap distance 1.25 in. 117
Figure D-7. Basic sensor phase angle response: Gap distance 1.50 in. 117
Figure D-8. Basic sensor phase angle response: Gap distance 1.75 in. 118
Figure D-9. Basic sensor phase angle response: Gap distance 2.0 in. 118
Figure D-10. Basic sensor phase angle response: Gap distance 2.25 in. 119
Figure D-11. Basic sensor phase angle response: Gap distance 2.50 in. 119

Figure D-12. Basic sensor phase angle response: Gap distance 2.75 in. 120
Figure D-13. Improved sensor phase angle response: Gap distance 0.0 in. 120
Figure D-14. Improved sensor phase angle response: Gap distance 0.25 in. 121
Figure D-15. Improved sensor phase angle response: Gap distance 0.50 in. 121
Figure D-16. Improved sensor phase angle response: Gap distance 0.75 in. 122
Figure D-17. Improved sensor phase angle response: Gap distance 1.0 in. 122
Figure D-18. Improved sensor phase angle response: Gap distance 1.25 in. 123
Figure D-19. Improved sensor phase angle response: Gap distance 1.50 in. 123

Figure E-1. Basic sensor: after one week curing period 124
Figure E-2. Basic sensor: concrete exposed to fresh water for 3 days 125
Figure E-3. Basic sensor: concrete exposed to fresh water for 7 days 125
Figure E-4. Improved sensor: after one week curing period 126
Figure E-5. Improved sensor: concrete exposed to fresh water for 3 days 126
Figure E-6. Improved sensor: concrete exposed to fresh water for 7 days 127
Figure E-7. Basic sensor: after one week of curing 128
Figure E-8. Basic sensor: concrete exposed to salt water for 3 days 128
Figure E-9. Basic sensor: concrete exposed to salt water for 7 days 129
Figure E-10. Improved sensor: after one week of curing 129
Figure E-11. Improved sensor: concrete exposed to salt water for 3 days 130
Figure E-12. Improved sensor: concrete exposed to salt water for 7 days 130

CHAPTER 1
Introduction

1.1 INTRODUCTION

Corrosion is a serious and ongoing problem in reinforced concrete structures, especially in marine environments or regions where deicing salts are used. Studies in 1999 indicated that 15% of the bridge decks in the US were structurally deficient due to corrosion (Koch, et. al., 1999). When left uncorrected, corrosion degrades the strength of a structure and extensive repairs are often required. Early detection of corrosion can significantly decrease the repair costs. What makes corrosion detection so difficult is that in most cases the effects of corrosion are not visible until some sort of structural damage has occurred. Many methods have been developed to detect corrosion but they are often unreliable, difficult to implement, or very expensive.

A prototype corrosion sensor has been developed that minimizes these unwanted characteristics. This sensor is wireless, inexpensive, and has expected life equal to the life of the structure. The conceptual design of this sensor is discussed in "Development of a Corrosion Sensor for Reinforced Concrete Structures" by Grizzle (2003). In her thesis, she proves the feasibility of the sensor and begins to test some of the performance characteristics of the sensor. This thesis intends to improve upon the sensor, demonstrate the feasibility of using the sensor to detect the onset of corrosion in large-scale reinforced concrete members, and investigate the performance characteristics of the sensor.

The prototype sensor is constructed using an inductive coil, two capacitors and a state switch. The inductive coil and one capacitor form a basic LC circuit

that can transmit data about the sensor using radio frequency technology. When the LC circuit is interrogated using a transmitter, it will resonate at a characteristic frequency. When the second capacitor and the state switch are added to the circuit the natural frequency will change. For the prototype sensor, the state switch is constructed using steel wire which is exposed to the same environment as the reinforcing steel. When this steel wire corrodes and fractures, the corresponding circuit will be broken and the sensor will resonate at a different frequency, thereby transmitting information about level of corrosion in the structure.

1.2 SCOPE OF WORK

The objective of this thesis is to demonstrate the feasibility of the prototype sensor by discussing improvements to the sensor, providing data on the performance of the sensors in representative applications, and performing control tests to better understand the overall behavior of the sensors. Also this thesis will present a second prototype sensor that has been developed to improve upon the original sensor. This new sensor will be called the improved sensor while the prototype sensor, will be called the basic sensor.

Basic design concepts are discussed in Chapter 2. This chapter introduces the fundamental behavior of the sensor and gives general characteristics of the basic and improved sensors.

Testing of the state switch is discussed in Chapter 3. Grizzle (2003) began investigating the relationship between the corrosion rates of the state switch with that of the reinforcing steel. These tests were conducted using accelerated corrosion tests that exposed steel wires and reinforcing steel to simulated concrete solutions. Because these tests provided a relatively quick way to test the state switch, these tests are continued in this thesis.

For the sensors to be successful the sensors must have several key characteristics: (a) they must be easy to install, (b) they must be sufficiently tough to survive the casting process, and (c) they must be reliable. These characteristics have been studied through the construction of four full-scale slabs. Thirty-two sensors were embedded in these slabs and their performance was studied. Chapter 4 discusses the full-scale slabs and the sensor performance in detail.

During the full-scale slab tests, some unexpected responses were observed. To understand these responses, several individual experiments were conducted and the results are discussed in Chapter 5. Chapter 5 also discusses some improvements to the prototype sensor, and the results of tests of sensor performance in different environments.

Chapter 6 provides a summary of the results and provides recommendations for future work related to this project.

CHAPTER 2
Conceptual Design of Sensors

2.1 INTRODUCTION

Two different sensors have been developed: a basic sensor and an improved sensor. Both of the sensors provide information about the level of corrosion within the reinforced concrete member by responding at two, distinct characteristic frequencies: an initial frequency, which corresponds to a state without corrosion, and a final frequency, which indicates that a threshold amount of corrosion has occurred.

2.2 TECHNOLOGY

Two issues dealing with the conceptual design are discussed in this section: data transmission and corrosion detection.

2.2.1 Data transmission

The sensors rely on radio frequency technology to transmit information about the state of the switch. In the simplest form the sensors can be described as an LC circuit that is powered by inductive coupling from a transmitter/receiver (Figure 2-1). Once the sensor is exited by the magnetic field generated by the transmitter, the sensor will resonate at its natural frequency. This natural frequency, as shown in Fig. 2-2, can be identified as a drop phase angle response. Theoretically, the phase angle should reach zero at the characteristic frequency, but the minimum phase angle does not reach this state in most applications. This does not represent a problem in obtaining data from the sensor because the

characteristic frequency can be identified reliably if the dip in the phase angle response exceeds a few tenths of a degree.

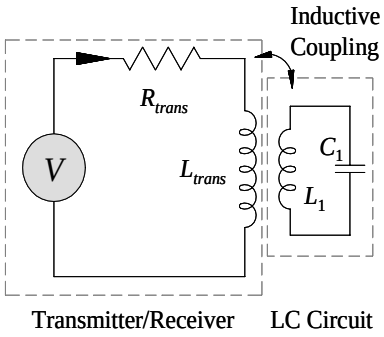

Figure 2-1. Typical LC circuit

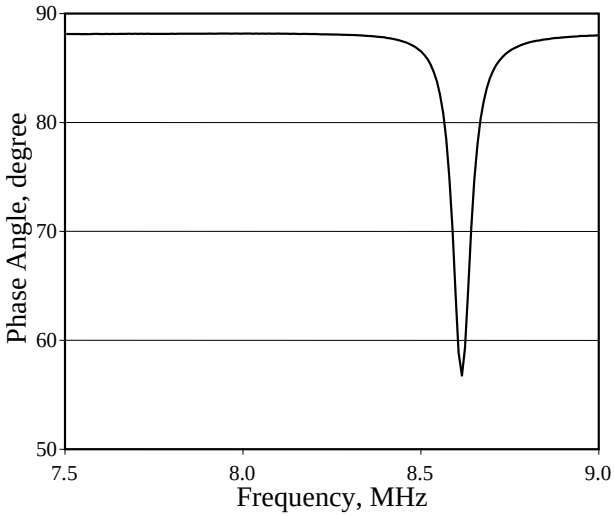

Figure 2-2. Typical phase angle response

Selecting RF technology to excite the sensors has several advantages. RF technology allows the sensors to be wireless, which simplifies placement and use during the life of the structure. Also this technology allows the sensor to be free of an internal power source, which means that the sensors will be readable throughout the life of the structure. Another important advantage is that the sensors are extremely inexpensive and simple to manufacture.

2.2.2 Corrosion detection

To achieve the two distinct natural frequencies, an external switch and a capacitor have been added to the basic LC circuit (Figure 2-3). Because the second capacitor is in parallel with the LC circuit and in series with the switch, the characteristic frequency of the sensor depends on the state of the switch (2-1, 2-2). When the external switch is closed, the circuit resonates at its initial frequency:

$$f_{res} = \frac{1}{2\pi\sqrt{L_1 \cdot (C_1 + C_2)}} \tag{2-1}$$

When the external switch is opened, the characteristic frequency shifts to an appreciably higher value (Figure 2-4):

$$f_{res} = \frac{1}{2\pi\sqrt{L_1 \cdot C_1}} \tag{2-2}$$

The external switch is essentially what provides the corrosion detection. The external switch is constructed using steel wire. The prototype sensors have been designed such that once the steel wire experiences enough corrosion it will break causing the characteristic frequency of the sensor to change. This change in frequency can then be correlated to corrosion of the nearby reinforcement.

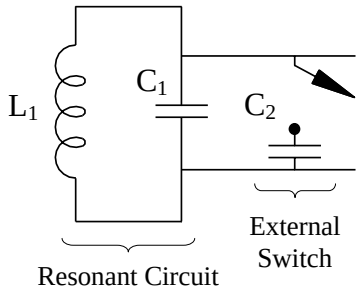

Figure 2-3. Typical LC circuit with added state switch and capacitor

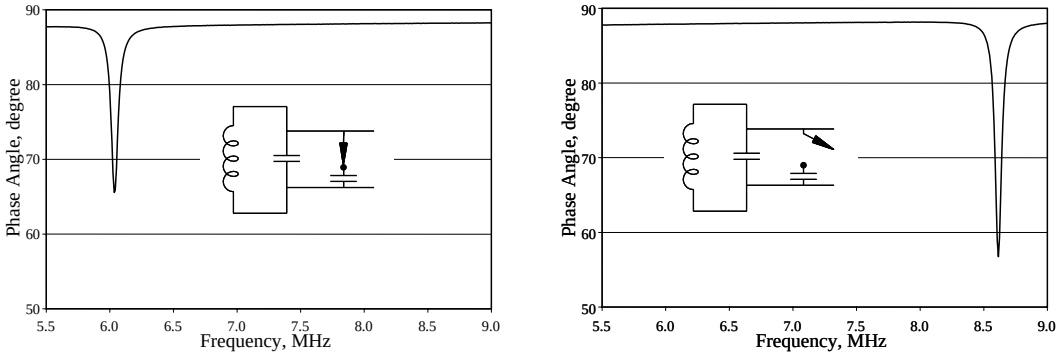

Figure 2-4. Phase angle response corresponding to state of switch

2.3 SENSOR DESCRIPTION

Two sensors have been developed: basic sensor and improved sensor. The basic sensor is very closely based on the prototype sensor developed by Grizzle (2003). The improved sensor was developed to improve the performance of the basic sensor.

2.3.1 Basic sensor

The basic sensor was first developed by Grizzle (2003) and it is constructed using one inductor, two capacitors, and one external switch, as shown in Fig. 2-5. The inductive coil is formed by wrapping an enamel coated wire around a 1.25-in. plastic ring five times. The number of loops was established experimentally and driven by a desire to generate a signal that could penetrate approximately 3 in. of concrete cover, while minimizing the overall depth of the sensor. Two, 150-pF capacitors are used in the sensor. The size of the capacitors was selected such that the characteristic frequencies corresponding to the initial and final states of the sensor would be in the range of 5 to 10 MHz.

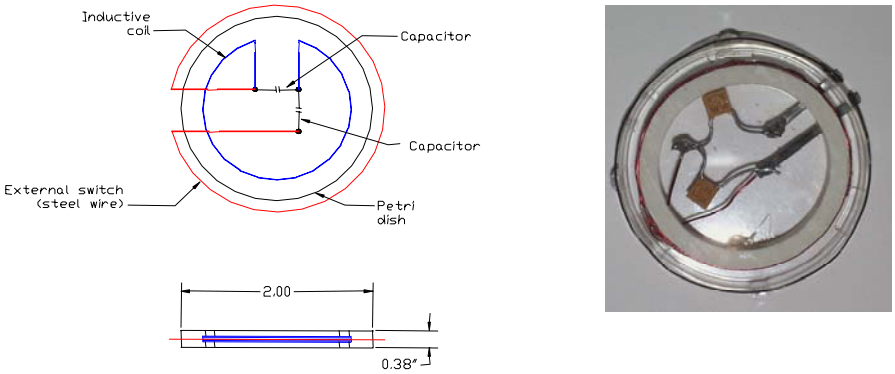

a) Basic sensor schematic b) Typical basic sensor

Figure 2-5. Basic sensor

The coil and capacitors are assembled inside a 2-in., plastic Petri dish, which is later filled with a potting compound. The steel wire is connected to the circuit within the Petri dish, but extends outside and is exposed to the environment.

The choice of potting compound proved to be important, as corrosion was observed inside the Petri dish during early tests. The selection of the potting compound is discussed later in Chapter 4.

The measured initial characteristic frequency of the basic sensor is approximately 6 MHz, while the final characteristic frequency is approximately 8.5 MHz (Fig. 2-4). This difference in frequencies is easily distinguishable, which minimizes the risk of the sensor output being corrupted by noise due to environmental factors.

The primary disadvantage of the basic sensor is that the characteristic frequency can not be detected during some periods in the life of the sensor. This behavior was not expected and it will be discussed more thoroughly in Chapters 3 and 4. The loss of the signal has been found to be caused by chlorides and moisture that have penetrated into the concrete. Because of these factors, the

signal from the basic sensor can be lost if the concrete is interrogated in a moist state. This characteristic limits the applicability of the sensor and can make locating the sensor impossible if the concrete is too moist.

2.3.2 Improved sensor

The improved sensor (Figure 2-6) represents a combination of the basic sensor and a reference circuit. The improved sensor is identical to the basic sensor with the addition of a reference circuit. The reference circuit is constructed using a 5-loop coil and a 500-pF capacitor. The characteristic frequency of the reference circuit is 4.5 MHz, and is only nominally affected by corrosion of the external switch. The sensing coil resonates at 7.0 MHz when in the initial state and at 9.0 MHz when in the corroded state (Figure 2-7). The shift is achieved by having the external switch corrode and break. When the switch breaks it changes the capacitance which is directly associated with the natural frequency (Equation 2-1, 2-2). The signal from the reference coil does interfere with that of the sensing circuit if the interrogation coil is positioned closer to the reference circuit. However, if the interrogation coil is positioned closer to the sensing circuit, the characteristic frequencies of both are clearly identifiable.

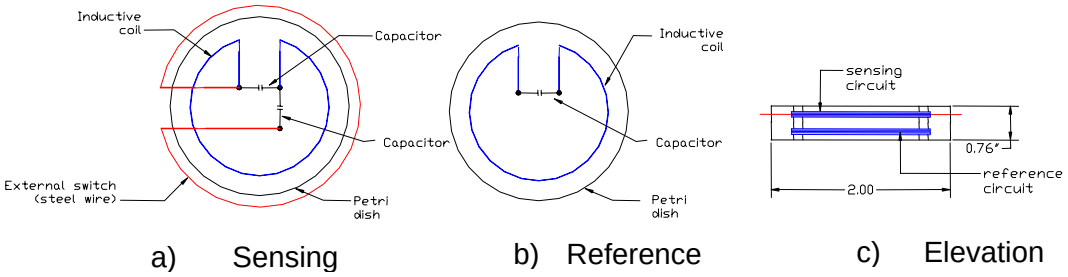

Figure 2-6. Improved sensor

The primary advantage of the improved sensor is that the reference circuit can be detected throughout the entire life of the sensor. The benefit of this characteristic is that the sensor can be located even if the sensing coil is not transmitting. This

sensor is also susceptible to reduced signal strength in the presence of moisture and chlorides and will not give reliable results if the concrete is too moist. The addition of the reference circuit more than doubles the thickness of the sensor, but the overall size was considered to be acceptable. The improved sensor is also encapsulated in a potting compound for environmental protection.

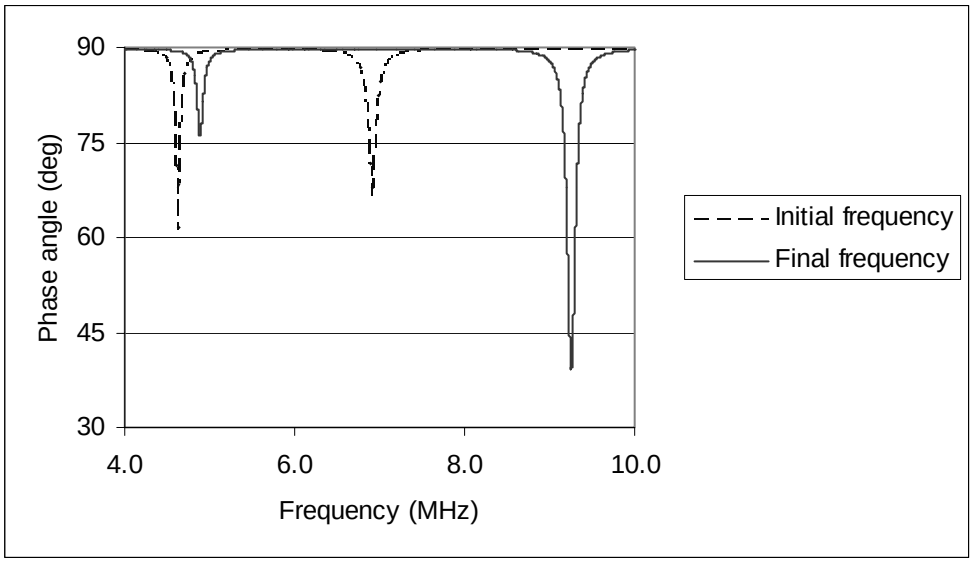

Figure 2-7. Typical response of a improved sensor

2.4 EXTERNAL SWITCH BEHAVIOR

As discussed earlier, the corrosion detection is performed using an external switch made of annealed steel wire. This wire is exposed to the same environmental conditions as the steel reinforcement, and therefore, monitoring the condition of the wire provides information about the condition of the adjacent reinforcing steel. As the corrosion process begins in the wire and in the reinforcement, the cross-sectional areas of both are reduced. Because the diameter of the wire is much smaller, the wire will fracture due to corrosion before appreciable corrosion damage has occurred in the reinforcement. To detect

different corrosion thresholds, three wire sizes were used to fabricate the prototype sensors: 26 gage, 24 gage, and 21 gage. The corresponding wire diameters are 0.0159 in. (0.40 mm), 0.0201 in. (0.51 mm), and 0.0285 in. (0.72 mm) respectively.

CHAPTER 3
Accelerated Corrosion Tests

Accelerated corrosion tests were conducted to relate the corrosion thresholds for each wire size to the progression of corrosion in rebar. Short sections of #5 reinforcing bars and wire (Figure 3-1) were suspended in a saturated calcium hydroxide solution, which simulates the pore water in concrete.

Figure 3-1. Accelerated corrosion test setup

3.1 TEST SETUP

This test solution has been proven by Grizzle (2003) to generate corrosion quickly. Saturated calcium hydroxide solution has also been used by other researchers to study corrosion in reinforced concrete environments. The solution is ideal for modeling the concrete surrounding the reinforcing steel because calcium hydroxide crystals occupy 20-25% of cement paste by volume (Kitowski, 1993). The test solution contains 1.85 g/L of CaHO to simulate a typical concrete environment. In typical concrete, the steel is protected by a passive layer created by the high alkalinity of the CaHO (Jones, 1996). The presence of chlorides

breaks down this layer and allows corrosion to occur. To simulate this condition 3.5 percent by weight of NaCl was added to the saturated calcium hydroxide solution.

The tests related the time it takes for a certain diameter of wire to fracture to the amount of corrosion in the #5 rebar. The #5 rebar was selected for these tests because it is the typical reinforcement size used in bridge decks. The wire for these tests was arranged in a loop configuration to model the wire that would be wrapped around the circumference of a typical sensor. The wires and the rebars were submerged in the solution for 5 days and then exposed to the atmosphere for 2 days. By allowing the specimens to dry, more oxygen is available for the corrosion process further increasing the corrosion rate. These cycles were continued until the wire fractured due to corrosion.

The reinforcing bars were then removed from the solution, cleaned, and weighed to determine the corresponding reduction of cross-sectional area. The reinforcing was cleaned using ASTM G1, designation C.3.5 standard which involves placing the specimen in a hydrochloric acid solution for ten minutes. The solution contained 500 mL of hydrochloric acid, 3.5 g of hexamethylene tetramine and 500 mL reagent water. This solution is used to remove the corrosion product from the rebar without destroying the good steel. Data reported from the accelerated corrosion tests include the length of the test and the weight loss by each rebar sample.

The scale that was used in early tests was found to give unreliable results and data from several sets of accelerated corrosion tests had to be discarded. The results of the latest tests were considered to be reliable. A more sensitive scale was used and it was calibrated before each measurement. The calibration was conducted by weighing the standard weight at the beginning of each test when the initial weights of the rebars were measured. The standard weight was weighed

again when the corroded rebars were weighed. To get reliable results, the difference between the initial and the final weights of the standard weight would be added to the rebar measurements to account for any fluctuations in the scale.

Two separate accelerated corrosion tests were conducted. Each test involved eight sets of tests for each diameter of wire. Each wire had a piece of rebar that was immersed in the solution at the same time as the wire. These rebars were weighed and their length was measured before they were exposed to the environment (Table 3-1, 3-2). The wires that were used for the experiments were 26 gage, 24 gage, and 21 gage.

3.2 RESULTS FROM ACCELERATED CORROSION TESTS

The accelerated corrosion tests were intended to provide information about the corrosion thresholds for various sizes of steel wire. The data from the Accelerated corrosion tests are illustrated in Tables 3-1 and 3-2. At the time of writing, data from the 21 gage wires were not available, because the wires had not fractured.

Table 3-1. Data from first set of accelerated corrosion test

Rebar ID	Wire gage	Initial rebar data		Final rebar data		
		Weight (g)	Length (in.)	Weight (g)	days	Reduction in cross sectional area (%)
1	26	251.865	16.9	250.43	50	0.57
2	26	242.165	16.2	241.06	43	0.45
3	26	250.775	16.9	249.36	43	0.56
4	26	247.92	16.65	246.35	50	0.63
5	26	252.32	16.85	249.88	57	0.97
6	26	252.31	16.9	250.49	50	0.72
7	26	239.05	16.05	237.58	63	0.61
8	26	246.945	16.6	245.37	63	0.63
9	24	250.805	16.85	247.37	94	1.36
10	24	245.68	16.45	243.22	99	1.00
11	24	255.565	17.15	251.73	92	1.5
12	24	242.435	16.22	238.66	92	1.56
13	24	255.94	17.2	253.31	99	1.03
14	24	242.25	16.3	240.05	112	0.91
15	24	246.07	16.5	242.35	94	1.51
16	24	246.855	16.5	243.22	120	1.47
17	21	248.095	16.55	*	*	*
18	21	250.045	16.8	*	*	*
19	21	248.555	16.7	*	*	*
20	21	248.565	16.7	*	*	*
21	21	247.965	16.65	*	*	*
22	21	238.55	16.65	*	*	*
23	21	235.56	15.75	*	*	*
24	21	243.965	16.37	*	*	*

* Tests are ongoing.

Table 3-2. Data from second accelerated corrosion test

Rebar ID	Wire gage	Initial rebar data		Final data		
		Weight (mg)	Length (in)	Weight (mg)	days	Reduction in cross sectional area (%)
A	26	225.82	15.07	223.83	78	.88
B	26	225.03	15.0	223.15	54	.83
C	26	224.83	15.04	222.24	53	1.15
D	26	224.09	14.92	221.65	53	1.08
E	26	225.61	15.03	223.6	72	.89
F	26	224.18	14.9	222.25	64	.86
G	26	226.68	15.09	223.63	84	1.34
H	26	225.24	15.06	222.46	78	1.23
I	24	226.88	15.23	223.37	80	1.54
J	24	220.61	14.69	217.87	78	1.27
K	24	228.06	15.19	225.42	72	1.15
L	24	222.86	15.02	220.13	72	1.22
M	24	228.87	15.24	226.75	93	.93
N	24	226.67	15.17	223.83	78	1.25
O	24	226.79	15.21	*	*	*
P	24	225.75	15.11	223.44	78	1.02
Q	21	225.87	15.06	*	*	*
R	21	24.86	14.96	*	*	*
S	21	227.2	15.15	*	*	*
T	21	229.24	15.28	*	*	*
U	21	226.11	15.12	*	*	*
V	21	227.71	15.14	*	*	*
W	21	230.56	15.35	*	*	*
X	21	225.3	15.02	*	*	*

* Tests are ongoing.

3.2.1 Wire Performance

These tests were run under the assumption that wires with smaller diameters will corrode and break in less time than wires with larger diameters. Therefore, different wire sizes could be used to detect different levels of corrosion. These times are represented in Figure 3-2 for the first set of accelerated corrosion tests and Figure 3.3 for the second set. The time to wire break for each gauge of wire was averaged and the results plotted (Figure 3.4).

The average time to wire breaks in test 1, for the 26 gage and 24 gage wires, were 50 days and 75 days respectively. During the second test average times of 67 days and 79 days were obtained for the 26 gage and the 24 gage, respectively.

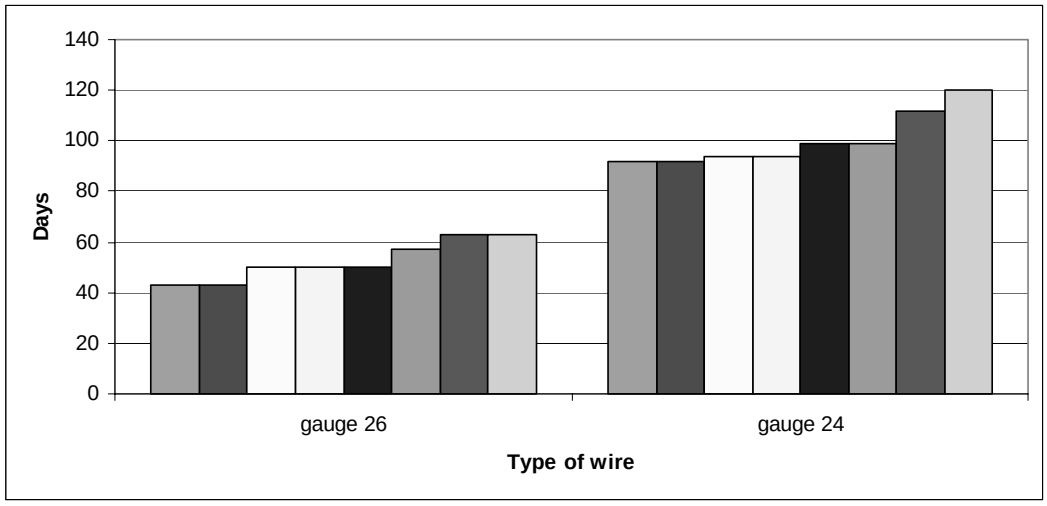

Figure 3-2. Time to wire break for accelerated corrosion test 1

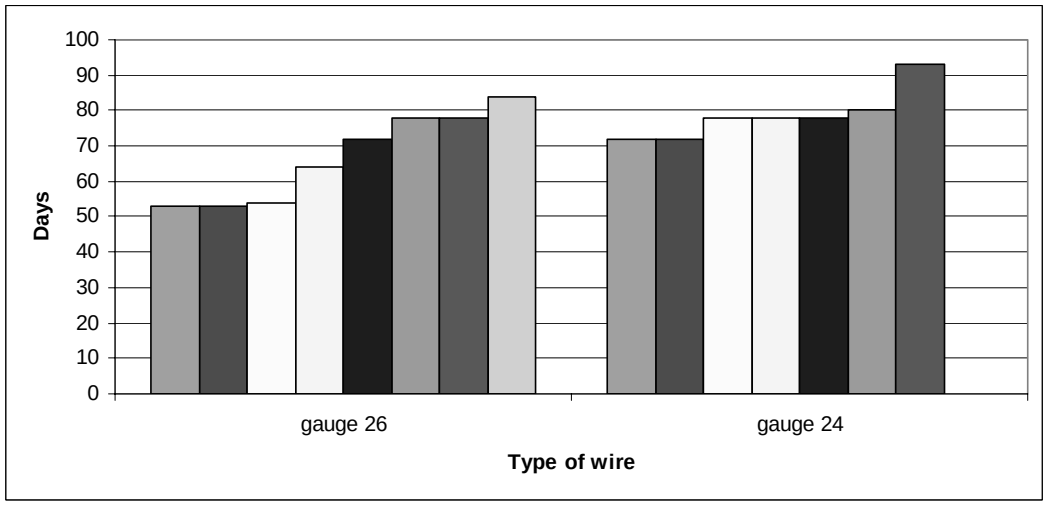

Figure 3-3. Time to wire break for accelerated corrosion test 2

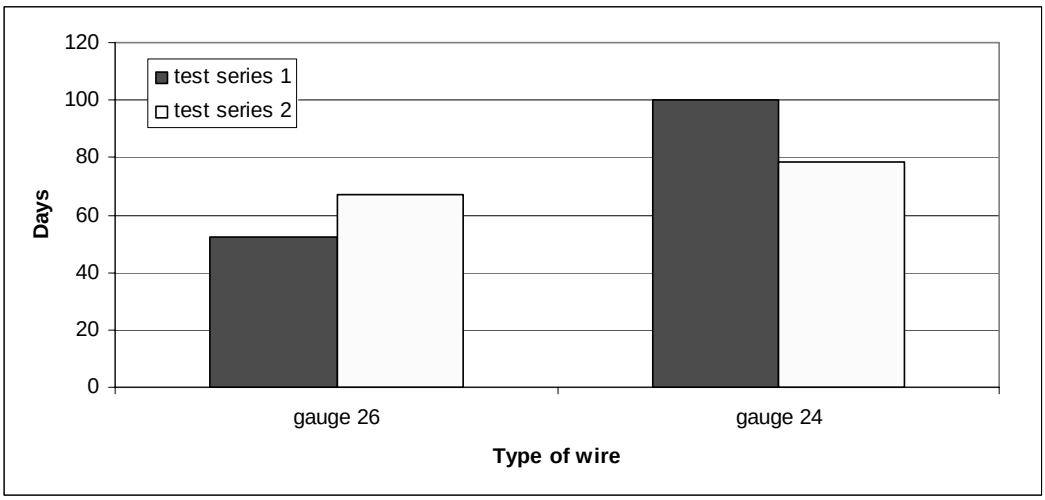

Figure 3-4. Average time to wire break for accelerated corrosion tests 1 and 2

The difference in the average time can be attributed to a slightly different solution mix. The results from both test series are consistent with the assumption that the smaller the wire diameter, the shorter the time required to corrode through the entire diameter. These results indicate that different diameter wires can be used to indicate different amounts of corrosion occurring in the concrete.

3.2.2 Reinforcement Performance

To be able to predict the condition of the reinforcement corresponding to failure of a given diameter wire is important. These tests related the amount of cross-sectional area that was lost to the steel wire diameter. The results for both accelerated corrosion tests are shown in Table 3-1 and Table 3-2. From the tests, it can be concluded that a larger wire gauge corresponds with a larger amount of cross-sectional area lost (Figures 3-5, 3-6). The average cross-sectional area reduction for the 26 gage wire specimens in test 1 and in test 2 were 0.64 % and 1.03 % respectively. The corresponding cross-sectional area reductions for the 24 gage wires were 1.29 % for test 1 and 1.19 % for test 2. Using a larger gage wire

will result in more damage to the reinforcement while a smaller gage wire produces less damage.

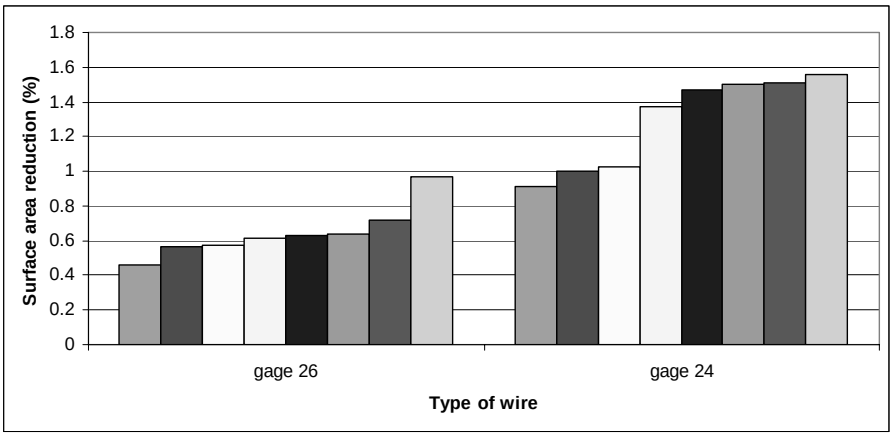

Figure 3-5. Cross-sectional area reduction of accelerated corrosion Test 1

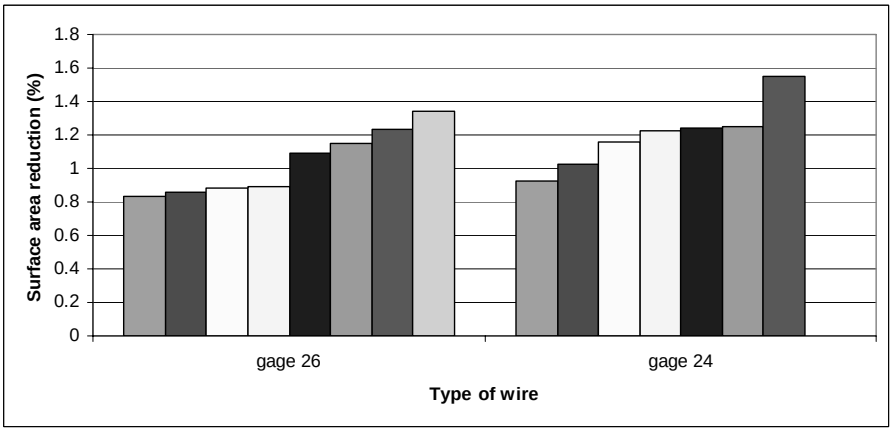

Figure 3-6. Cross-sectional area reduction for accelerated corrosion test 2

3.3 SUMMARY OF ACCLERATED CORROSION TESTS

The accelerated corrosion tests prove the hypothesis that smaller gage wires will detect a smaller amount of damage. However, more data are needed to accurately predict the amount of damage expected from a certain gage wire.

CHAPTER 4
Full Scale Slab Tests

4.1 INTRODUCTION

The performance of sensors that were embedded in concrete slabs are reported in this chapter. A successful sensor must possess several key qualities: (a) easy to install, (b) durable enough to survive concrete casting process, and (c) reliable. The large scale slabs were designed to test the performance of the sensors in these key areas.

4.2 SLAB DESCRIPTION

Four reinforced concrete slabs were cast as part of this project. The test specimens were selected to simulate a section from a typical bridge deck. Each slab was 8-in. deep, 18-in. wide and 10-ft long. The slabs were reinforced using #5 bars which is the typical size for the top layer of reinforcement in bridge decks. Eight sensors were attached to the reinforcing bars near the top surface of each slab. The specimens were designed to accelerate corrosion of the reinforcement in several different ways. The concrete cover to the longitudinal reinforcement was selected to be 1 in. to ensure that the chlorides would penetrate to the level of the reinforcement quickly. Also, a low-strength concrete with high amounts air-entraining admixture was used to cast the slabs. The typical 28-day compressive strength of the slabs was between 2000 psi and 2100 psi, while the amount of air-entraining admixture was 1.25 oz of air per 100 lb of Portland cement, which is twice the recommended dosage. This combination of low compressive strength

and high air content makes the concrete very permeable, which further increases the rate of chloride ion penetration through concrete.

4.3 TEST SETUP

The slabs were subjected to sustained loads (Figures 4-1 and 4-2): the beams rested on two supports placed at 3.5 feet from each end. Loads were applied at each end creating a region of constant negative moment in the beam between the two supports. The applied load was sufficient to crack the slabs. Measured crack widths were in the range of .013 to .016 in. A typical crack limit recommended by ACI committee 224 for structures exposed to salt water is .006 in. Inducing wider cracks in the slabs provides a mechanism for salt water to penetrate into the concrete very rapidly.

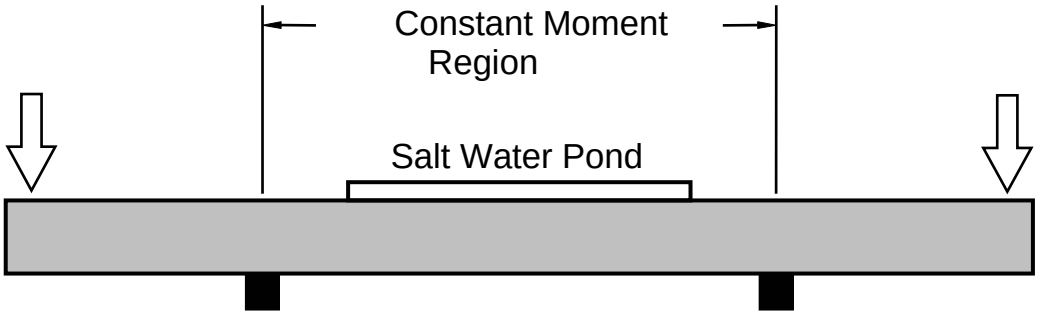

Figure 4-1. Slab layout

Figure 4-2. Slab layout

The salt water was ponded in the constant moment region of each slab. The salt water solution contained 3.5 percent of NaCl by weight, the same amount as typical sea water. This salt water solution was cycled in the ponds using a two week wet / two week dry interval. This setup was designed to accelerate the process of corrosion in the top level of reinforcement in the constant moment region.

4.3.1 Salt Water Ponds

The salt water ponds were constructed using 36-in. long, 16-in. wide and 6-in. deep plastic containers (Figure 4-2). The bottom of each container was removed to put the salt water in direct contact with the top surface of the concrete. To insure a water tight seal between the container and the slab, a silicone adhesive was used to affix the container to the concrete. Also the seams between the container and the concrete were filled with a silicone sealant. The cracks on the sides of the slabs were also sealed with a silicone sealant. The sealant was applied on the surface of the cracks and then forced in to the cracks to ensure a

watertight seal. Although care was taken to waterproof the system, leaks were found along the corners of the ponds and around the cracks in the slabs. Because the ponds leaked, the salt water was replaced periodically to ensure that the specimens stayed moist during the two week wet cycle.

4.4 SENSOR PLACEMENT

Thirty two sensors were placed in the slabs; 16 basic sensors and 16 improved sensors. The sensors were placed in the middle of the beam where the concrete would experience the most cracking and therefore the fastest penetration of chlorides (Figure 4-3). The sensors were embedded with 1-in. cover corresponding to the level of the reinforcement. Each beam included eight sensors, four of each type. Also, two different arrangements of external switches were used for the sensors: a circumferential loop and an elongated loop (Figure 4-4). Installation of the sensors was executed by attaching the sensor to the adjacent rebar using two zip ties (Figure 4-3b). Attaching the sensors to the rebar ensured that they would be exposed to the same environment as the reinforcing steel.

a) Layout of sensors

b) Positioning of sensor

Figure 4-3. Typical sensor placement

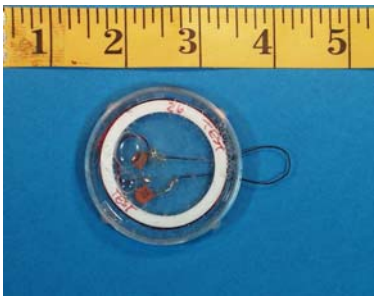

(a) Basic sensor with elongated loop

(b) Basic sensor with circumferential loop

Figure 4-4. Switch configurations

4.5 DURABILITY

The durability of the sensors is very important especially during the construction process. Casting of the slabs was used as a test of the durability of the sensors in an actual construction process.

The slabs were cast in Ferguson Laboratory using a ready mix truck and a 1–yd^3 concrete hopper. Concrete from the truck was placed in the hopper and then the hopper was transported to location of the forms. The hopper was suspended over each slab and concrete was dropped into the forms. Once enough concrete was placed into the forms, the concrete was vibrated and the surface was finished with trowels. No special care was taken to protect the sensors.

The slabs were allowed to cure for four weeks before they were transported outside and subjected to sustained loads. Before the slabs were cracked, the sensors were interrogated for the first time after being embedded in to the concrete. Of the thirty two sensors, two sensors responded at their final frequency indicating that the external switch had broken during the construction process. Both of the damaged sensors were constructed using the elongated loop configuration (Figure 4-4a). From this data, it was concluded that the elongated loop configuration was too fragile to be investigated further. Since the loop

extends about an inch beyond the sealed environment, it is vulnerable to being broken by a vibrator, a worker's boot, or a piece of sharp aggregate. However, the circumferential loop layout proved to be durable. Since the external wire of the circumferential loop is wrapped around the circumference if the sensors, it is better protected from being damaged. The durability of the circumferential loop was proven during construction of the slab. Overall durability of the sensors was found to be acceptable.

4.6 INTERROGATION OF THE SLABS

The sensors in the slabs were interrogated once a month using a Hewlett Packard 4194A impedance/gain-phase analyzer (Table 4-1). During the first interrogation, the 30 sensors that had survived the construction process responded at their initial characteristic frequencies, indicating that the state switches had not corroded. Representative data from a basic sensor and an improved sensor are shown in Figure 4-5(a) and 4-6(a), respectively. One characteristic frequency was clearly defined when the basic sensors were interrogated, and two characteristic frequencies (one corresponding to the reference coil and the other to the sensing coil) were observed in the response of the improved sensors. The amplitudes of the dips in the phase angle response were considerably less than had been observed when the sensors were interrogated in air. This behavior was expected, however, because the transmitter/receiver coil was placed adjacent to the coil in the sensor when the tests were conducted in air, while the two coils were separated by the concrete cover in the slabs. In addition, free water is present in the concrete. Both factors are believed to reduce the coupling efficiency of the system. The influence of these factors is discussed in detail in Chapter 5.

When the sensors were interrogated after the first month of exposure to the salt water, most of the sensors appeared to have malfunctioned. The characteristic

dip in the phase angle response was not observed (Figure 4-5b). The reference frequency could still be identified in the improved basic sensors, but the characteristic frequency of the sensor circuit was missing (Figure 4-6b).

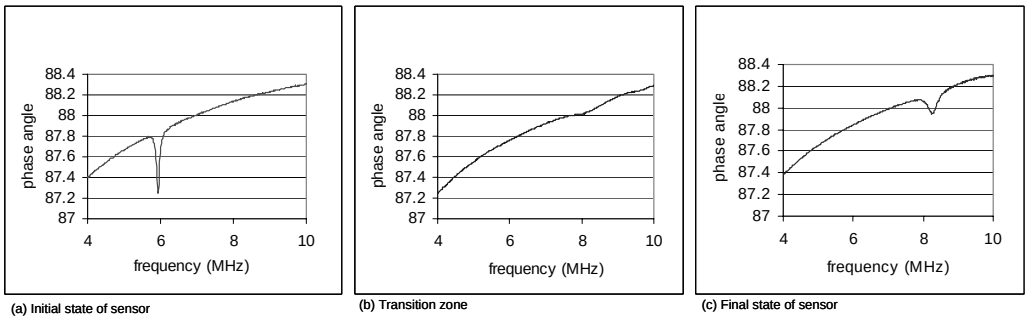

Figure 4-5. Basic sensor response

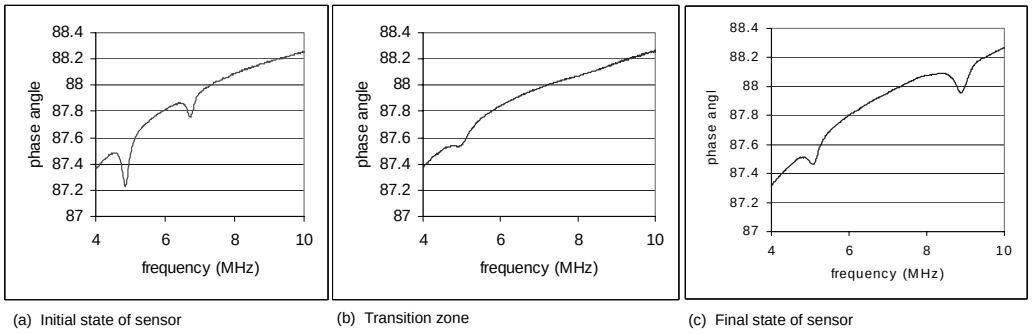

Figure 4-6. Improved sensor response

Since this response was not expected, one of the slabs was broken apart to evaluate the condition of the sensors. It was not possible to determine the condition of the external switches, but in retrospect, it is unlikely that any had fractured due to corrosion. A very small amount of corrosion was observed on the steel wires and on the surface of the reinforcement in the immediate vicinity

of the cracks. The decision was made to continue monitoring the sensors in the other three specimens for several more months.

After 5 months of exposure, few of the sensors started showing a large amplitude dip corresponding to a fractured wire. The variation of the characteristic frequencies with time is shown in Figure 4-7 for a typical basic sensor and a improved sensor that demonstrated a dip corresponding to a fractured wire. The frequency response of the improved sensor showed that the sensing coil could not be detected in the readings one, two, and three months after the initial interrogation (Figure 4-7). This same behavior was also observed in the basic sensor during the third and fourth months. However, after several months, the signal from the sensing coils reappeared for the sensors, and the characteristic frequencies corresponded to the final state, indicating that the external switch had fractured (Figure 4-7).

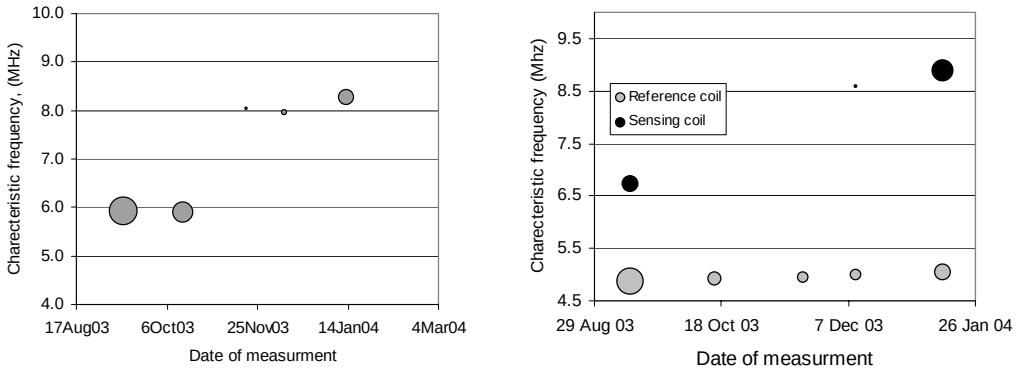

a) Basic sensor b) Improved sensor

Figure 4-7. Characteristic frequency with time

Although few sensors behaved as expected, many more exhibited behavior that was unexpected (Table 4-2). Most sensors never responded with a frequency that corresponded to a fractured wire (table 4-1). These sensors either exhibited a small dip in the phase response near the frequency corresponding to a broken wire or they exhibited no characteristic frequency. Also some sensors indicated a

broken wire when interrogated one month, but the characteristic frequency had disappeared when interrogated the next month. This behavior was not expected, and therefore, more tests were conducted to understand the observed response. The results from these investigations are described in Chapter 5. Although a clear indication of a fractured wire was not observed in many of the sensors, the remaining slabs were visually inspected on April 2, 2004.

Table 4-1. Response of sensors by date

Slab/ Date cast	Date of interrogation	Number of sensors responding in each state		
		Initial	Transition	Final
1	9/8/03	8	0	0
	10/15/03	4	4	0
	11/19/03	3	5	0
	12/10/03	3	5	0
	1/13/04	3	5	0
	2/18/04	1	6	1
	3/20/04	1	6	1
2	9/8/03	8	0	0
	10/15/03	1	4	3
3	9/8/03	6	0	2
	10/15/03	2	6	0
	11/19/03	2	5	1
	12/10/03	1	6	1
	1/13/04	1	6	1
4	9/8/03	8	0	0
	10/15/03	5	3	0
	11/19/03	3	4	1
	12/10/03	1	5	1
	1/13/04	1	5	2
	2/18/04	1	4	3
	3/30/04	1	3	4

Table 4-2. Sensor response at the time of autopsy

Beam/date	Sensor	Type of sensor	Final frequency (MHz)
Slab 1 02 April 04	4	Basic/circumferential	(8.2) Transition
	13	Basic/elongated loop	(8.5) Transition
	15	Basic/elongated loop	(5.9) Initial
	17	Improved/elongated loop	(8.9) Final
	18	Improved/elongated loop	(N/A) Transition
	26	Improved/circumferential	(N/A) Transition
	27	Improved/circumferential	(8.7) Transition
	30	Improved/elongated loop	(8.8) Transition
Slab 2 16 Oct 03	2	Basic/circumferential	(N/A) Transition
	3	Basic/circumferential	(N/A) Transition
	14	Basic/elongated loop	(8.5) Transition
	20	Improved/elongated loop	(6.8) Initial
	21	Improved/circumferential	(8.8) Transition
	23	Improved/circumferential	(8.9) Final
	24	Improved/elongated loop	(9.0) Final
	25	Improved/circumferential	(9.0) Transition
Slab 3 19 Jan 04	7	Basic/circumferential	(N/A) Transition
	8	Basic/circumferential	(N/A) Transition
	9	Basic/elongated loop	Broken during construction
	11	Basic/elongated loop	(6.0) Initial
	16	Basic/elongated loop	Broken during construction
	28	Improved/elongated loop	(N/A) Transition
	29	Improved/circumferential	(N/A) Transition
	31	Improved/elongated loop	(8.9) Final
Slab 4 02 April 04	1	Basic/circumferential	(N/A) Transition
	5	Basic/circumferential	(8.1) Final
	6	Basic/circumferential	(6.0) Initial
	10	Basic/elongated loop	(8.5) Final
	12	Basic/elongated loop	(N/A) Transition
	19	Improved/elongated loop	(9.0) Final
	22	Improved/circumferential	(8.9) Transition
	32	Improved/circumferential	(9.0) Final

Initial = Sensor responding with initial frequency

Final = Sensor responding with final frequency (indicating corrosion)

Transition = Sensor responding with no signal or very faint signal

4.6.1 Visual Inspection

To determine if corrosion was actually occurring in the slabs, the sensors and reinforcing bars had to be visually inspected. The visual inspection of the slabs was conducted by removing the concrete cover around the rebar and the sensors. This concrete removal was performed using both a 30-lb impact hammer and a hand chisel Figure 4-8. Most of the cover was removed using the impact hammer. The remainder of the concrete around the rebar and the sensors was removed using the chisel. This method was used to minimize the damage to the sensors during the concrete removal process. However, some of the sensors were damaged during the concrete removal process. Removing the concrete around the external wire proved to be especially difficult. Because the wire had bonded to the concrete, removing it from the concrete required some force and usually the wire broke during this process. Due to these accidental wire breaks, differentiating between breaks caused by corrosion and breaks caused by concrete removal was almost impossible.

Figure 4-8. Concrete removal

(a) Observed corrosion of reinforcement in the vicinity of improved sensor

(b) Observed corrosion of reinforcement in vicinity of basic sensor

Figure 4-9. Corrosion around reinforcement

From the visual inspections of the rebar and the sensors, it was evident that corrosion had initiated in the slabs. Corrosion on the rebar was always found near sensors where the frequency had shifted (Figure 4-9). But, corrosion was also found around sensors that were responding in transition zone. This was most evident in the last slab to be autopsied. This slab had the least leaks and had been moist for most of the time. Only one sensor in this beam indicated that its wire had fractured. During the autopsy it was discovered that the slab was still saturated even after being allowed to dry for two weeks. The corrosion in the slab was excessive and some areas of the bars showed significant corrosion damage (Figure 4-10). It was also evident from the autopsies that areas of the rebar that crossed cracks showed more corrosion than locations that were surrounded by uncracked concrete (Figure 4-11). From the autopsies it was concluded that the sensors do detect corrosion but their response was not as simple as originally assumed. It was hypothesized that moisture and chlorides in the beam affect the response of the sensors. This hypothesis is discussed in more detail in Chapter 5.

Figure 4-10. Heavy reinforcement degradation caused by corrosion

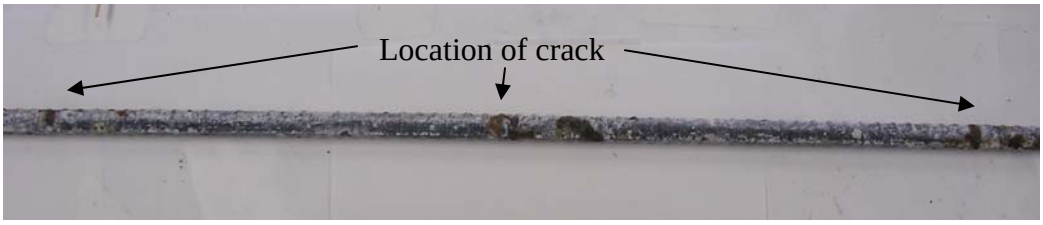

Figure 4-11. Section of reinforcement in the cracked region

4.6.2 Half cell measurements

The last two slabs were also monitored using half cell potentials to confirm the visual evidence. These half cell measurements were conducted on March 4, 2004 using a 10 in. grid covering the entire slab. Measurements were taken at the intersection points of this grid and the potentials were plotted on to a contour chart (Figure 4-12). These half cell potential measurements indicate a probability of corrosion in the salt water pond region. The measurements were conducted according to ASTM C 876 standard and readings were interpreted according to these guidelines: (a) measurements more negative than -350 mV indicate that there is a 90 percent probability that corrosion is occurring in that

area, and (b) measurements more positive than -200 mV indicate that there is a 90 percent probability that corrosion is not occurring. As can be seen in Figure 4-12, the center of the slab, under the salt water pond, has a 90 percent probability that corrosion is occurring.

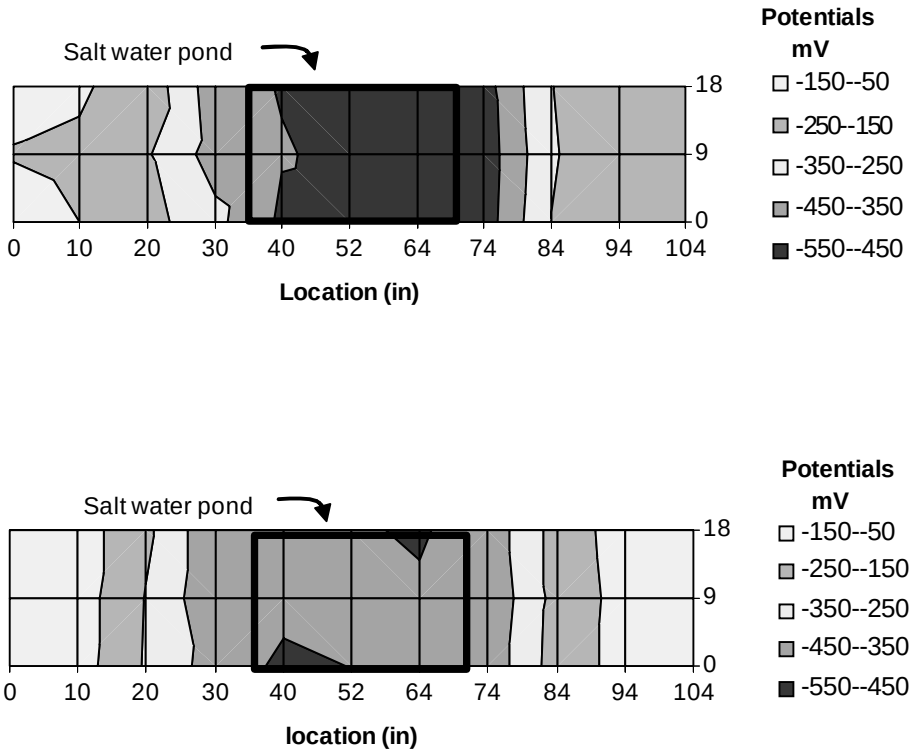

Figure 4-12. Half cell potential measurements

4.6.3 Chloride penetration

To verify that chloride ions were penetrating the concrete, chloride penetration measurements were taken from one of the slabs. The samples were

taken on April 02, 2004 from the last slab autopsied. The samples were taken at three different locations: (1) at the surface, (2) at the level of the reinforcement few inches away from a crack and (3) at the level of reinforcement at a crack.

The level of chlorides that were present at the surface was found to be 0.11 % and at the level of the reinforcement these levels were found to be 0.10 % and 0.13 % depending on location (Table 4-3). The level of chlorides found are less than what is accepted by the ACI. The ACI 318-02 code recommends a chloride content less than 0.15 % for structure exposed to chlorides (ACI 318-02 Table 4.4.1). The corrosion found on the rebar suggests that the chloride levels should be higher. Because the cracks in the slabs were very large, it is possible that the salt water did not have time to penetrate into the surrounding concrete, rather it flowed right through. This theory is supported by the results because more chlorides were found at the location of the crack. These chloride values seem to explain why so much corrosion was found right under a crack and no corrosion was found in the uncracked concrete.

Table 4-3. Chloride penetration results

Location of sample	**mV**	**Chloride concentration (%)**
At the surface	19.3	.11
At the level of reinforcement (away from a crack)	20.7	.10
At the level of reinforcement (at a crack)	17.4	.13

4.7 SUMMARY

The large scale tests were successful in demonstrating the key attributes of the sensors. The installation process of the sensors in a construction site needs to be fast and simple. Because the sensors are small and relatively durable, the installation process can be conducted efficiently without losing much time. Another important quality, which is closely related to the installation ease, is durability. A typical concrete cast is a harsh environment that requires a tough sensor. The large scale slabs proved that the sensors are tough enough to survive this process. The sensors reliability in detecting corrosion was also found to be somewhat successful. The visual inspections and the half cell measurements confirmed that corrosion was occurring in the slabs and some of the sensors detected this reliably. However, some of the sensors did not respond with an expected response. It is hypothesized that the variance in the signal was due to the moisture and the chloride content in the slabs. These variables are studied further in Chapter 5.

CHAPTER 5
Sensor Testing and Behavior

5.1 INTRODUCTION

During the full scale slab-tests, some of the sensors exhibited unexpected response. Individual experiments were conducted to evaluate these behaviors in a controlled manner.

5.2 INTERNAL CORROSION

During some early tests of the sensors, internal corrosion of the electrical components was noticed. This behavior was also observed in the full-scale slab tests.

5.2.1 Causes

This internal corrosion has been attributed to several environmental factors. These factors are hypothesized to be corrosion caused by the flux used in the soldering process, moisture penetrating the potting compound along the external switch, and by the chemical composition of the potting compounds.

Using solder to attach steel is fairly difficult and flux must be used to clean the surface. The construction process as described by Grizzle (2003) for the prototype sensors uses flux to attach the steel to the other electrical components. The prototype sensors were constructed using a drop of flux on the steel before solder was applied. The problem with using flux is that it contains a strong acid. This acid will corrode the steel wire and cause corrosion to occur inside the sensor. Also, the solder that was used for the prototype sensors incorporated the

flux with the solder. These types of solders should be avoided in applications that are designed to be corrosion free. For the new sensors, a non-clean solder is used to try to minimize the problem. This solder does not contain flux on the inside; so therefore, the only flux that is used is applied before soldering. This flux can be cleaned with alcohol after the connection is made. Also to further inhibit the progress of the corrosion caused by the flux a suitable potting compound must be used.

Moisture penetration has been observed at the interface of the area where the external switch exits the potting compound. This corrosion was found to be the cause of wire breaks in early tests conducted by Grizzle (2003). These tests involved embedding the sensors into small concrete prisms that were exposed to salt water. Suitable potting compound is essential for protecting against this type of corrosion.

5.2.2 Protecting Against Internal Corrosion Using a Potting Compound

Potting compounds help to protect the vital electronics in the sensor from impact and corrosion. The crucial elements that must be protected from the corrosive environment are the inductor, the capacitors and the area of the external switch that is located inside the sensor. If the corrosion attacks the electronics, the sensor will malfunction and become unreliable. Also, the external switch must be protected inside the sensor where it is not designed to corrode. To protect the sensors several different compounds have been used: (a) GE silicone RTV615A, (b) Envirogel^{TM} by Glotrax Polymers inc., (c) hot glue, and (d) marine epoxy.

The selection of a potting compound is based on several key qualities. The potting compound should have low viscosity for easy application, it should be fairly inexpensive, and transparent, or at least translucent. Several potting

compounds were not considered because they were not translucent. Having translucent potting compound is important because it allows the sensors to be visually inspected. Visual inspection allows the research team to identify problems, such as corrosion forming on the electronics, defective connections, and other manufacturing flaws, that could be missed otherwise. Also some compounds were not considered because they had a high viscosity. Very viscous materials are hard to place into the Petri dish, might not coat every part of the electronics, and may cause voids in the Petri dish. All of the selected compounds were transparent and had a very low viscosity.

5.2.3 Testing Potting Compounds

The ability of the compound to protect against corrosion was tested by creating sensors using all of the compounds and testing the sensors using the accelerated corrosion tests. The sensors were placed into beakers containing the same solution as used in the accelerated corrosion tests in Chapter 3. The sensors were also subjected to wetting and drying cycles as described in Chapter 3. The performance of the potting compounds was evaluated by visually inspecting the interior components. These inspections were conducted once a week. From the inspections it was evident that the RTV615A and the Envirogel^{TM} did not protect against corrosion (Figure 5-1a, 5-1b). These sensors showed evidence of corrosion within the first week and this level increased during subsequent inspections. The hot glue and the marine epoxy performed well in keeping the corrosion from occurring inside the Petri dish. The marine epoxy did not show any evidence of corrosion while the hot glue had a minimal amount of corrosion present inside of the sensor (Figure 5-1c, 5-1d).

a) RTV615A

b) Envirogel^{TM}

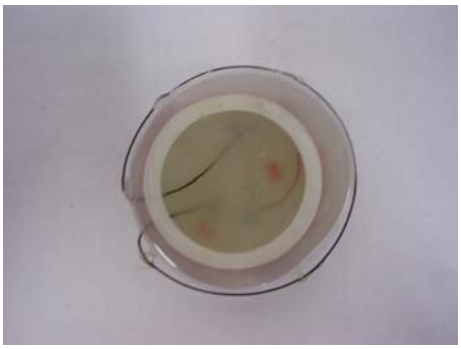

c) Hot glue

b) Marine epoxy

Figure 5-1. Different types of potting compounds

From the accelerated corrosion tests, it was concluded that adhesion of the potting compound to the electrical components was crucial in preventing corrosion from occurring inside of the sensors. The RTV615A and the Envirogel^{TM} do not adhere to the components, thereby allowing corrosion to attack the components. Both of the adhesive compounds prevented corrosion of the electrical components from occurring because the moisture does not appear to penetrate along the switch into the Petri dish.

The final potting compound selection was conducted between the hot glue and the epoxy. Both of the compounds are transparent, marine epoxy more so

than the hot glue, and have low viscosity. The advantage of the hot glue is that it does not have to be mixed like the marine epoxy. The marine epoxy is very sensitive to the mix proportions, so care has to be taken to ensure proper mix proportions. But the marine epoxy was selected because it offers better corrosion protection, it cures harder offering more impact resistance, and once the mix proportions are correct, it is easier to apply.

5.3 BEHAVIOR / PERFORMANCE

Understanding the behavior of the sensors once they become embedded in concrete is crucial. The behavior characteristics that are important to study are the variations of the response with time, the influence depth, and moisture and chloride ions in the concrete, and the embedment depth of the sensors

5.3.1 Response with Time

During the full-scale slab tests, it was discovered that the sensors have a transition zone between the initial and final frequencies. In this transition zone, the signal becomes weak and sometimes can not be detected. Tests were conducted to understand the causes of this behavior.

5.3.1.1 Effect of corrosion of the external switch

The effect of the corrosion on the external switch has been studied by placing sensors in a salt water solution and interrogating them frequently. After the discovery of the transition zone, it was hypothesized that as the external switch corroded its resistance would change and this would cause the sensor to go into the transition zone. With this test setup, the behavior of two basic sensors and two improved sensors were investigated.

The daily tests were run using the same simulated concrete solution as in the accelerated corrosion tests used to test the steel wires (Chapter 3). The

presence of chloride ions in the solution decreases the pH, allowing corrosion to attack the steel. The sensors are cycled in the solution using a 5 days wet / 2 days dry intervals. In the beginning the sensors were interrogated 5 days a week, and the frequency and the amplitude of the phase angle are monitored. However after a few days it became apparent that the signal was not changing the sensors were interrogated less frequently.

It was hypothesized that once the steel wire started corroding, the resistance in the wire changed, and therefore the signal from the sensor would be affected. The daily tests were used to test this hypothesis. However as the corrosion increased in the wire, the signal did not change significantly and the transition zone was not observed (Figure 5-2, 5-3). A small variation in the signal response was observed but this could be attributed to the amount of moisture that was present on the wire during measurement (Figure 5-3). From these tests, it was concluded that the amount of corrosion on the external switch did not affect the response of the sensor.

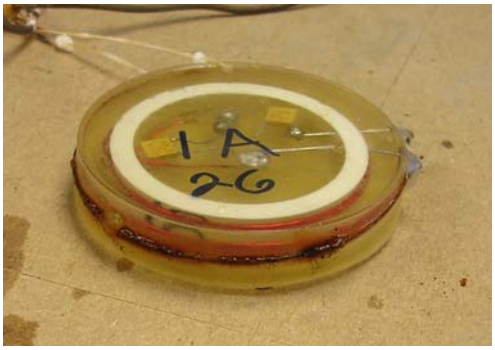

a) Basic sensor heavily

a) Improved sensor heavily

Figure 5-2. Sensors after being exposed to accelerated corrosion tests

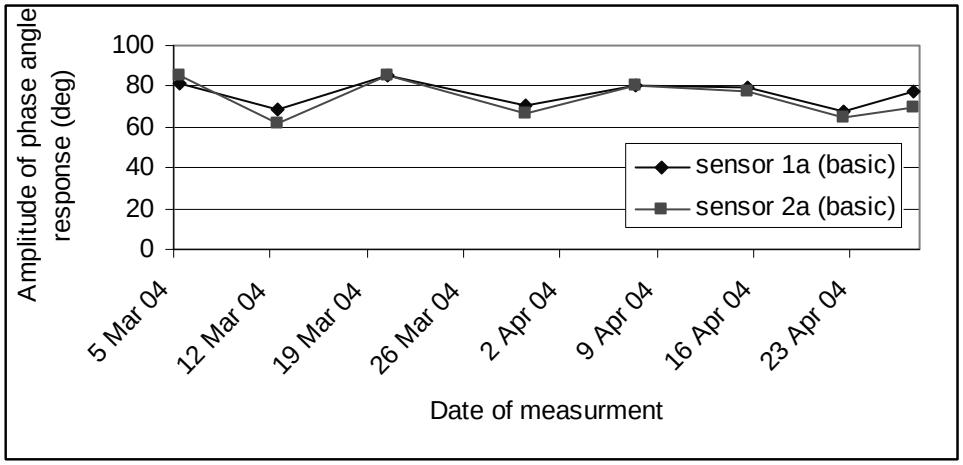

Figure 5-3. Time response of basic sensors

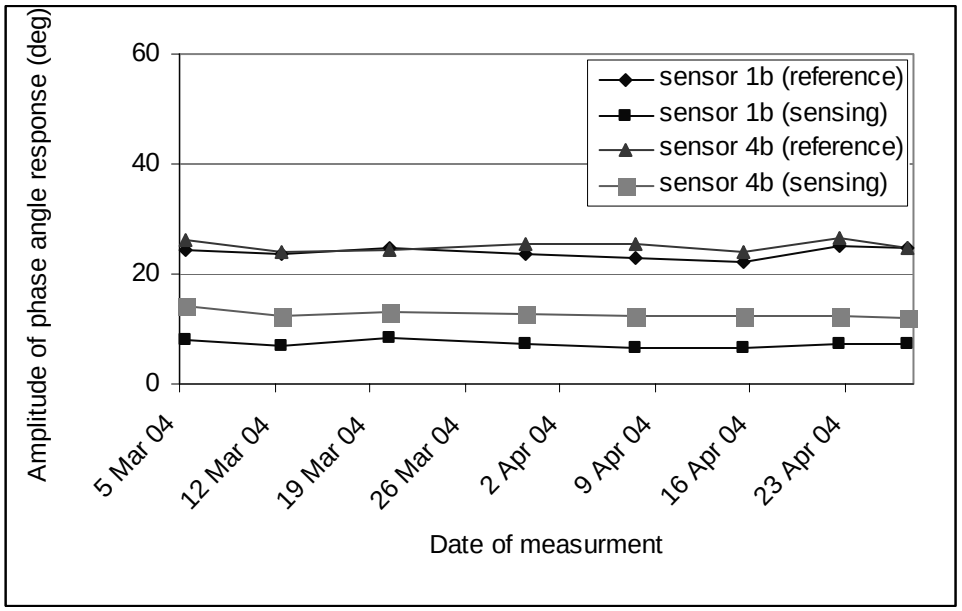

Figure 5-4. Time response of improved sensors

5.3.1.2 Effect of moisture and chlorides

Since the change in the signal could not be attributed to the condition of the wire, a new experiment was devised to test the effect of the surrounding environment.

Concrete in a dry state is a nonconductive medium, but once it becomes wet and is penetrated by chloride ions, its electrical conductivity increases. Due to this characteristic of concrete, it was believed that the current was flowing from the steel wire to the concrete and back to the steel wire. This behavior would mean that even when the wire was broken, the switch would still respond in its closed state.

This hypothesis was tested by interrogating a sensor in several different conditions. The sensor was first interrogating with the external switch intact and a typical initial frequency was observed (Figure 5-5(a)). The switch was then cut using wire cutters and again the sensor was interrogated and a frequency corresponding to a broken wire was observed (Figure 5-5(b)). These results were expected and proved that the sensor was working properly. The sensor was then placed in a cup of tap water and the response was recorded (Figure 5-5(c)). Results of this behavior show that the frequency had shifted slightly toward the initial value and the strength of the signal had decreased. This behavior resembles the behavior observed in the full-scale slabs. To test the hypothesis further, salt was added to the tap water and the sensor was interrogated again. Once the salt was added the sensors signal had shifted back to the initial value indicating that the wire was intact (Figure 5-5(d)). The distance between the sensor and the transmitter was kept constant through the test.

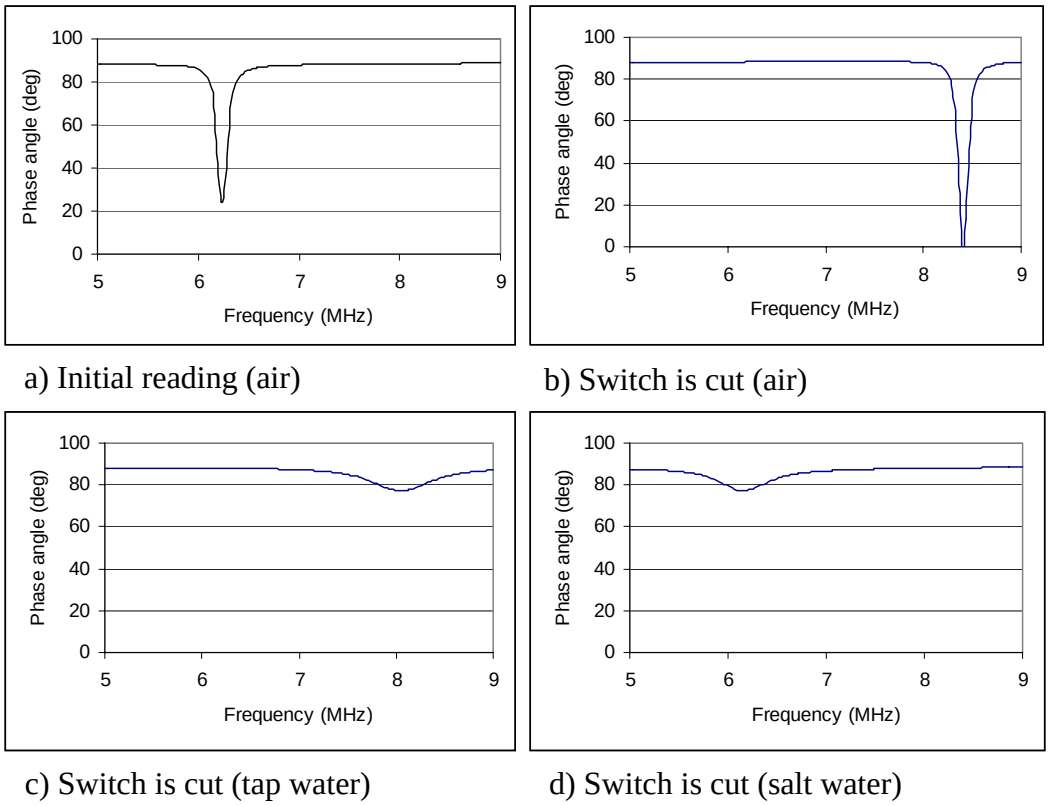

a) Initial reading (air)

b) Switch is cut (air)

c) Switch is cut (tap water)

d) Switch is cut (salt water)

Figure 5-5. Sensor response in different environments

These tests demonstrate that the sensors are affected by the environmental conditions in the surrounding concrete. The chloride ions and moisture present in the concrete complete the circuit between the two sides of a broken wire. The amplitude of the signal is not as strong as that with an intact wire because the resistance is higher when the current goes through the water. This experiment explains the behavior observed in the full-scale slabs. The signals that appeared to be in the transition zone were actually indicating that the wire had broken and that the current was being transmitted through the surrounding concrete. Presence of moisture and chloride ions does not affect a sensor that has an intact wire because the current will follow the path of least resistance which is along the wire.

5.3.2 Embedment depth

The embedment depth of the sensors has a significant influence on their performance. A typical concrete structure exposed to corrosive environments is required to have a concrete cover of at least 2.5 in. (ACI 318-02). Because the sensors are typically going to be monitoring the conditions in the concrete around the rebar, the signals from the sensors must be able to penetrate at least 2.5 in. through concrete. Embedment depths of approximately 3 in. are preferred. Also since different types of sensors are being developed it is beneficial to be able to evaluate the relative performance of the sensors.

Tests with different distances between the sensor and interrogation coil are discussed in this section. Some tests were conducted in air, while sensors were embedded in concrete for other tests.

5.3.2.1 Read depths in air

The tests were run using a Solartron 1260 Impedance/Gain Phase analyzer. The frequency sweep of the sensors was conducted from 4 MHz to 10 MHz using 200 frequency intervals. The size of the frequency step was selected to make the frequency steps small enough to capture the fundamental behavior of the sensors. Different read depths were achieved by stacking 0.25-in. plastic rings on top of each other. Plastic rings were used because plastic will not influence the signal. The signals of both the basic and improved sensors were analyzed at different distances from the interrogation coil and the amplitude of the dip in the phase angle was recorded. Initial response was measured with the sensors in contact with the interrogation coil (gap of 0 in.) and the gap was increased in 0.25-in. increments until the signal became too weak to distinguish.

5.3.2.1.1 Results

From Figure 5-6, it is concluded that the basic sensor can be interrogated a larger distance from the interrogation coil than the improved sensor. Both sensors had very strong signals when the sensors were placed directly on the interrogation coil. But once the first plastic ring was placed between the sensors and the reader, a large change in the amplitude was observed. This trend continued as the gap increased. The improved sensor could not be identified if the gap exceeded 1.5 in. The rapid reduction in signal strength is attributed to interference from the two coils.

The signal from the basic sensor was still identified at a gap of 2.75 in., which is nearly twice the range of the improved sensor. This range is considered to be satisfactory for the proposed application.

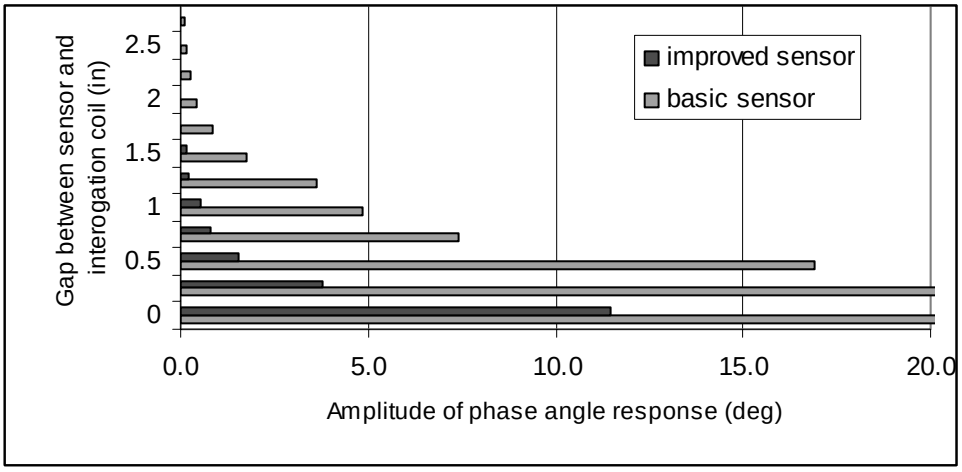

Figure 5-6. Variation of sensor response with distance to interrogation coil in air

At this stage in the sensor development, the transmission range is thought to be limited by the interrogating coil rather that the sensor. Other members of the project team are working to increase this important parameter.

5.3.2.2 Influence of moisture and chloride ions on transmission range

The transmission range is also affected by the medium that is placed between the transmitter and the sensor. Because these sensors will be embedded in concrete, it is important to understand how the concrete will influence the signal. Concrete becomes more conductive as the moisture content and chloride ion levels increase. In view of the fact that most reinforced concrete with corrosion problems has been infiltrated by moisture and chloride ions, the influence of the parameters must be investigated.

5.3.2.2.1 Experiment setup

To test the influence of moisture and chloride ions several sensors were cast in concrete discs with one inch of cover. The discs were exposed to three different environments: dry air, fresh water, and salt water. One of each type of sensor was subjected to each environment. The concrete used in these tests was made with very amounts of entrained air to facilitate penetration of the different solutions. The salt water and the fresh water discs were allowed to cure 7 days at room temperature and humidity. After 7 days the discs were interrogated using the Solartron 1260A Impedance/Gain Phase Analyzer. After the initial interrogation, the discs were placed in to either salt water or fresh water. The discs were subjected to these environments for 3 days and then the sensors were interrogated. After the interrogation, the discs were placed into their environments for additional 4 days and interrogated once again. The phase angle response during each interrogation was recorded. Also the weights of the discs were also recorded at each interrogation to ensure fresh and salt water penetration (Tables 5-1 and 5-2).

Table 5-1. Weights of discs exposed to fresh water

Days exposed to environment	Weight of cylinder (basic sensor) (g)	Weight of cylinder 2 (improved sensor) (g)
0	1031	1054
3	1082	2012
7	1089	2017

Table 5-2. Weights of discs exposed to salt water

Days in moisture	Weight of cylinder (basic sensor) (g)	Weight of cylinder 2 (improved sensor) (g)
0	1033	1048
3	1084	2009
7	1087	2014

5.3.2.2.2 Results

From the chloride and moisture penetration tests it was concluded that neither influenced the signal dramatically. The variations in the readings are illustrated in Figures 5-7 through 5-10. The signal strength in each environment produced a dip in the phase angle that is comparable to the dip seen in air. The only factor found to be a factor in the read depth was the distance between the sensor and the interrogator.

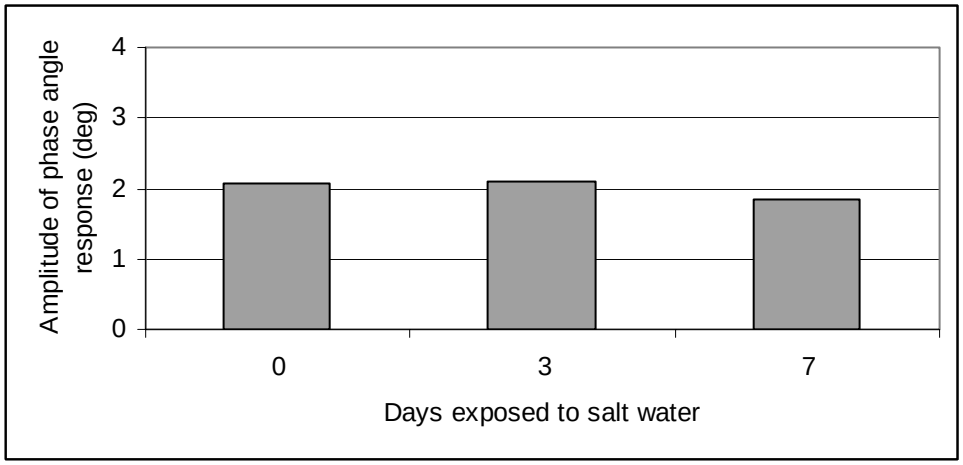

Figure 5-7. Basic sensor: variation in phase angle response after salt water exposure

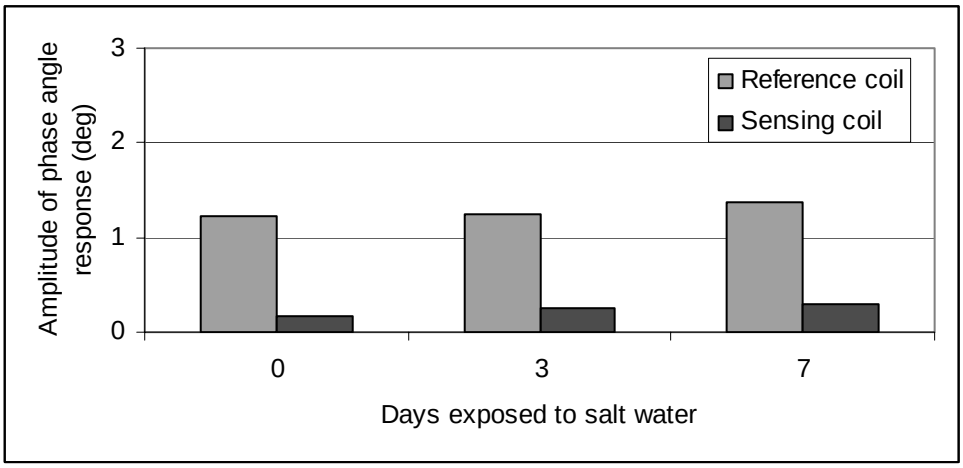

Figure 5-8. Improved sensor: variation in phase angle response after salt water exposure

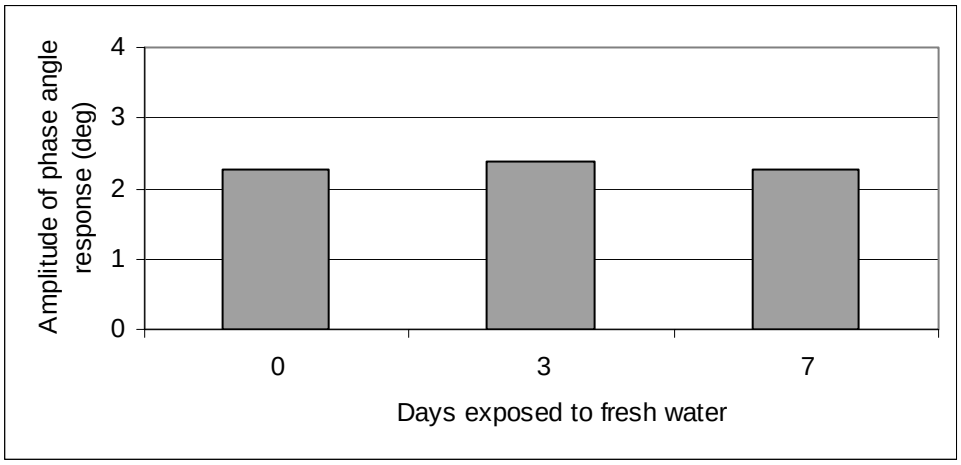

Figure 5-9. Basic sensor: variation in phase angle response after fresh water exposure

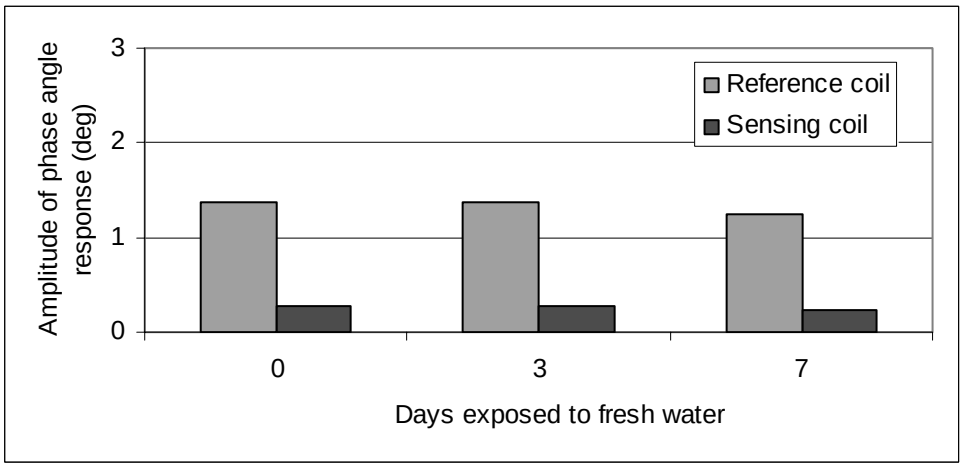

Figure 5-10. Improved sensor: variation in phase angle response after fresh water exposure

5.4 SUMMARY

During the full-scale slab tests some unexpected sensor responses were encountered. These responses were concluded to be caused by moisture and chloride ions in the concrete. The moisture and the chloride ions increase the

concretes conductivity which causes the sensor to malfunction. However these factors were found not to affect the amplitude of the phase angle response. But, it is not known how many chloride ions had penetrated into the concrete discs. Due to this uncertainty, monitoring of the concrete discs should be continued.

CHAPTER 6
Conclusion

6.1 SUMMARY

Corrosion of reinforcement in concrete structures is a serious problem worldwide and usually leads to expensive repairs. The cost of many of these repairs could be reduced if there was a reliable way to detect corrosion before it can cause damage. By developing a corrosion sensor that is inexpensive, easy to use and reliable, some of these structures could be repaired before major damage occurs.

The wireless sensors discussed and tested in this thesis have the pre-mentioned qualities. The objective of this thesis was to test the performances of the two wireless corrosion sensors. The two prototype sensors were investigated using several different experiments. These experiments investigated several different characteristics of the sensors: (a) ease of application, (b) durability in representative applications and (c) performance of the sensors in representative applications.

The basic design concepts were discussed in Chapter 2. Also in this chapter the general characteristics of the sensors were discussed. Chapter 3 continued the accelerated corrosion tests that were first conducted by Grizzle (2003). These tests proved that steel wires can be used as the state switch.

The installation, durability, and reliability of the sensors were discussed in Chapter 4. During the full-scale slab tests, it was found that the sensors are very easy to apply and that they can survive the casting process. However, the

reliability of the sensors came into question. During the interrogation of the slabs many unexpected behaviors were encountered. The sensors did not behave as they were originally designed. During the tests, it was discovered that the sensors experience a transition zone that makes the sensors unreadable. The reason for this behavior was discussed in Chapter 5. Overall the full-scale slab tests were a success and some of the sensors did detect corrosion reliably.

During the course of the sensor development and the full-scale slab tests some flaws in the sensors performance were discovered. Chapter 5 discussed and tested these flaws. Some of the flaws included internal corrosion and the behavior of the sensors in the transition zone. The internal corrosion was eliminated by the selection of a suitable potting compound. This chapter also tested the performance of the sensors in different environments as well as different embedment depths.

6.2 FUTURE RECOMMENDATIONS

The experiments conducted in this thesis indicate that the sensors can be used in real applications. However before installation of the sensors can be conducted some of the flaws that were discovered during this project must be corrected. To continue the development of the sensor, the following recommendations are proposed:

- Investigate different combinations of capacitors and inductors to eliminate the effects of the chlorides and moisture present in the concrete. The sensors respond in the transition zone when the resistance of the external switch exceeds a certain limit. This limit is governed by the equation:

By manipulating the inductance (L) and the capacitance (C) the resiatnce (R) can be changed. If the R is lower than that of salt water the transition zone can be eliminated.

- Cast more large-scale slabs and embed more sensors in them. Instead of only using 26 gage wire switches embed sensors that utilize the 21 and 24 gage wire switches. These tests could provide data about the amount of corrosion that a certain gage wire can detect.
- Test the new large-scale slabs for corrosion using half cell measurements, chloride penetration, and polarization resistance. These tests can be used to calibrate the data from the prototype sensor.
- Refine the sensor to be smaller in diameter. Also try to make sensor cigar shaped to capture any possible cracks that might form in the concrete.
- Investigate the feasibility of a sensor that relies on the decrease in the magnetic field to detect corrosion. The electronics of this sensor could be completely sealed from the environment eliminating the chance of internal corrosion.

APPENDIX A
Full Scale Slab Test Results

A.1 INTERROGATION OF THE SLABS

The slabs were interrogated about once a month until they were visually inspected. The phase angle of the sensors was recorded at each interrogation. The results of the interrogations are shown here. All slabs were cast on 24 July 03.

A.1.1 Slab 2 results

Five of eight sensors responded with an unexpected response. One sensor was still in its initial state while two sensors responded in their corroded state. The signals of the five sensors were very faint but here was some evidence that there was a dip in the signal around 8.5 MHz. The slab was autopsied on October 16, 2004.

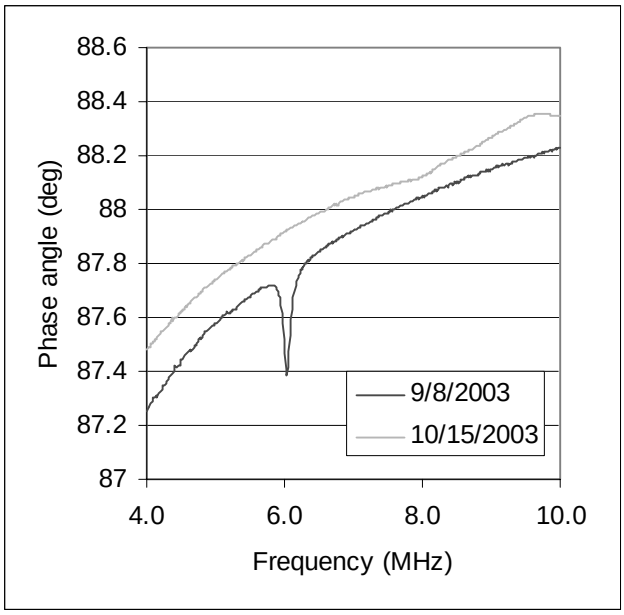

Figure A-1 Sensor 2 response

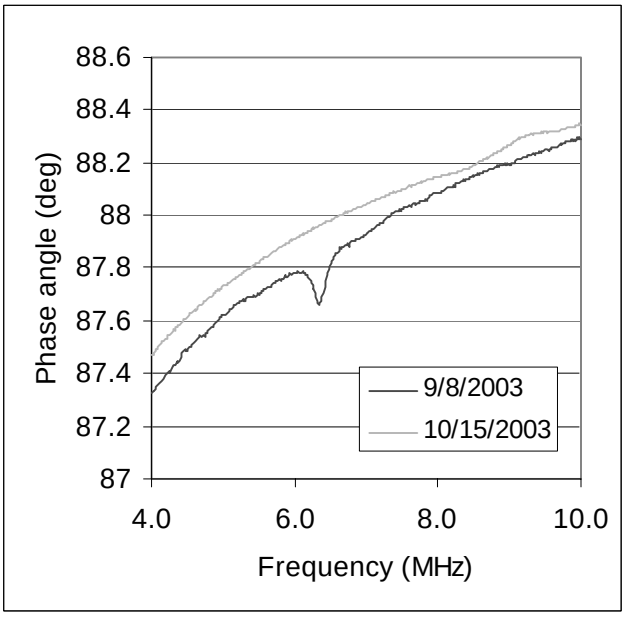

Figure A-2. Sensor 3 response

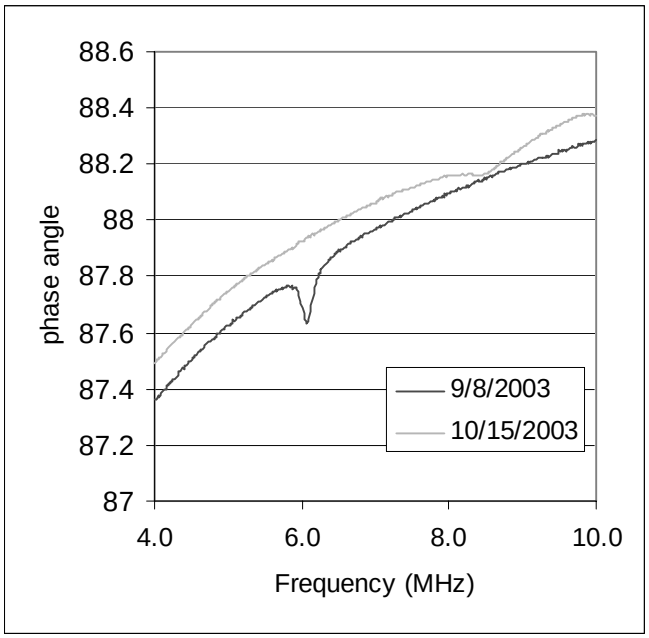

Figure A-3. Sensor 14 response

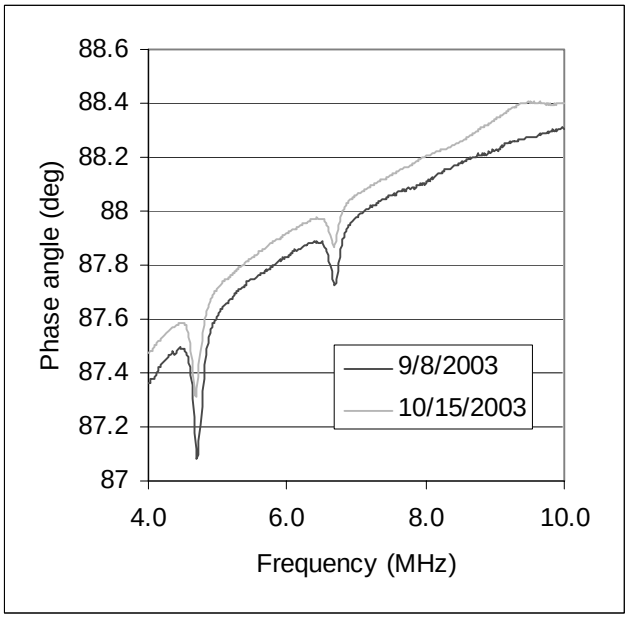

Figure A-4. Sensor 20 response

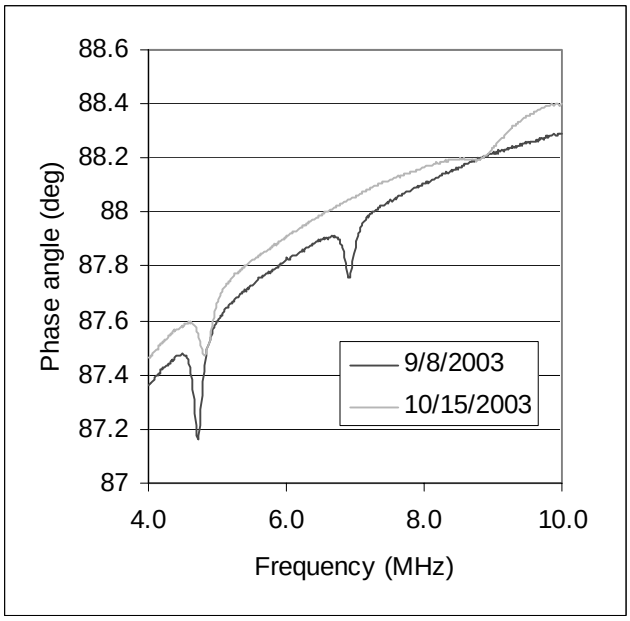

Figure A-5. Sensor 21 response

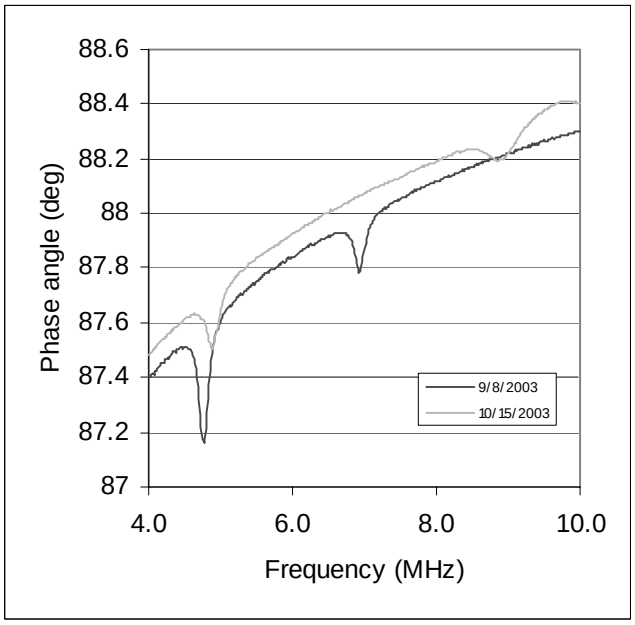

Figure A-6. Sensor 23 response

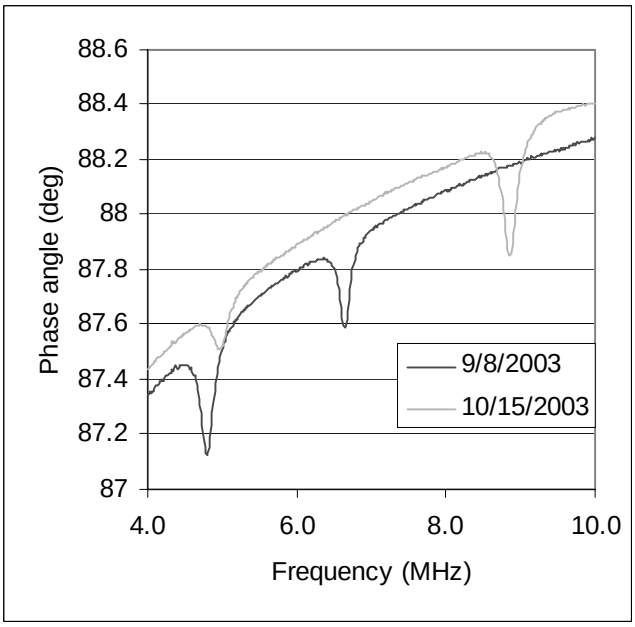

Figure A-7. Sensor 24 response

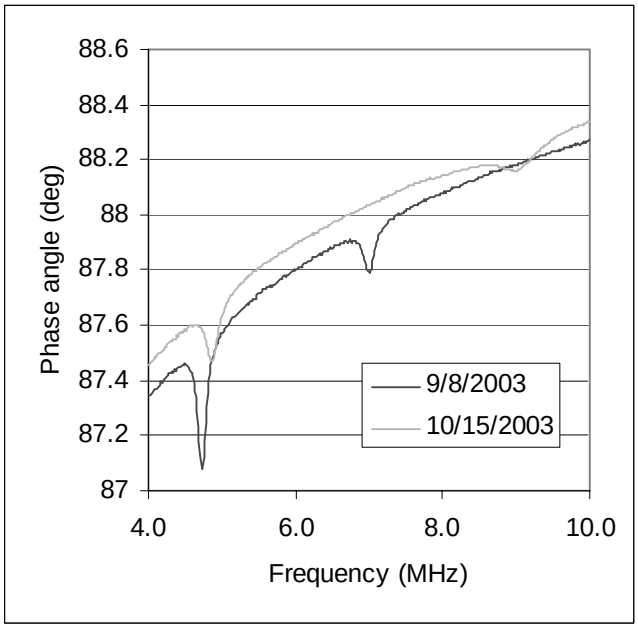

Figure A-8. Sensor 25 response

A.1.2 Slab 3 results

Four of eight sensors were in the transition zone, two sensors had been broken during construction, one sensor was still in its initial state and one was indicated corrosion. An autopsy was performed on this slab on January 19, 2004.

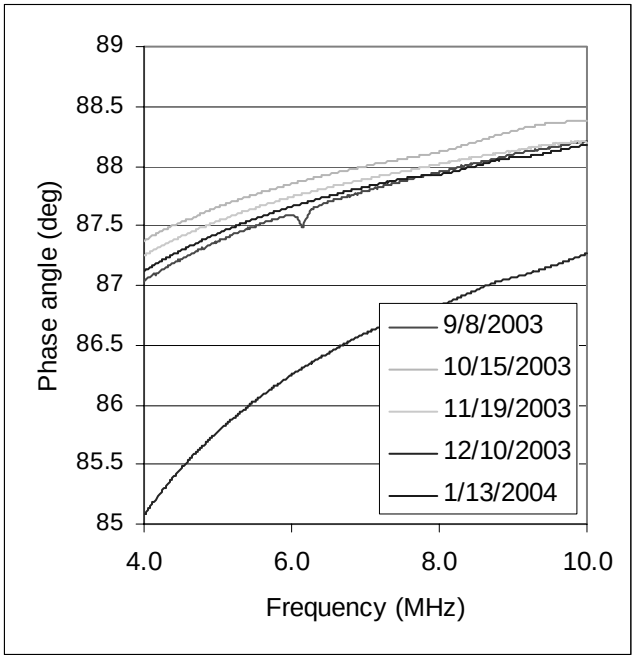

Figure A-9. Sensor 7 response

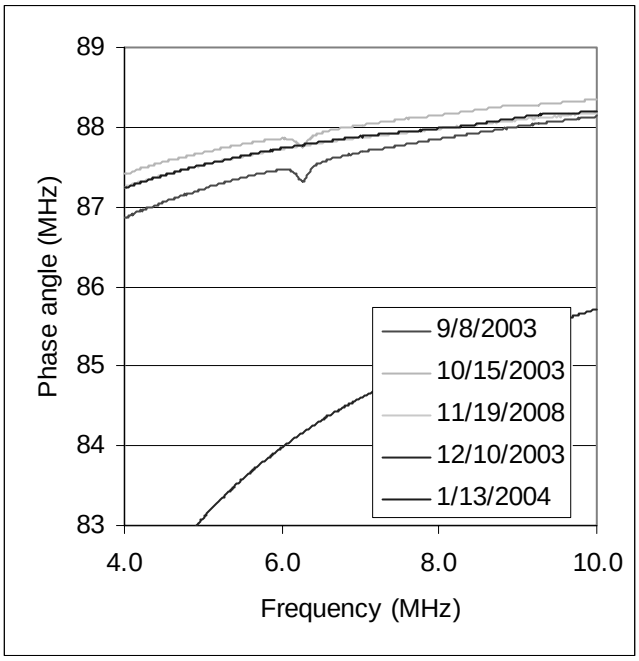

Figure A-10. Sensor 8 response

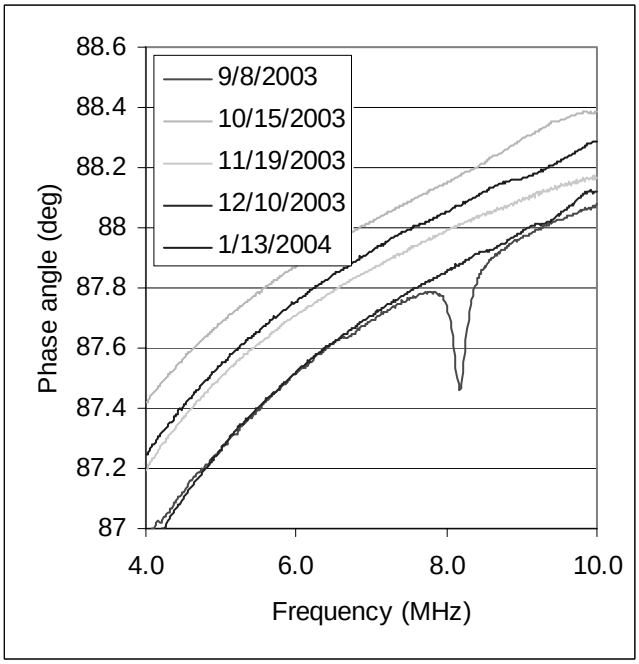

Figure A-11. Sensor 9 response

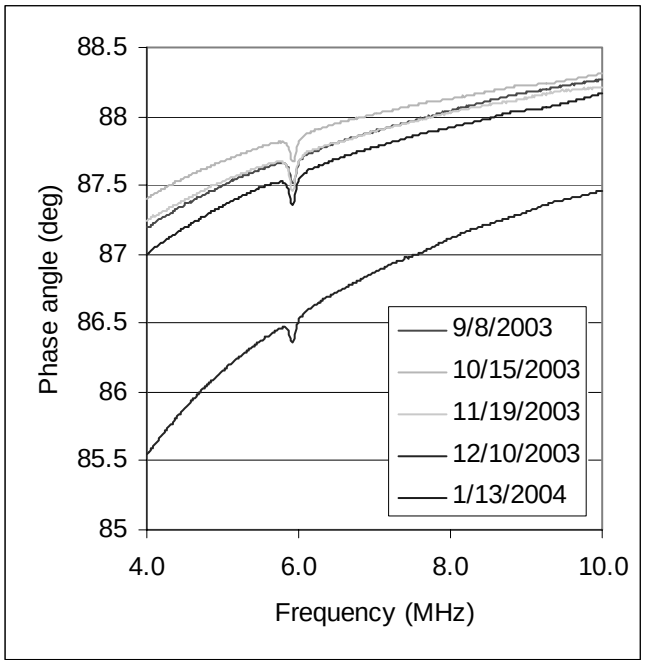

Figure A-12. Sensor 11 response

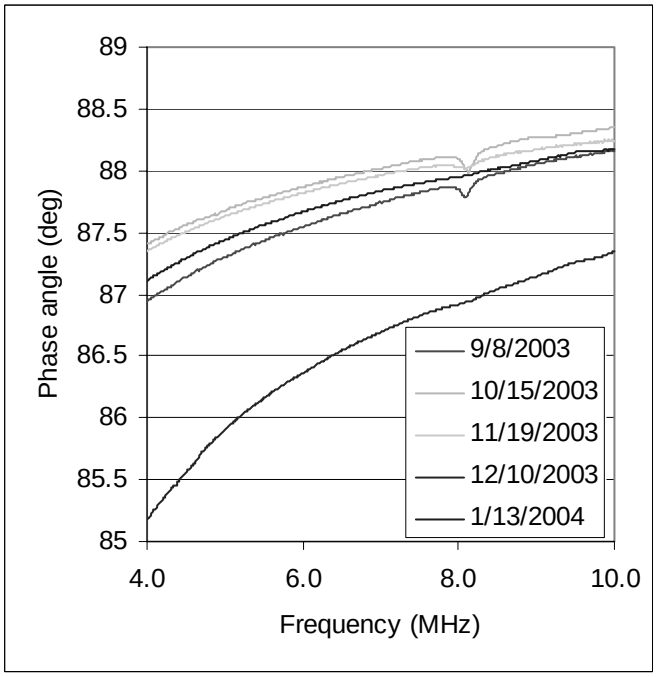

Figure A-13. Sensor 16 response

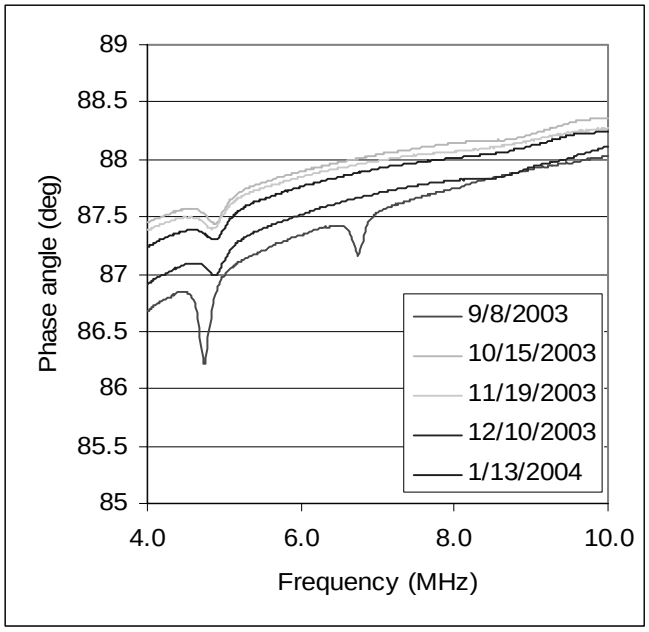

Figure A-14. Sensor 28 response

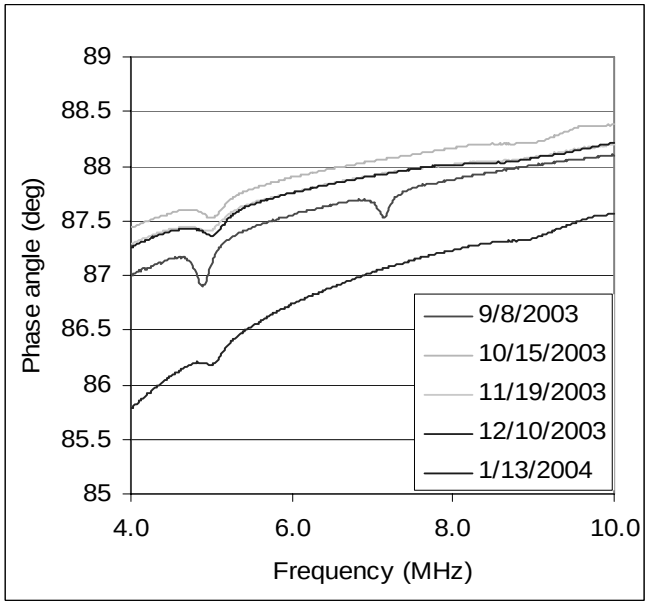

Figure A-15. Sensor 29 response

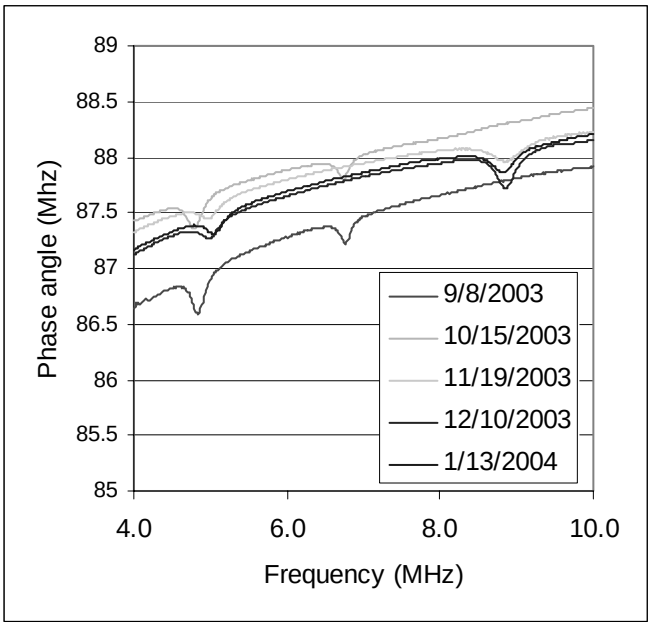

Figure A-16. Sensor 31 response

A.1.3 Slab 4 results

Three of eight sensors were in the transition zone, one was in the initial state and four sensors were in the final state indicating corrosion. An autopsy was performed on this slab on April 02, 2004.

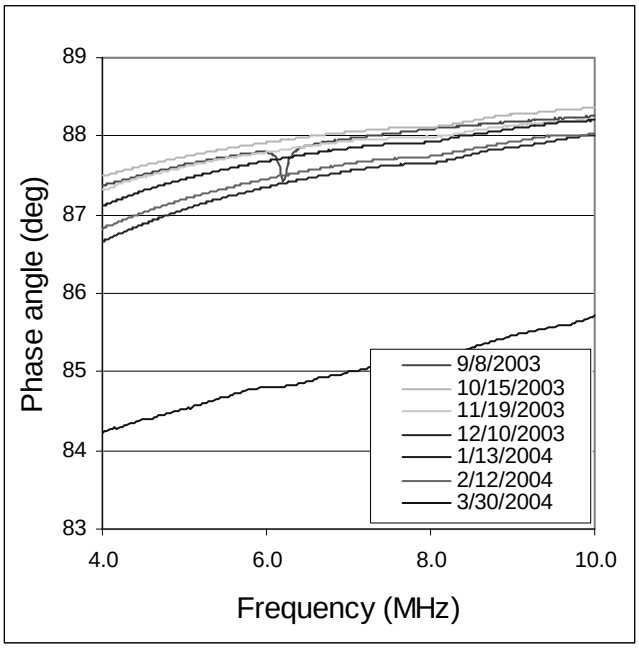

Figure A-17. Sensor 1 response

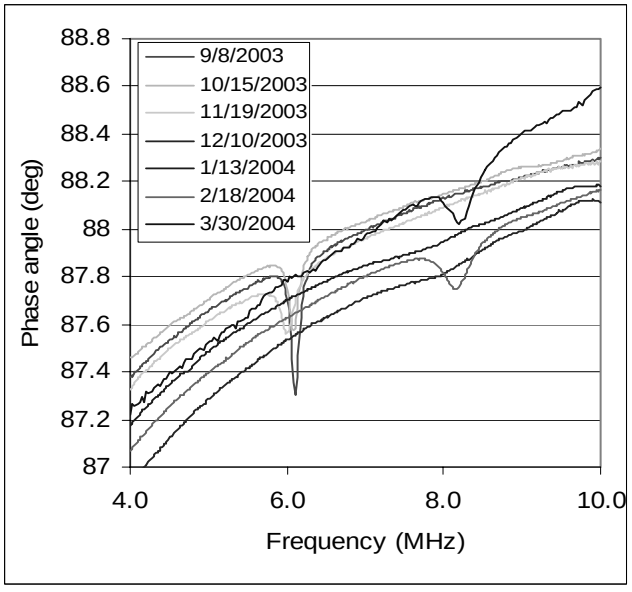

Figure A-18. Sensor 5 response

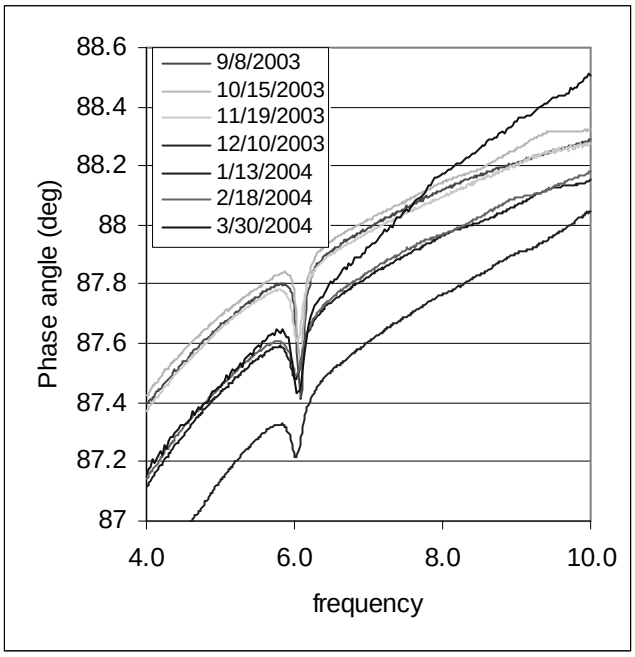

Figure A-19. Sensor 6 response

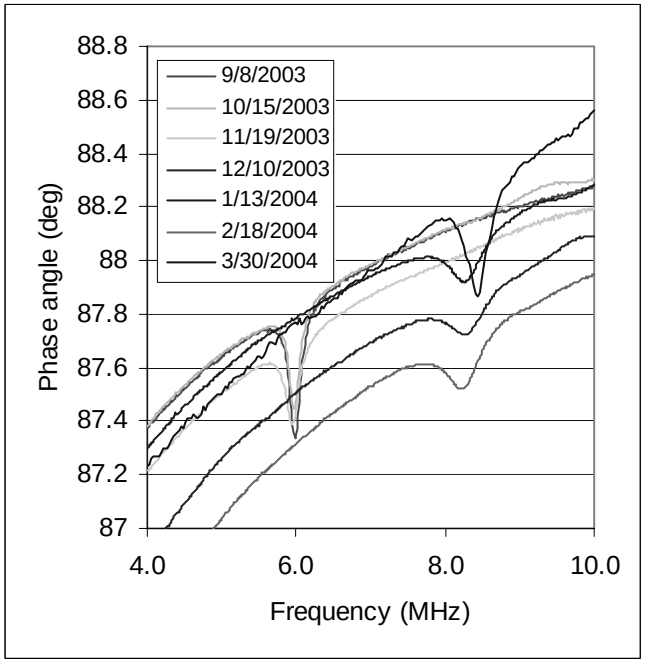

Figure A-20. Sensor 10 response

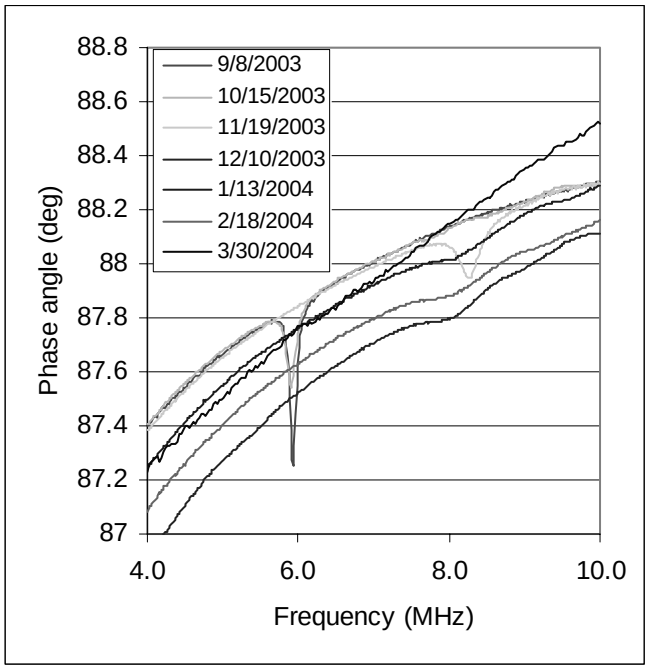

Figure A-21. Sensor 12 response

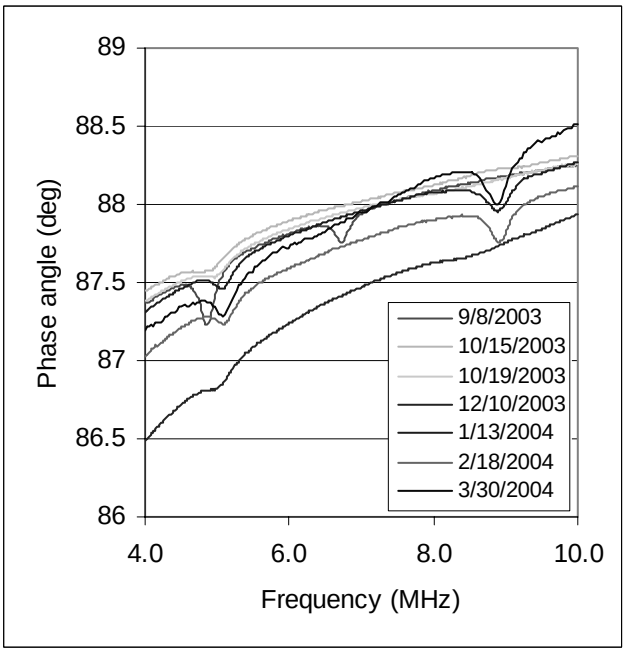

Figure A-22. Sensor 19 response

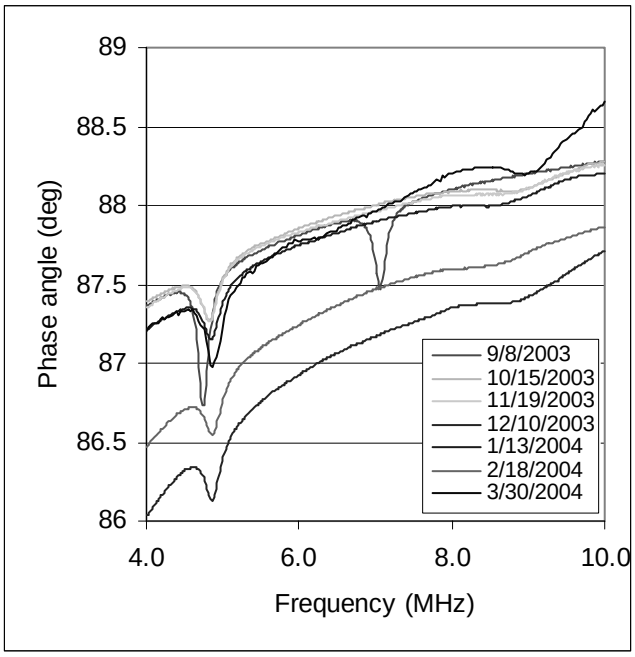

Figure A-23. Sensor 22 response

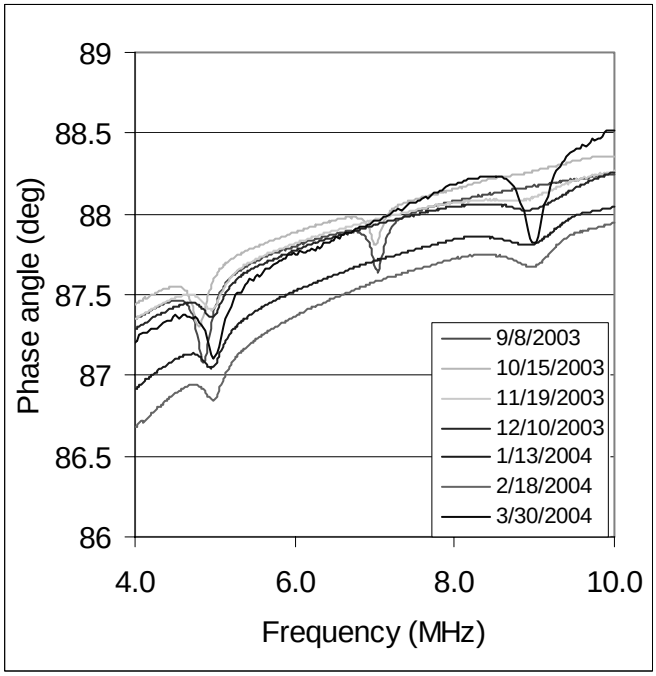

Figure A-24. Sensor 32 response

A.1.4 Slab 1 results

six of eight sensors were in the transition zone, one sensor was in the initial stat and one was in the final state indicating corrosion. An autopsy was performed on this slab on April 02, 2004.

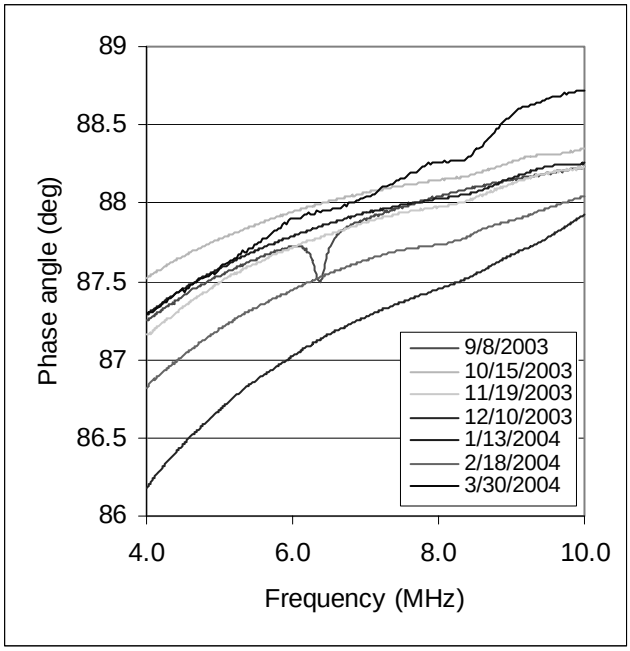

Figure A-25. Sensor 4 response

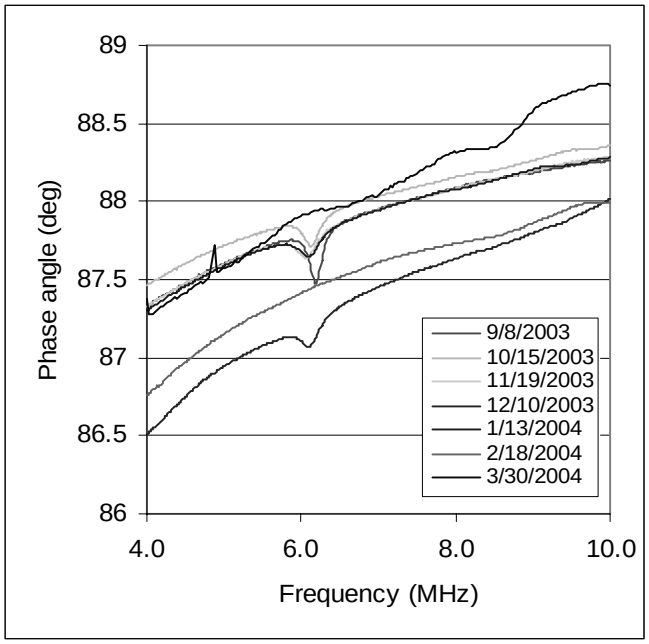

Figure A-26. Sensor 13 response

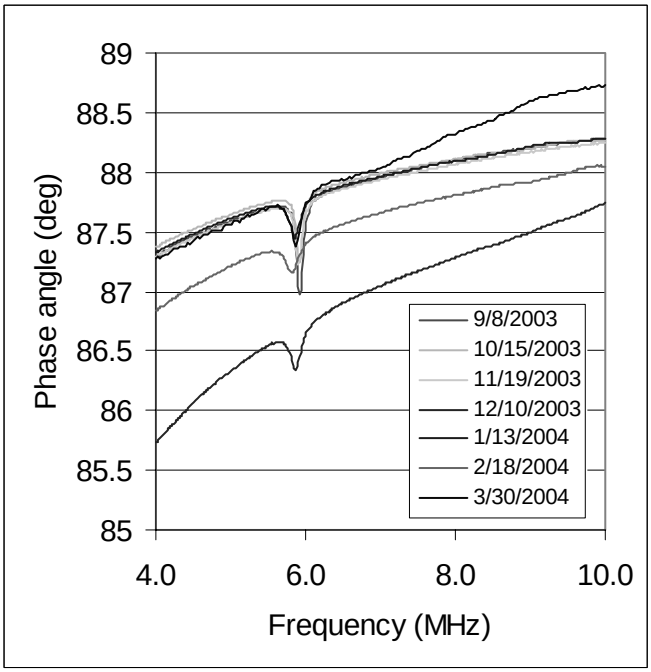

Figure A-27. Sensor 15 response

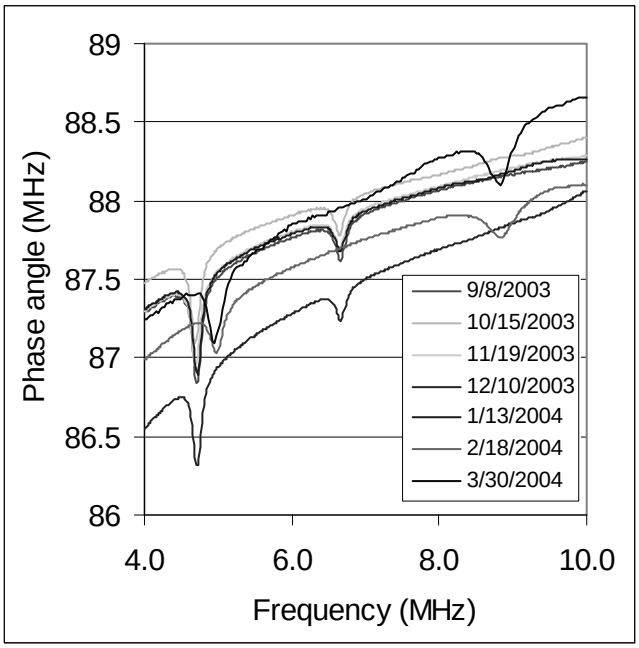

Figure A-28. Sensor 17 response

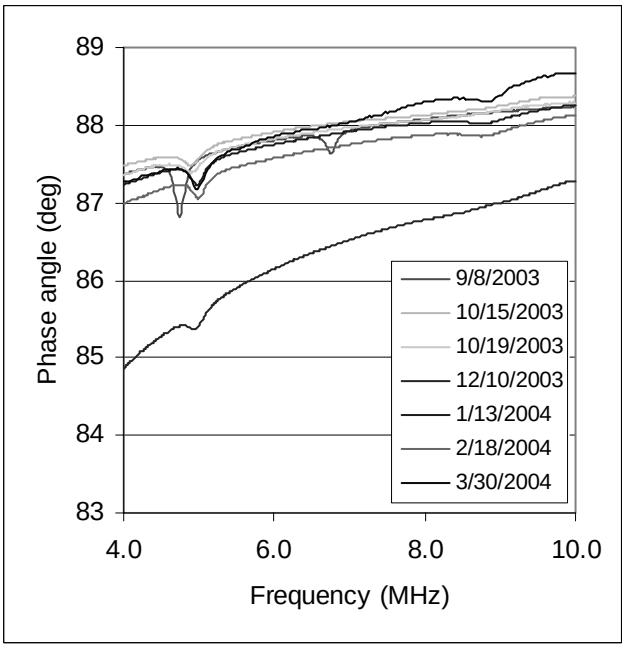

Figure A-29. Sensor 18 response

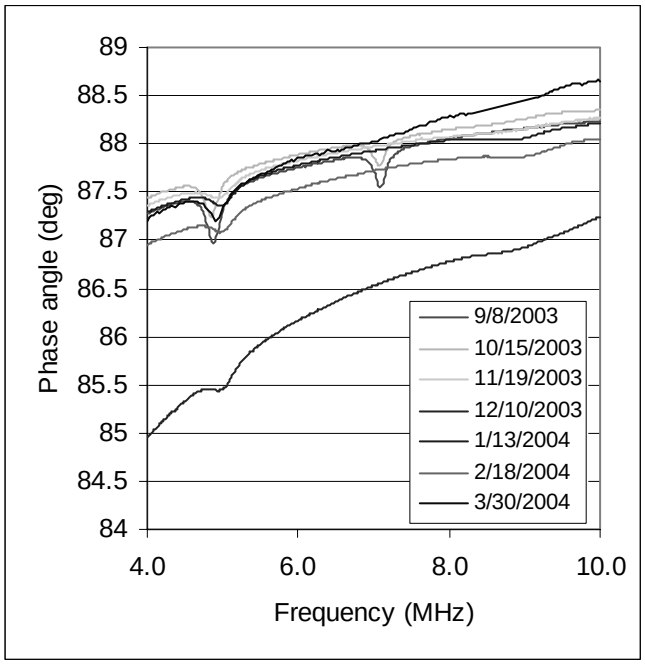

Figure A-30. Sensor 26 response

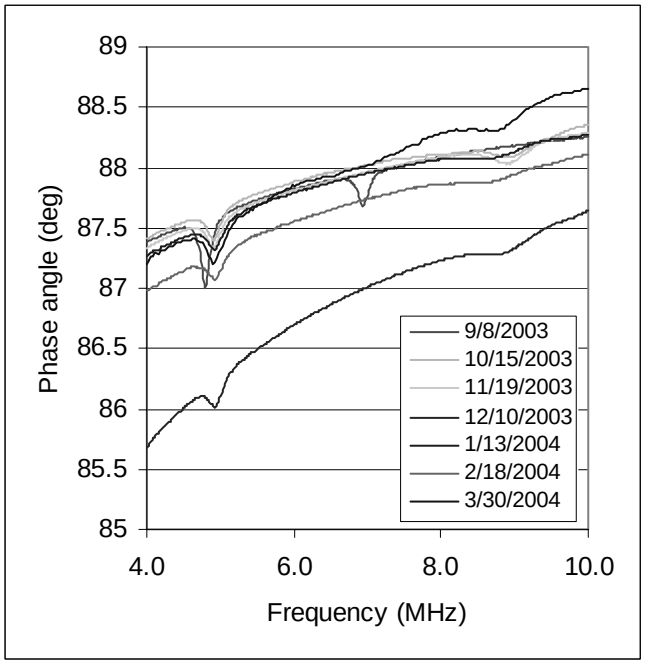

Figure A-31. Sensor 27 response

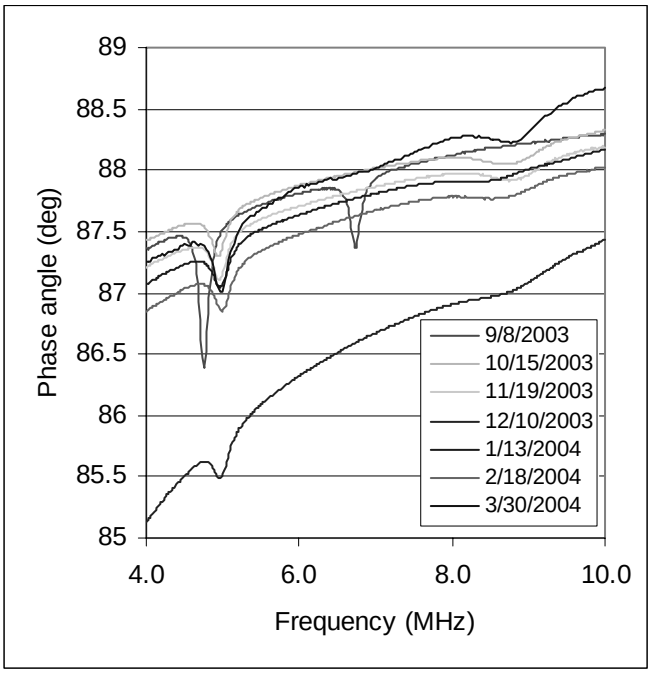

Figure A-32. Sensor 30 response

APPENDIX B
Results from Chloride Penetration Tests

B.1 CHLORIDE PENETRTATION

Chloride samples were taken from slab number 1 after it had been autopsied. The samples were taken at three different locations: (1) at the surface, (2) at the level of the reinforcement few inches away from a crack and (3) at the level of reinforcement at a crack. The chloride measurements were conducted using a James chloride field test unit following the ASTM 1050 standard. The chloride content of the specimens is derived by using a reference plot which relates mV readings to chloride concentration. The plot is created by measuring the mV reading of solutions with know concentrations and plotting a best fit curve for those points. The mV readings for each location are shown in Table B-1 and the corresponding plots are illustrated in figures B-1 through B-3.

Table B-1. Chloride concentration

Location of sample	**mV**	**Chloride concentration (%)**
At the surface	19.3	.11
At the level of reinforcement (away from a crack)	20.7	.10
At the level of reinforcement (at a crack)	17.4	.13

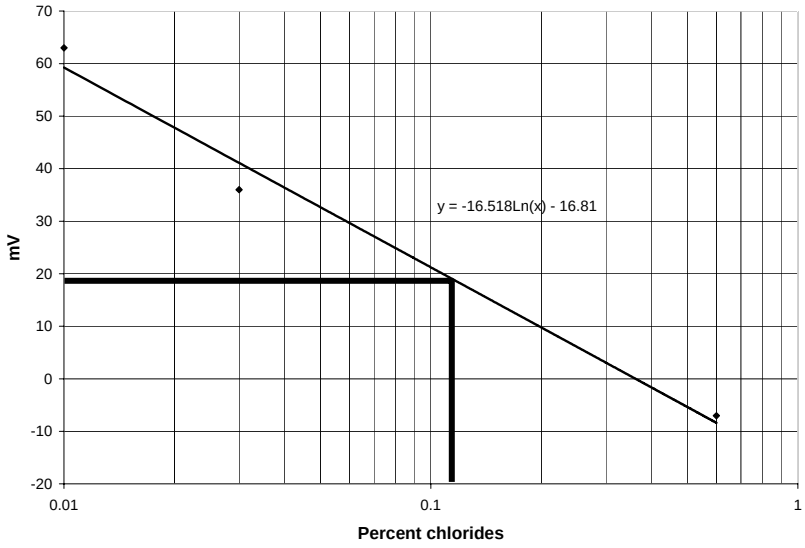

Figure B-1. Chloride concentration at the surface

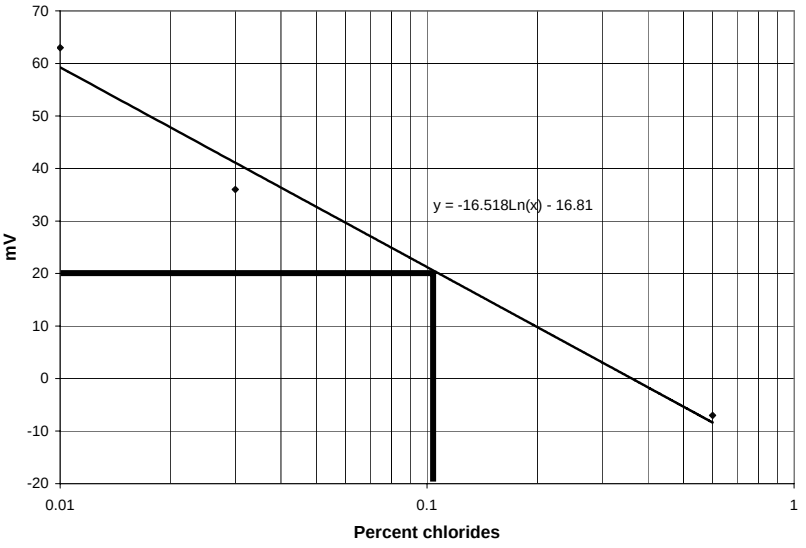

Figure B-2. Chloride concentration at level of reinforcement (away from crack)

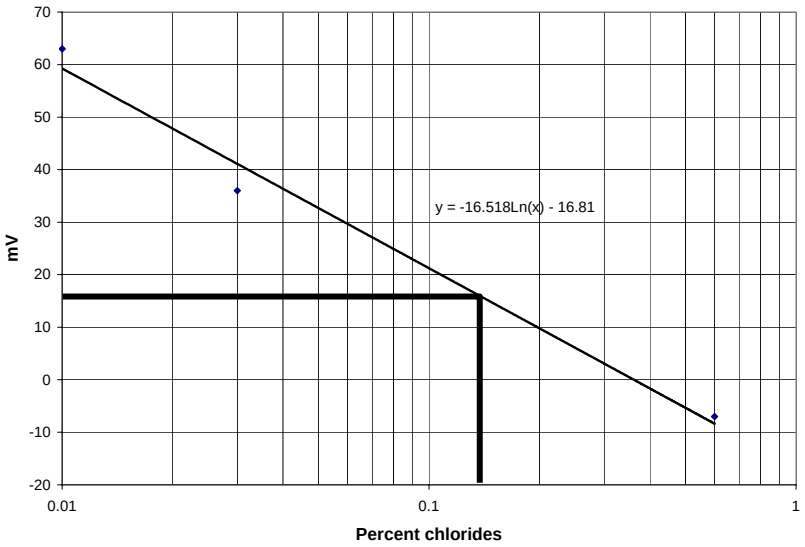

Figure B-3. Chloride concentration at level of reinforcement (at a crack)

APPENDIX C

Effect of Corrosion on Sensor Response

C.1 RESULTS OF DAILY SENSOR INTEROGATIONS

Two basic sensors and two improved basic sensors were subjected to daily measurements. The objective of these interrogations was to investigate the influence of corrosion of the external switch on the measured phase angle response of the sensors. In the beginning, the sensors were interrogated daily, but as it became evident that the response was not changing, the interrogations became less frequent. Also at the time of writing, none of the external switches had corroded enough to break.

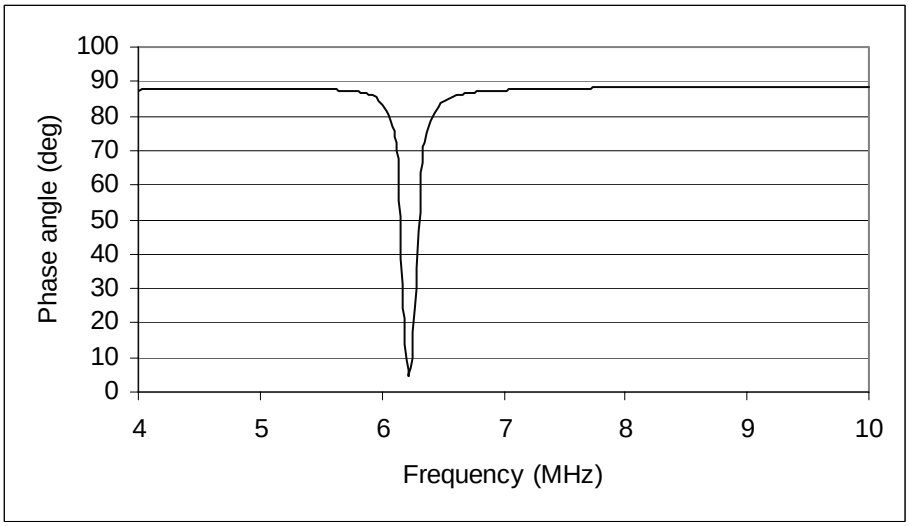

Figure C-1. 05 March 04: Basic sensor 1a

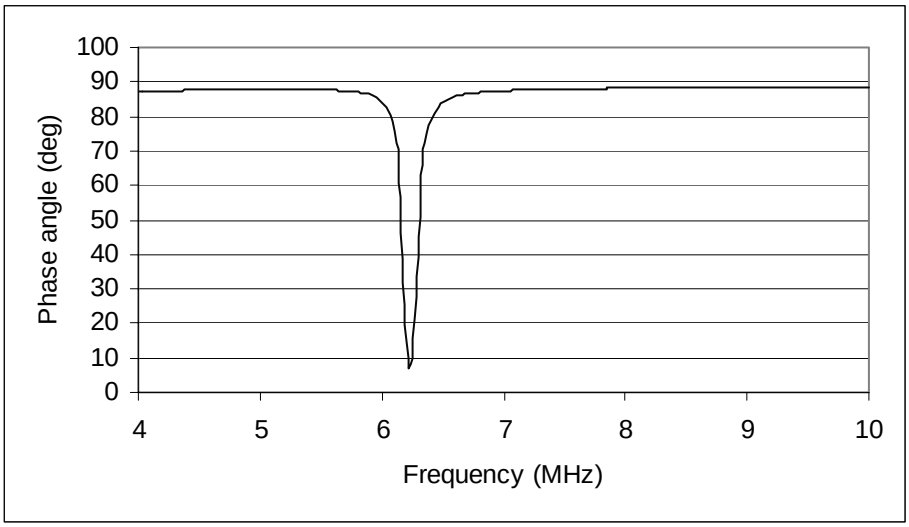

Figure C-2. 08 March 04: Basic sensor 1a

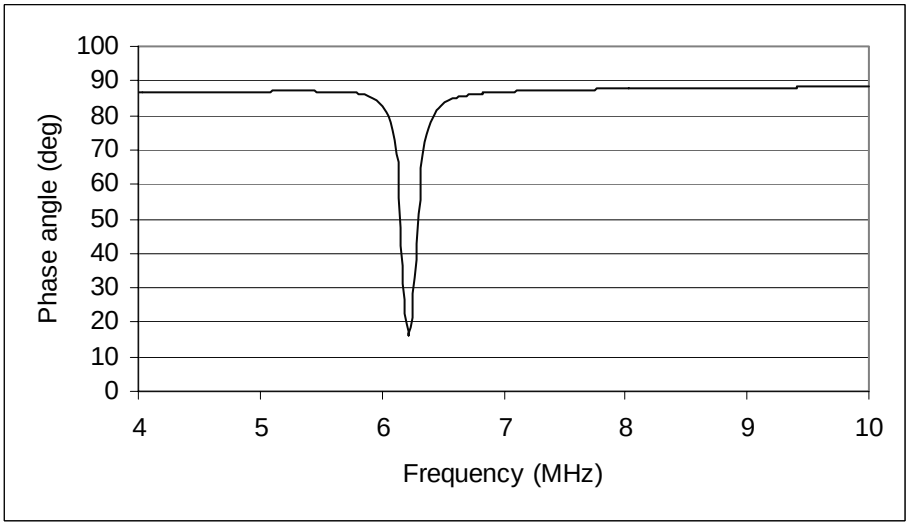

Figure C-3. 09 March 04: Basic sensor 1a

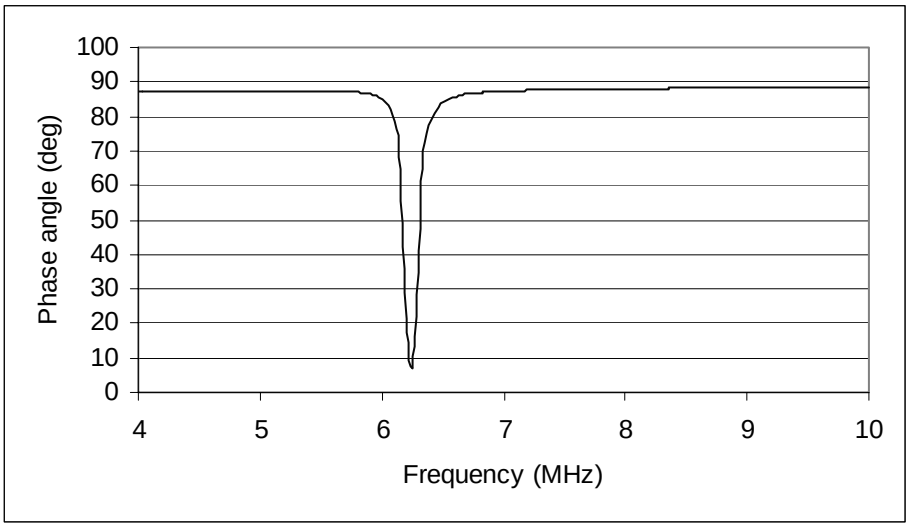

Figure C-4. 11 March 04: Basic sensor 1a

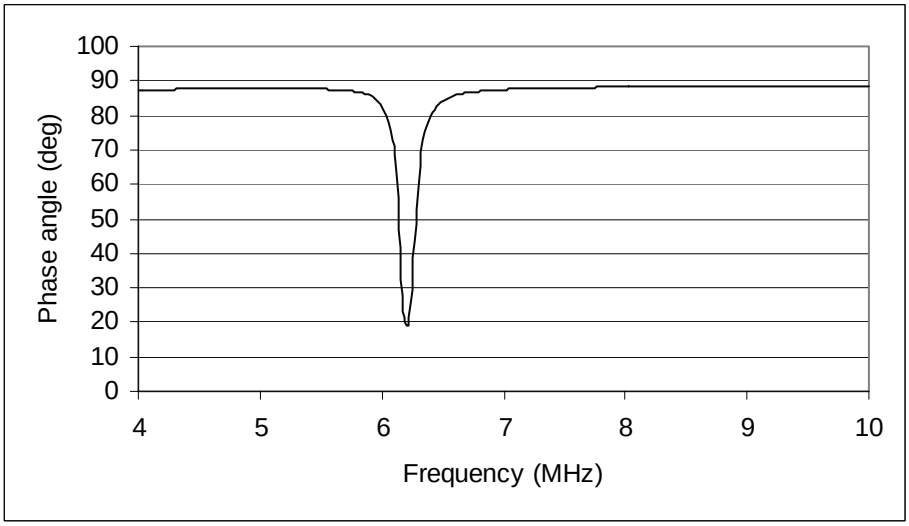

Figure C-5. 12 March 04: Basic sensor 1a

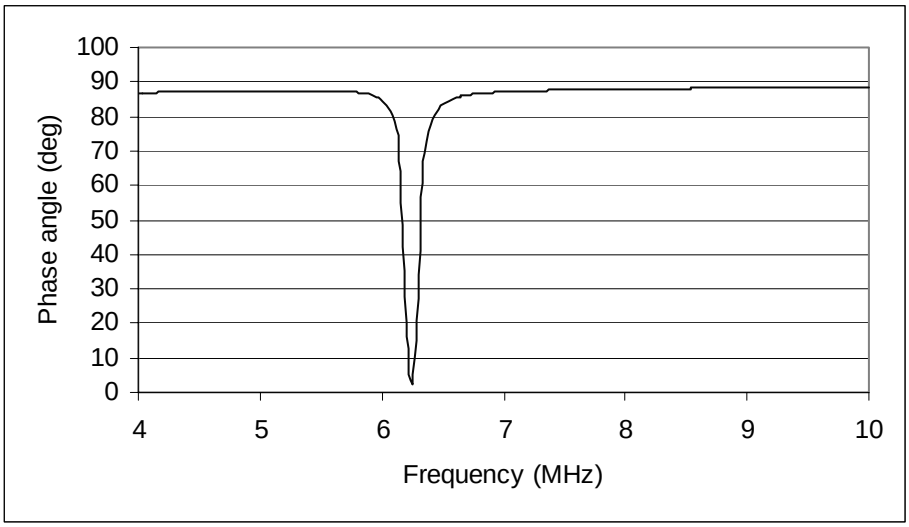

Figure C-6. 22 March 04: Basic sensor 1a

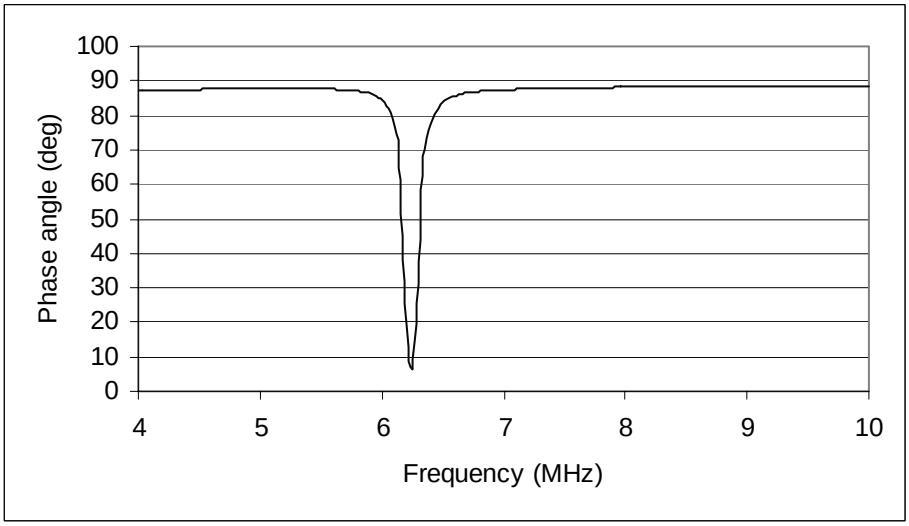

Figure C-7. 23 March 04: Basic sensor 1a

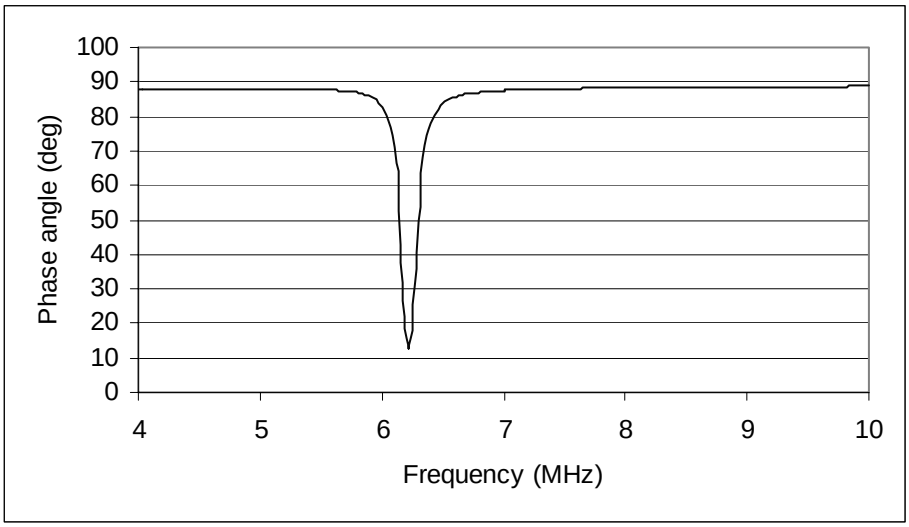

Figure C-8. 24 March 04: Basic sensor 1a

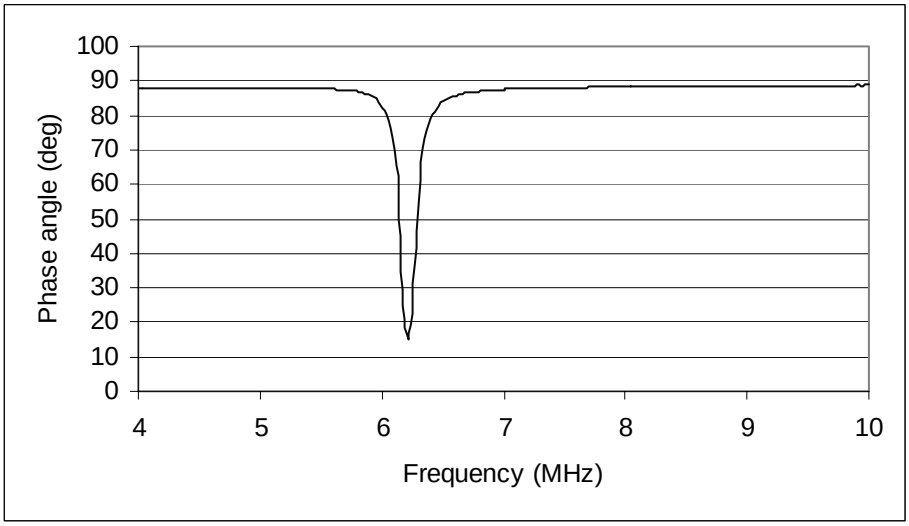

Figure C-9. 25 March 04: Basic sensor 1a

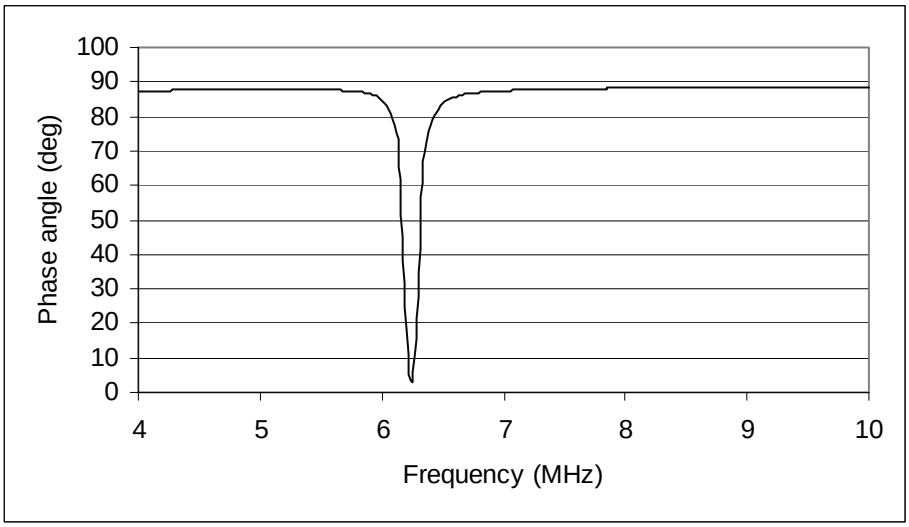

Figure C-10. 26 March 04: Basic sensor 1a

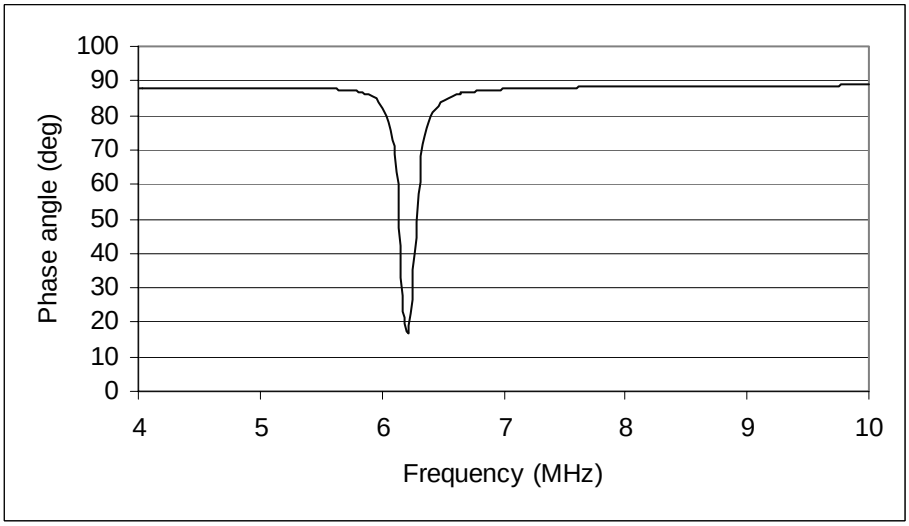

Figure C-11. 30 March 04: Basic sensor 1a

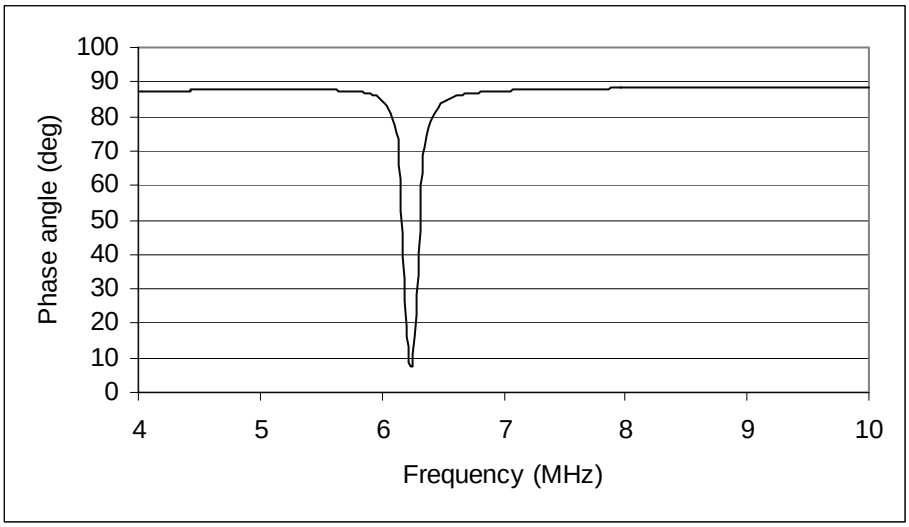

Figure C-12. 01 April 04: Basic sensor 1a

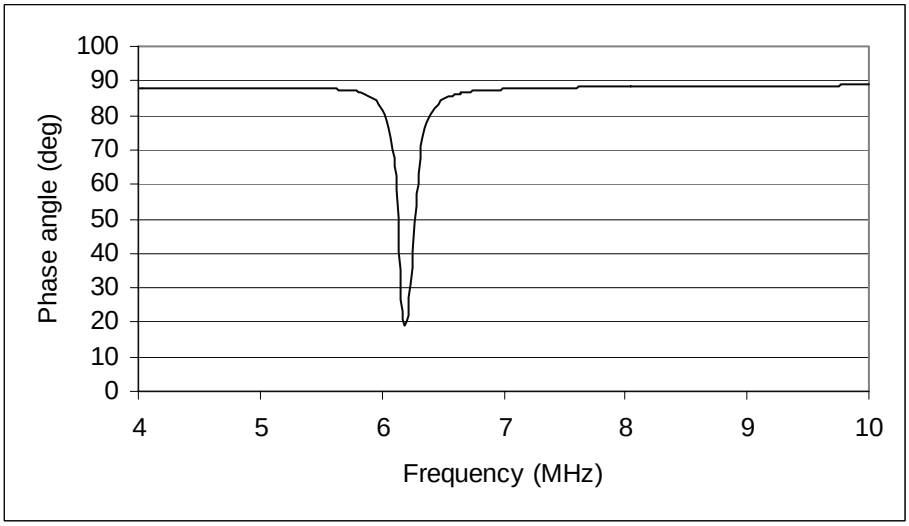

Figure C-13. 06 April 04: Basic sensor 1a

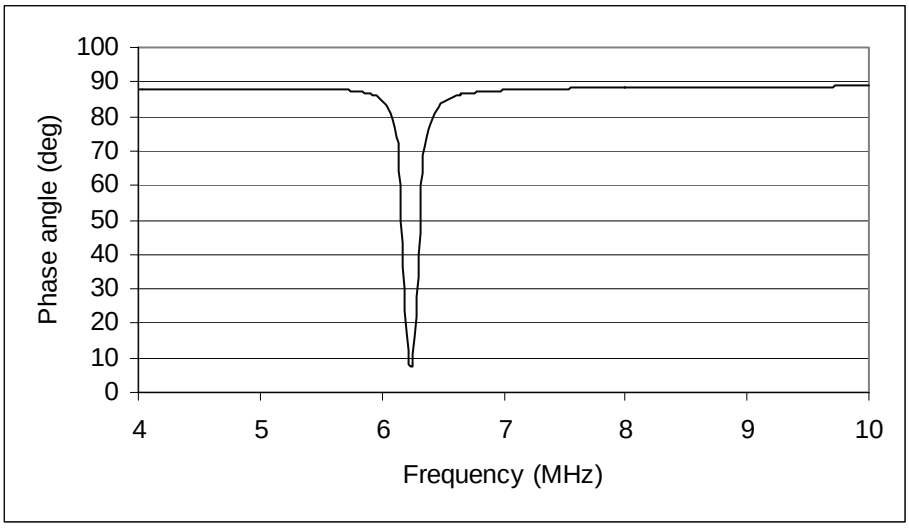

Figure C-14. 07 April 04: Basic sensor 1a

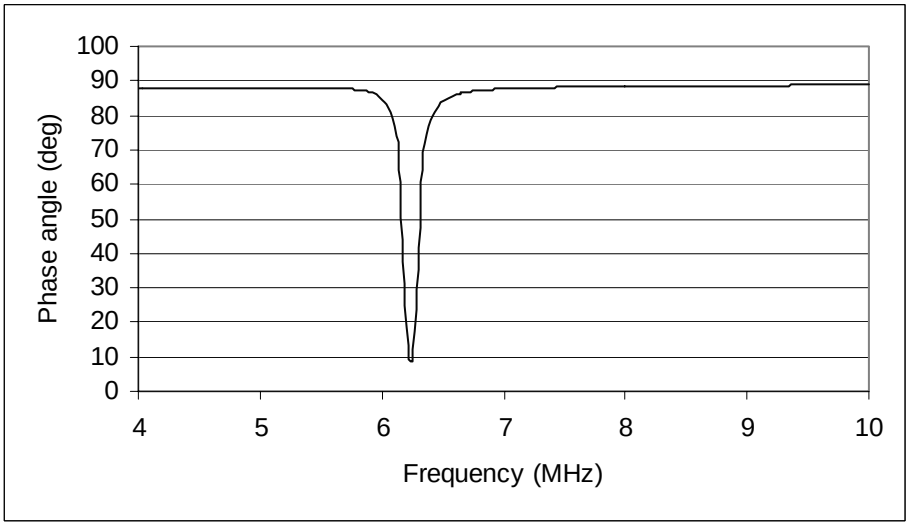

Figure C-15. 15 April 04: Basic sensor 1a

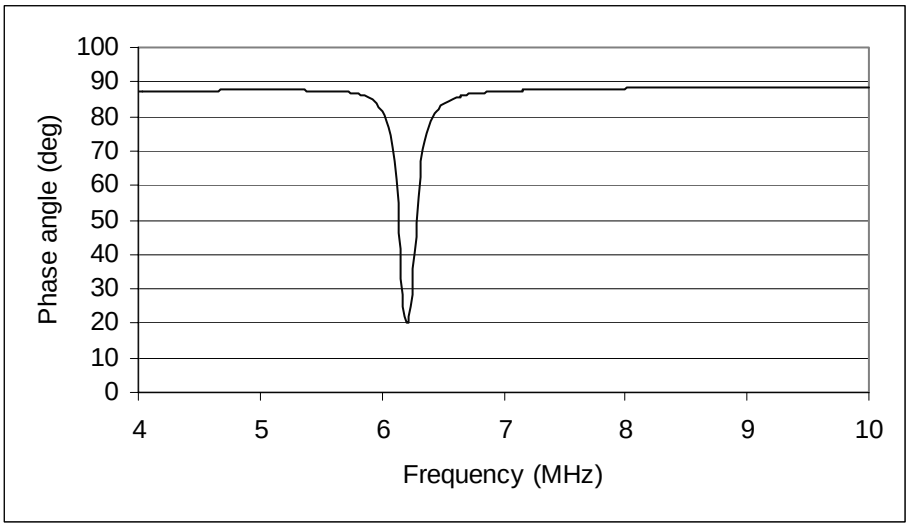

Figure C-16. 20 April 04: Basic sensor 1a

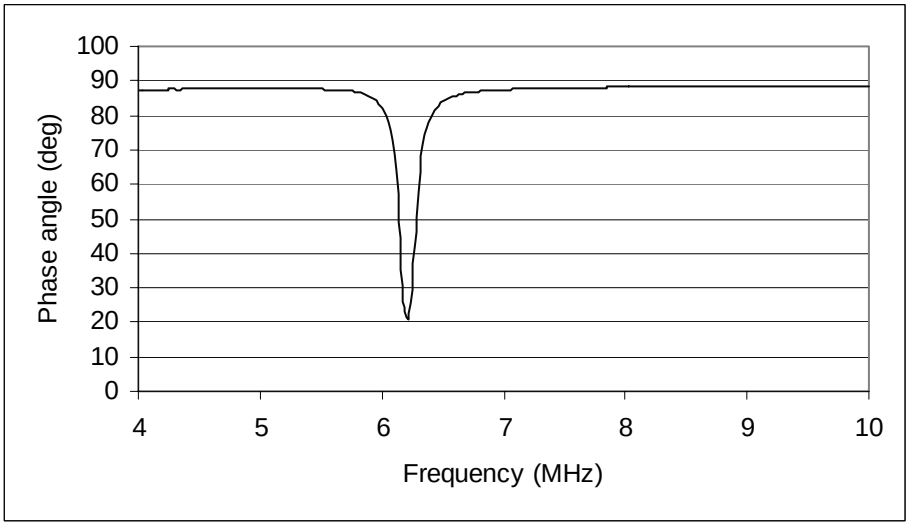

Figure C-17. 22 April 04: Basic sensor 1a

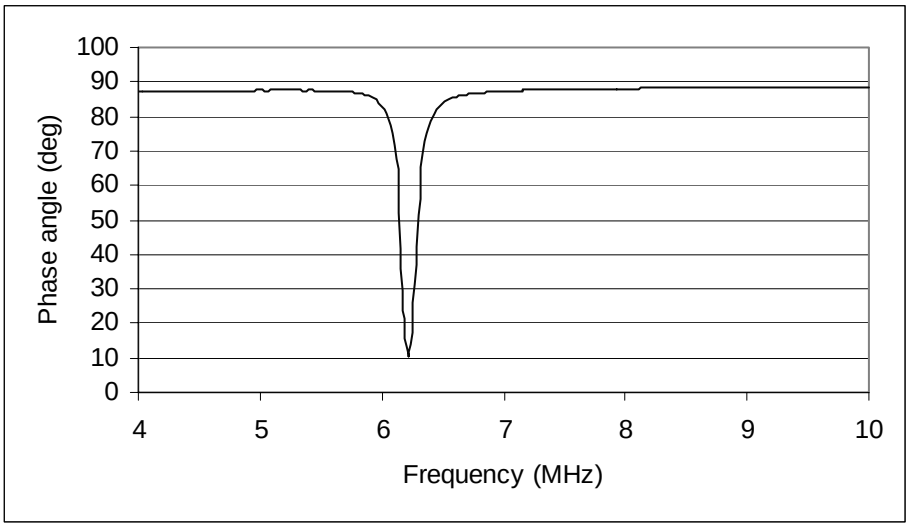

Figure C-18. 27 April 04: Basic sensor 1a

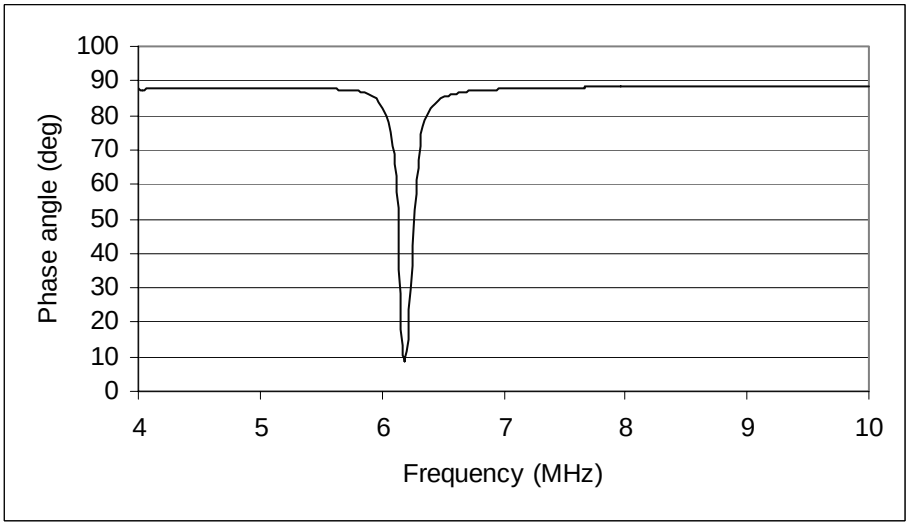

Figure C-19. 05 March 04: Basic sensor 2a

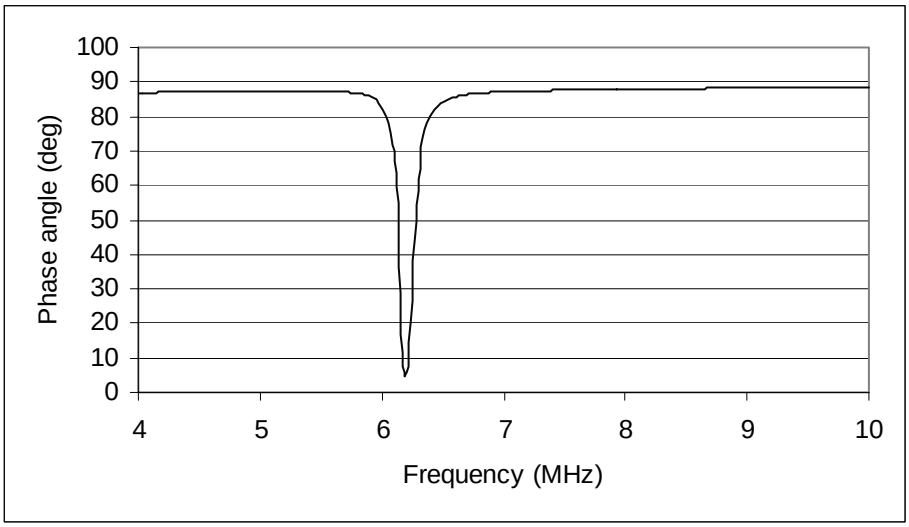

Figure C-20. 08 March 04: Basic sensor 2a

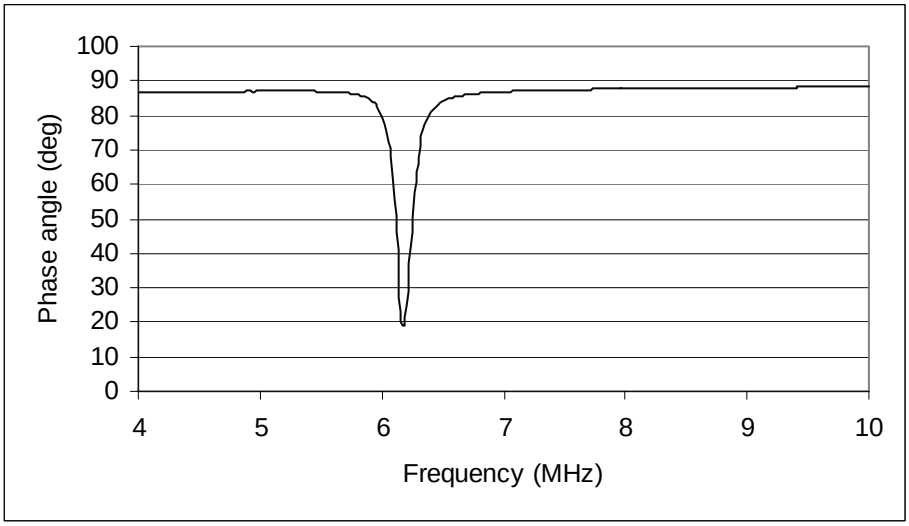

Figure C-21. 09 March 04: Basic sensor 2a

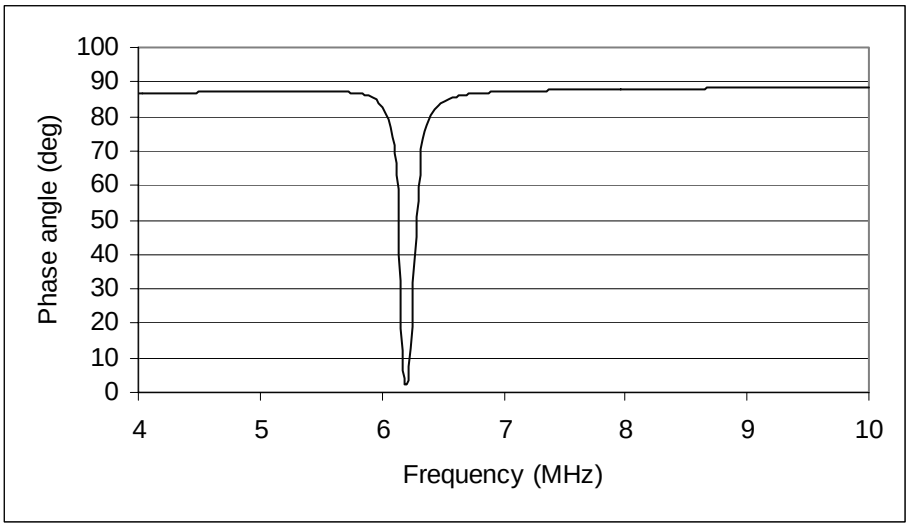

Figure C-22. 11 March 04: Basic sensor 2a

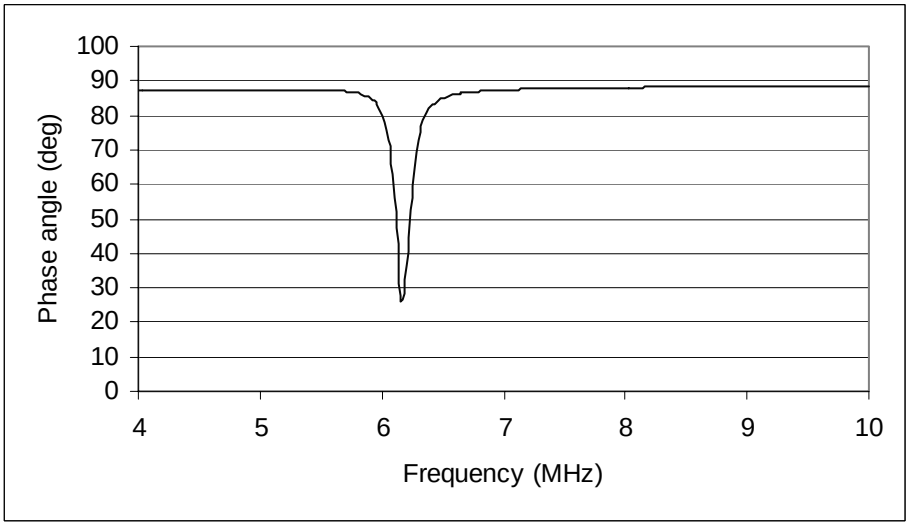

Figure C-23. 12 March 04: Basic sensor 2a

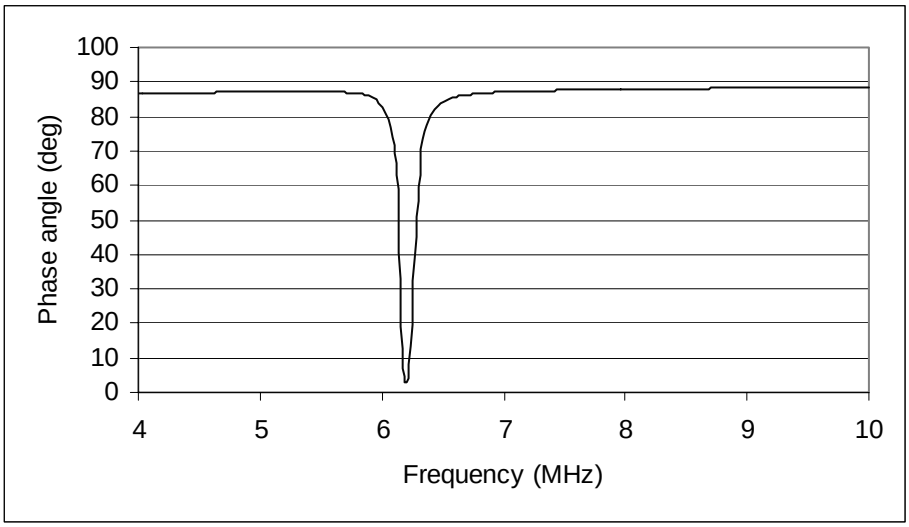

Figure C-24. 22 March 04: Basic sensor 2a

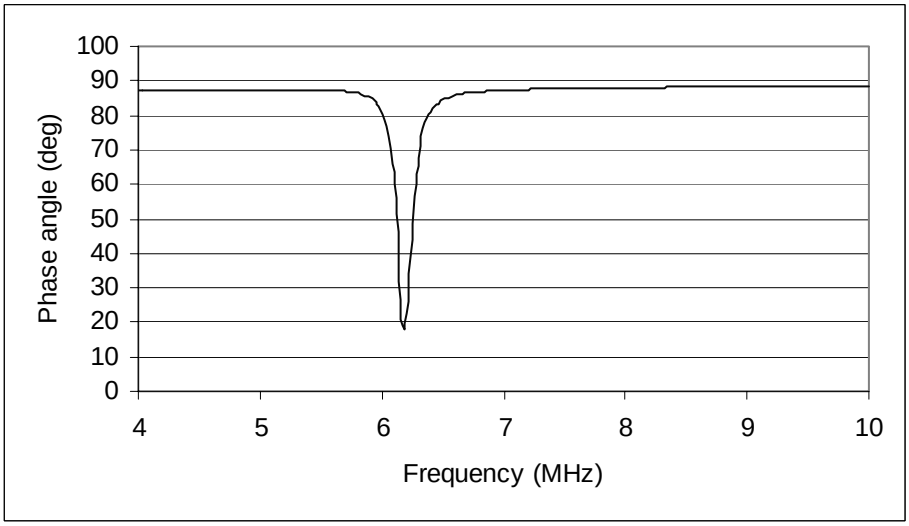

Figure C-25. 23 March 04: Basic sensor 2a

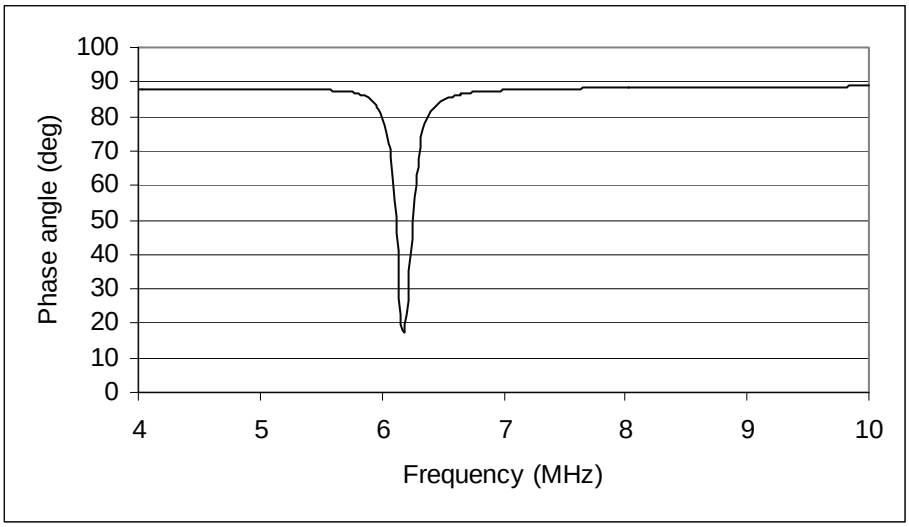

Figure C-26. 24 March 04: Basic sensor 2a

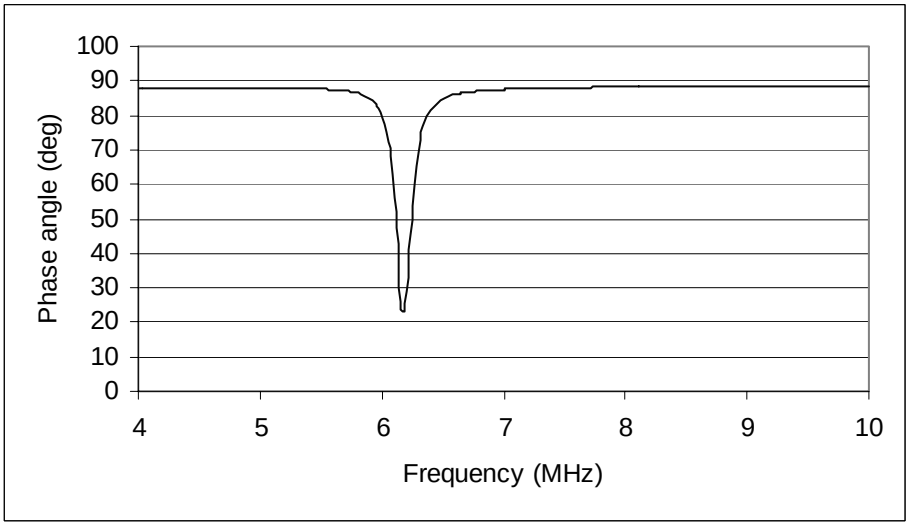

Figure C-27. 25 March 04: Basic sensor 2a

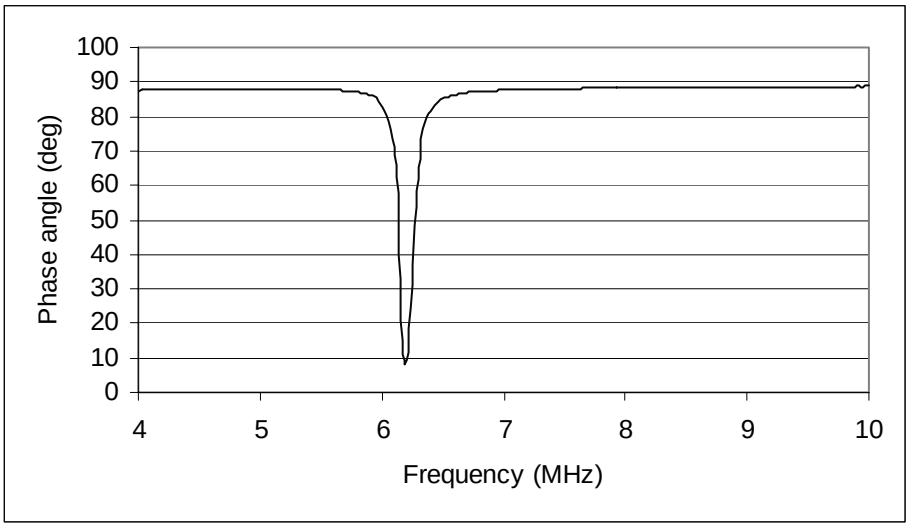

Figure C-28. 26 March 04: Basic sensor 2a

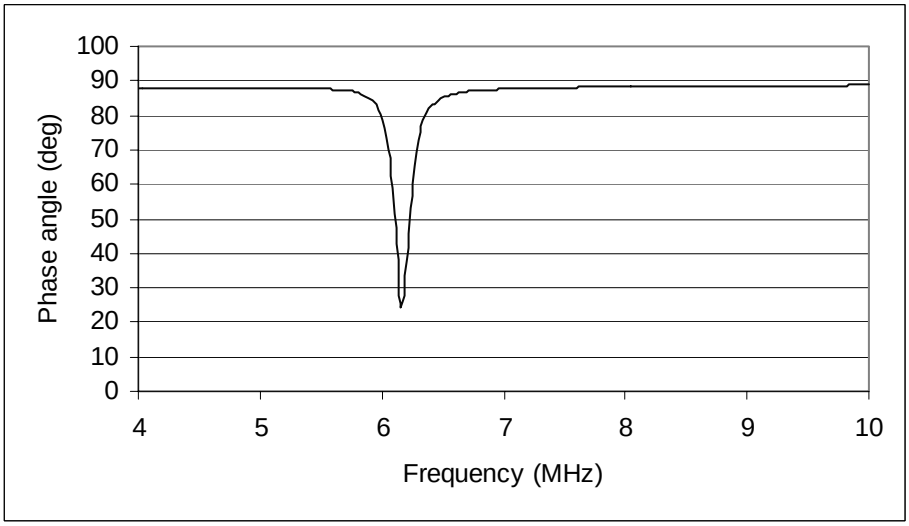

Figure C-29. 30 March 04: Basic sensor 2a

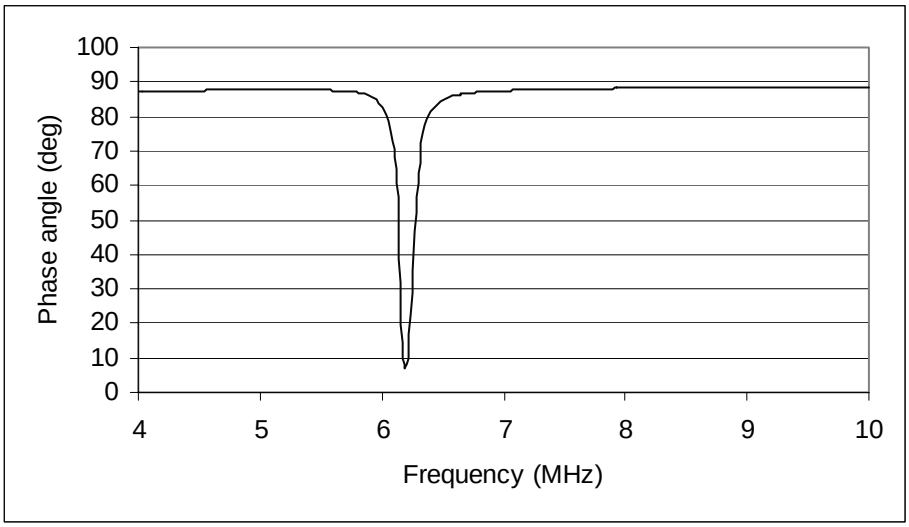

Figure C-30. 01 April 04: Basic sensor 2a

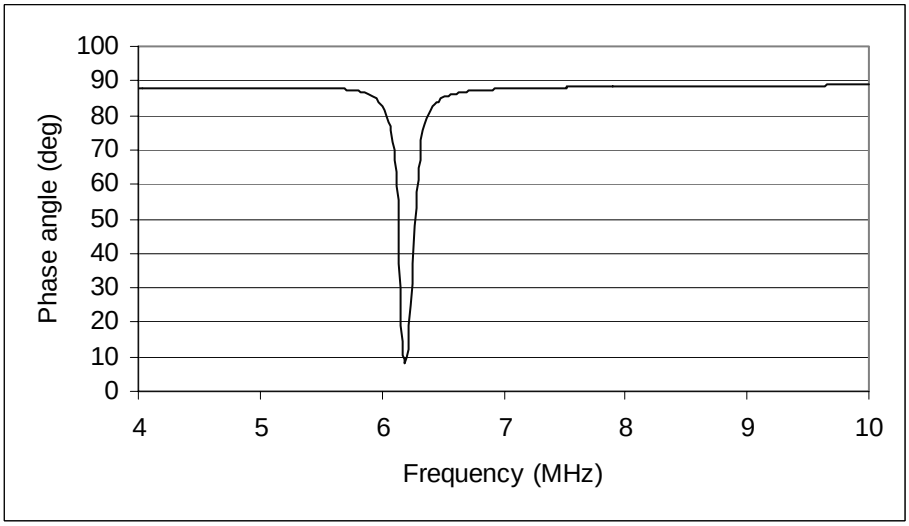

Figure C-31. 06 April 04: Basic sensor 2a

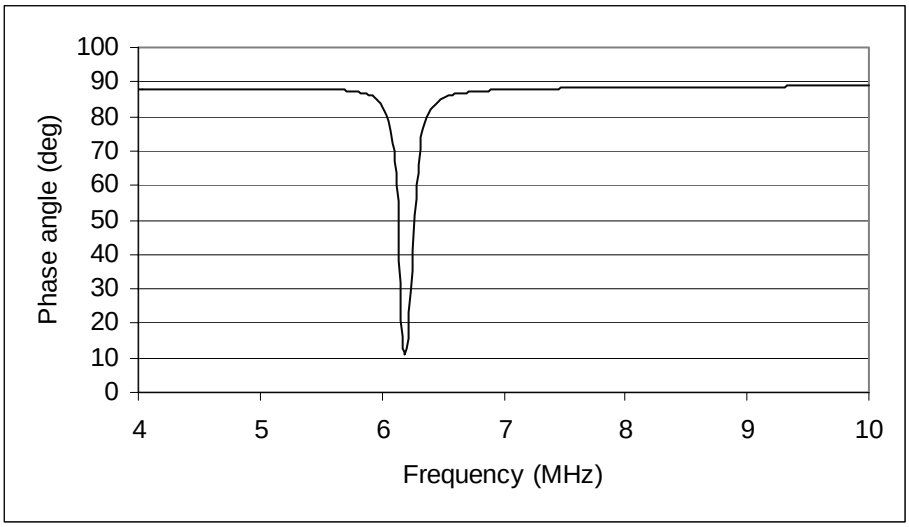

Figure C-32. 07 April 04: Basic sensor 2a

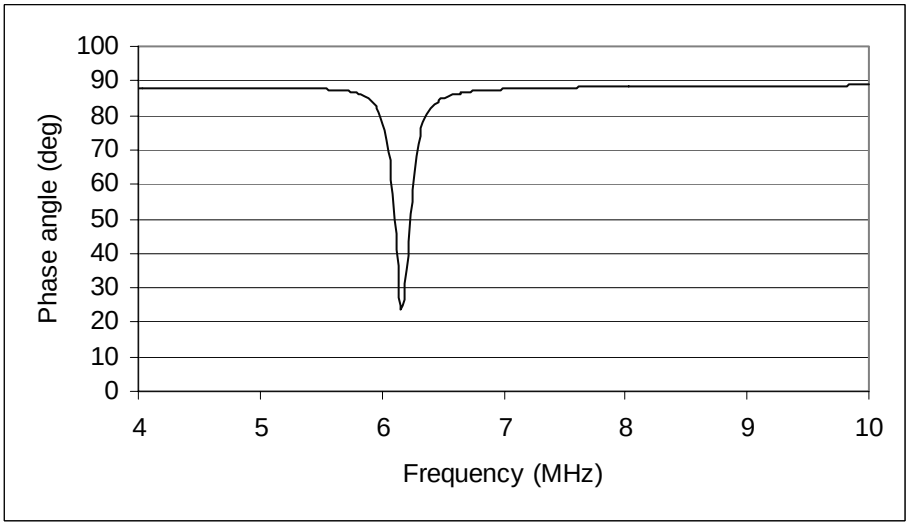

Figure C-33. 15 April 04: Basic sensor 2a

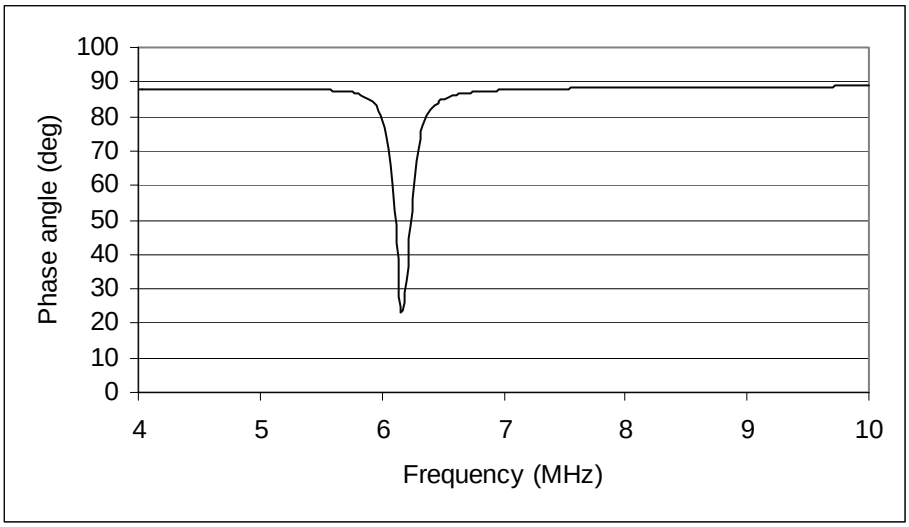

Figure C-34. 20 April 04: Basic sensor 2a

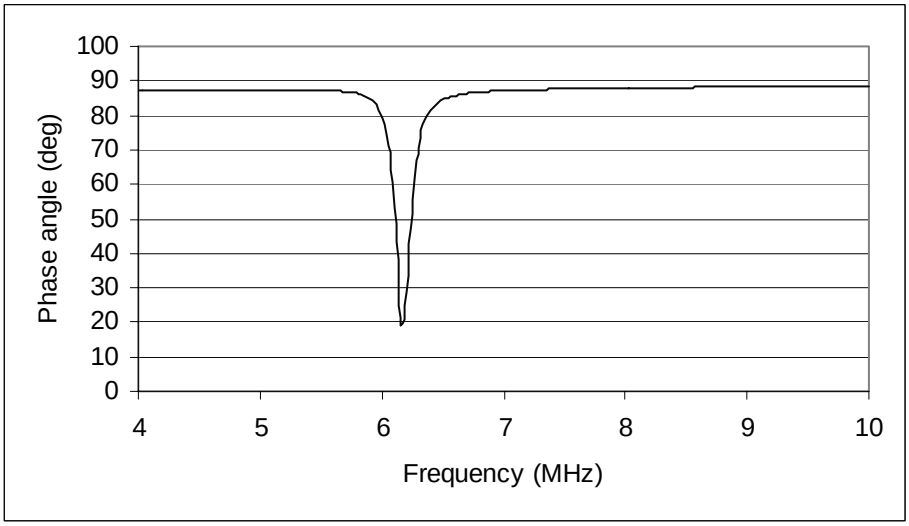

Figure C-35. 22 April 04: Basic sensor 2a

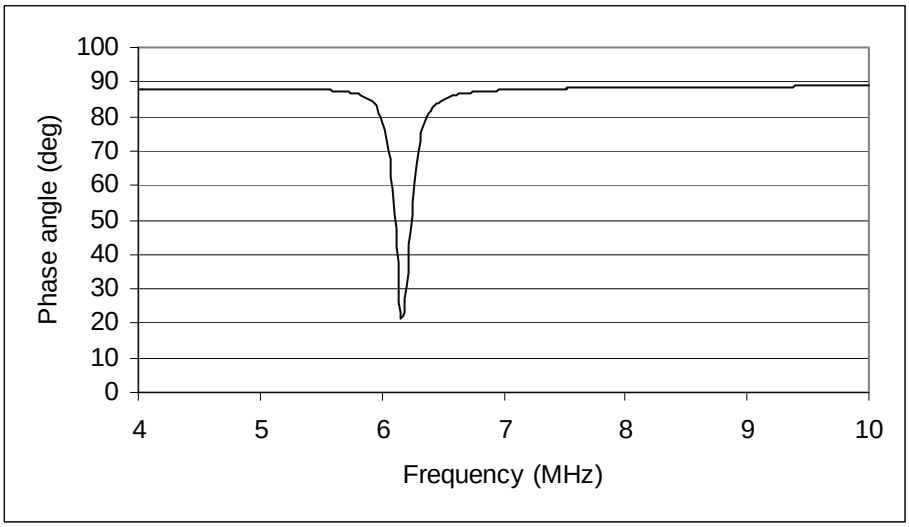

Figure C-36. 27 April 04: Basic sensor 2a

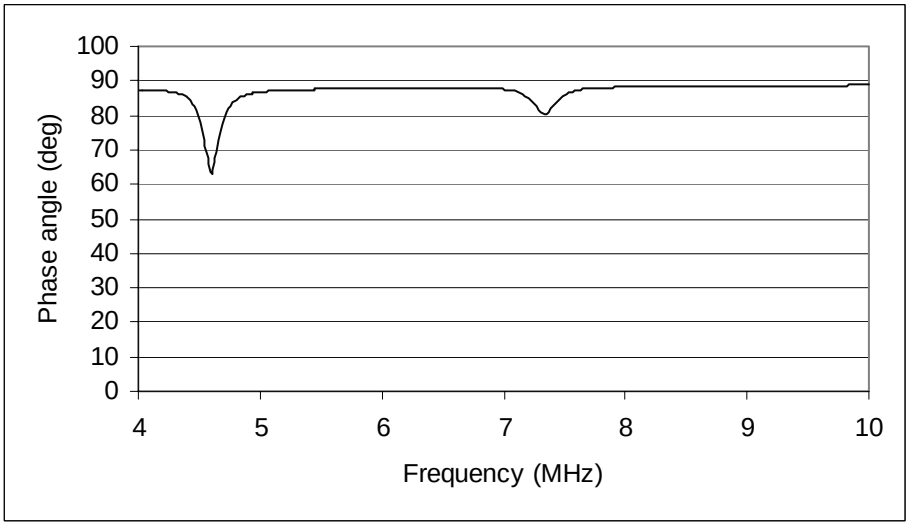

Figure C-37. 05 March 04: Improved sensor 1b

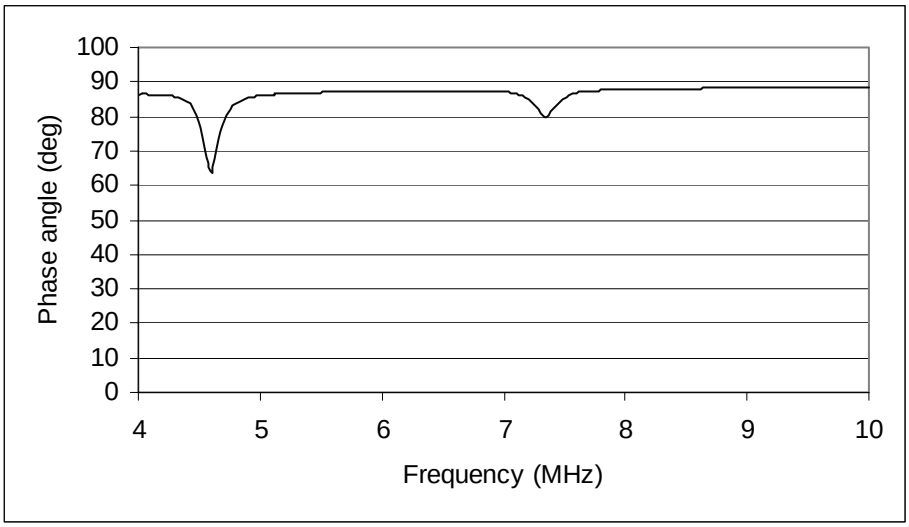

Figure C-38. 08 March 04: Improved sensor 1b

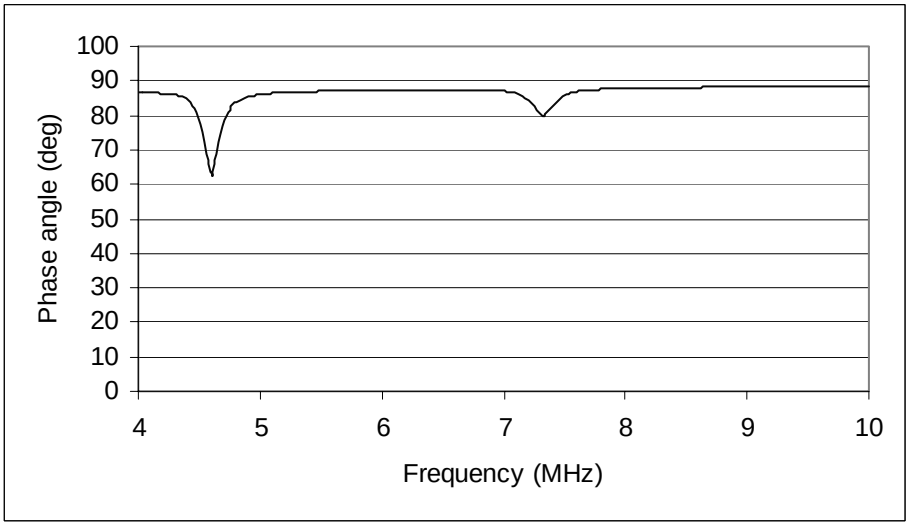

Figure C-39. 09 March 04: improved sensor 1b

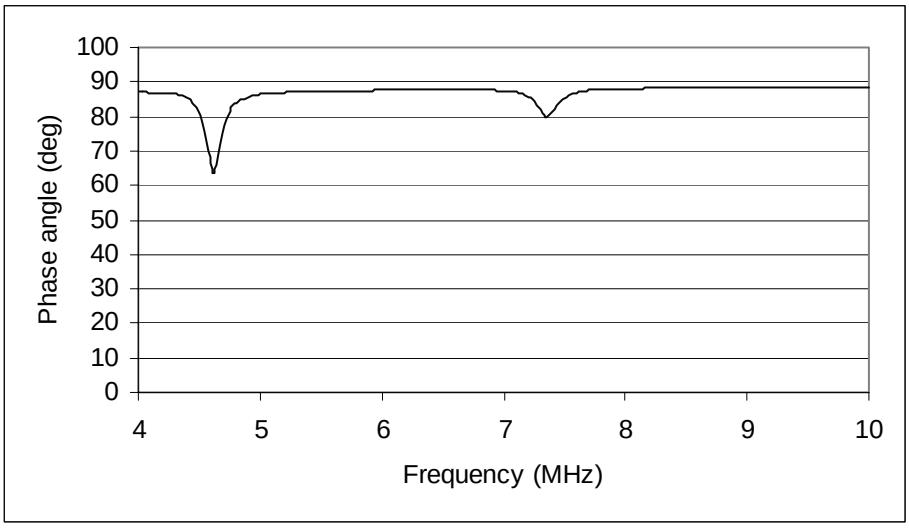

Figure C-40. 11 March 04: Improved sensor 1b

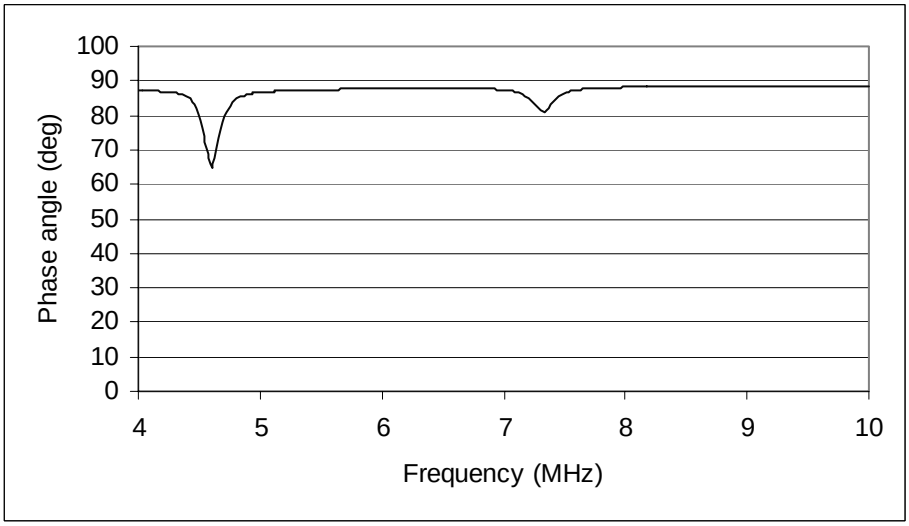

Figure C-41. 12 March 04: Improved sensor 1b

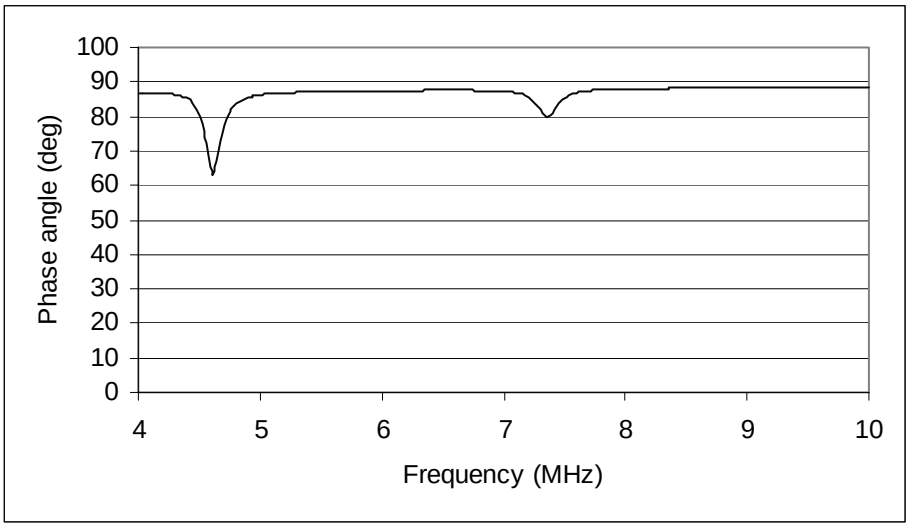

Figure C-42. 22 March 04: Improved sensor 1b

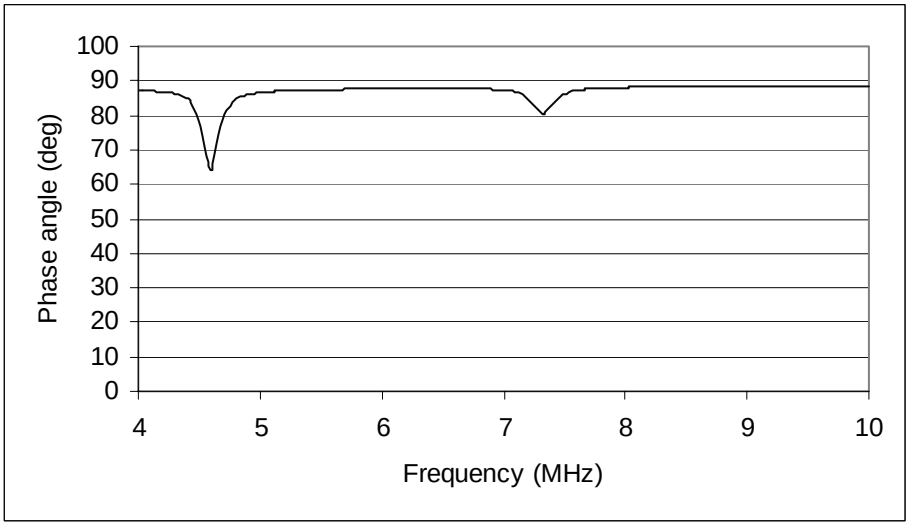

Figure C-43. 23 March 04: Improved sensor 1b

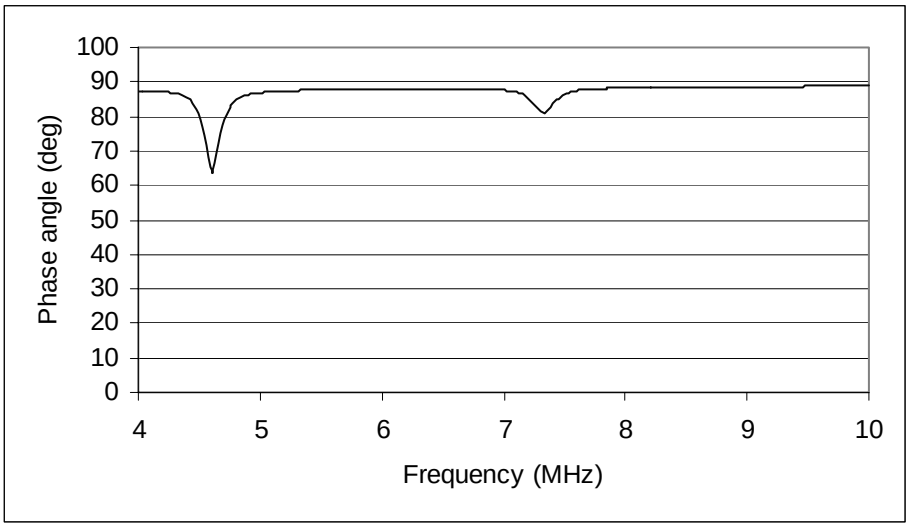

Figure C-44. 24 March 04: Improved sensor 1b

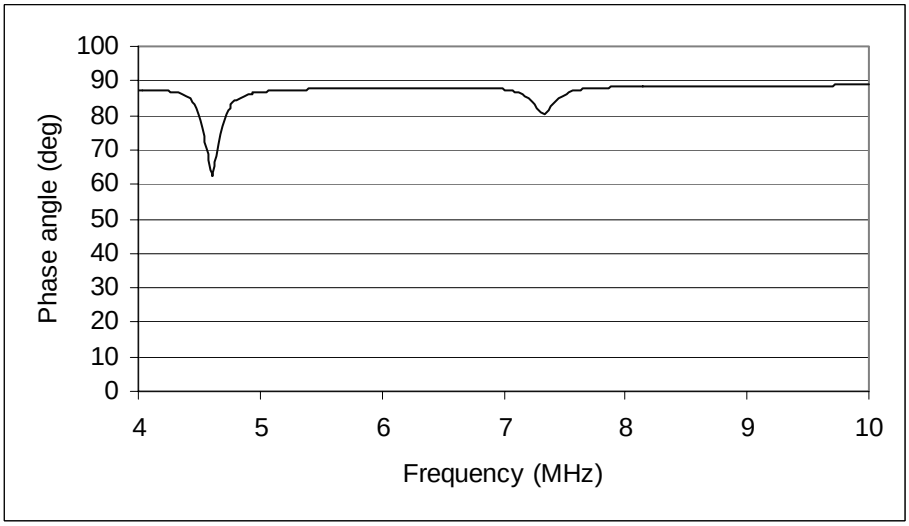

Figure C-45. 25 March 04: Improved sensor 1b

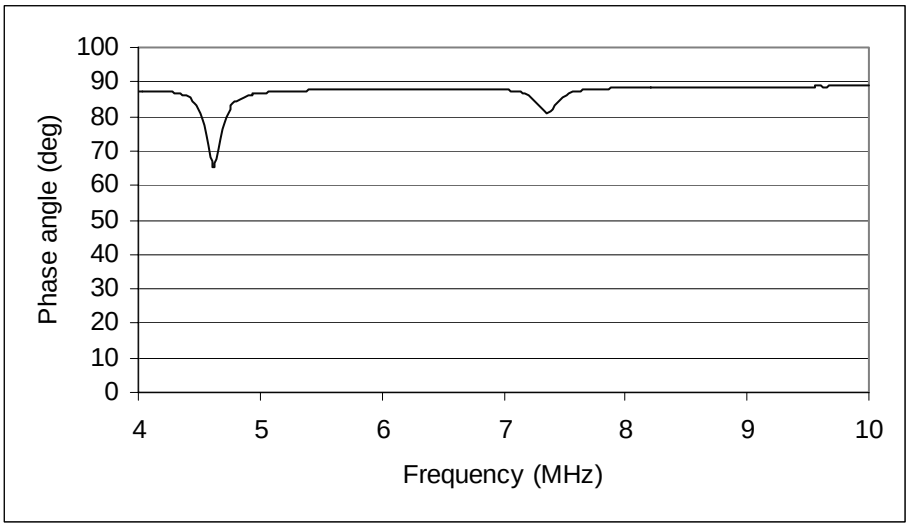

Figure C-46. 26 March 04: Improved sensor 1b

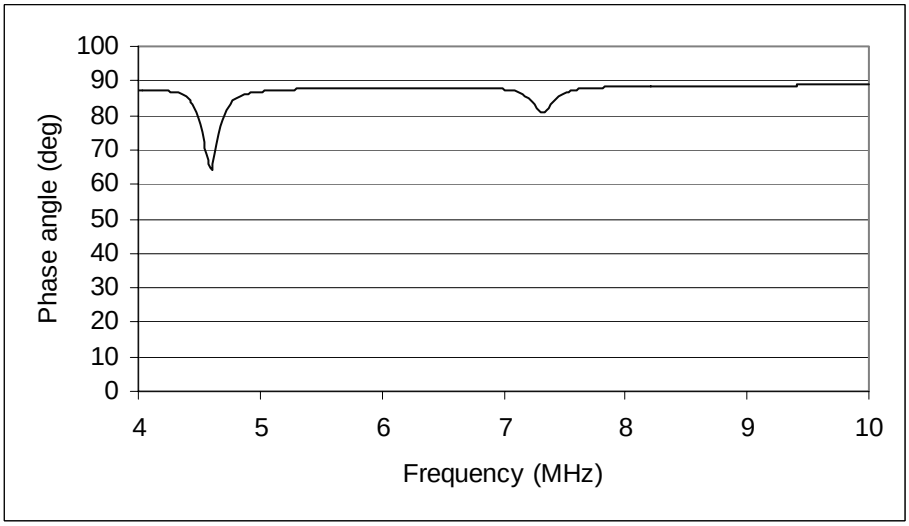

Figure C-47. 30 March 04: Improved sensor 1b

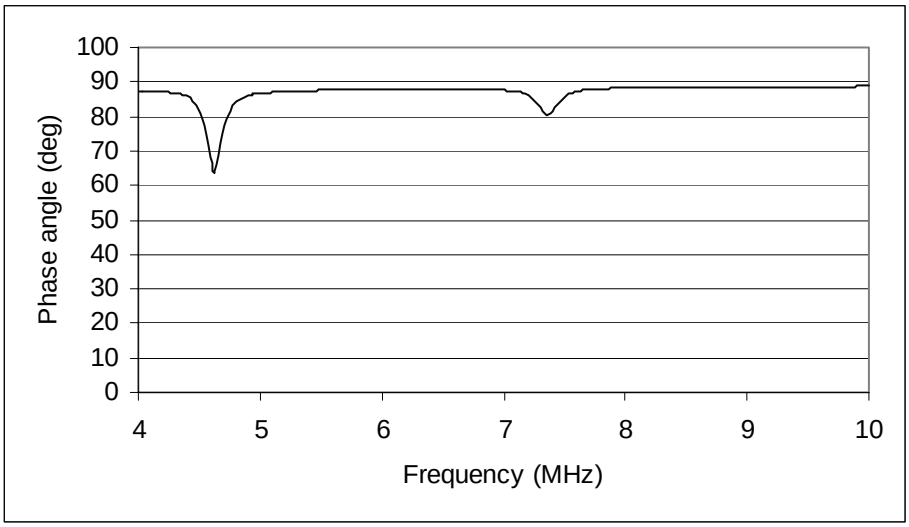

Figure C-48. 01 April 04: Improved sensor 1b

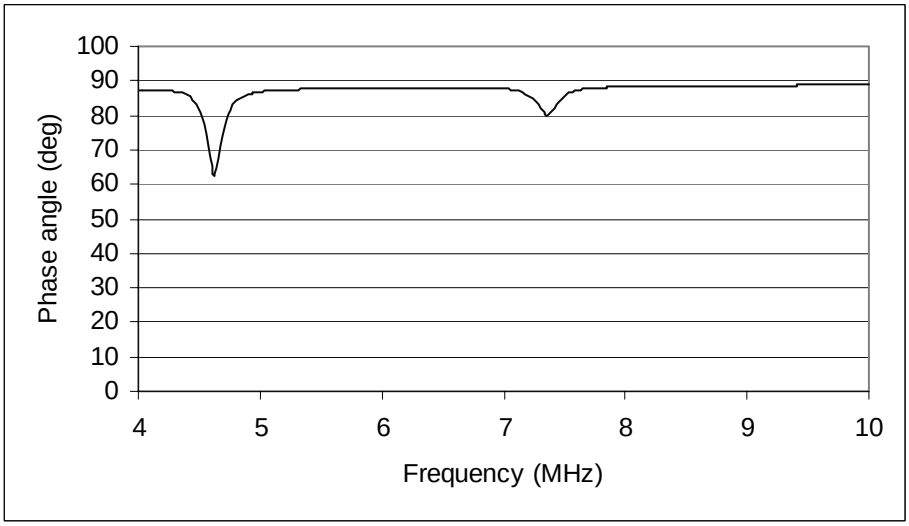

Figure C-49. 06 April 04: Improved sensor 1b

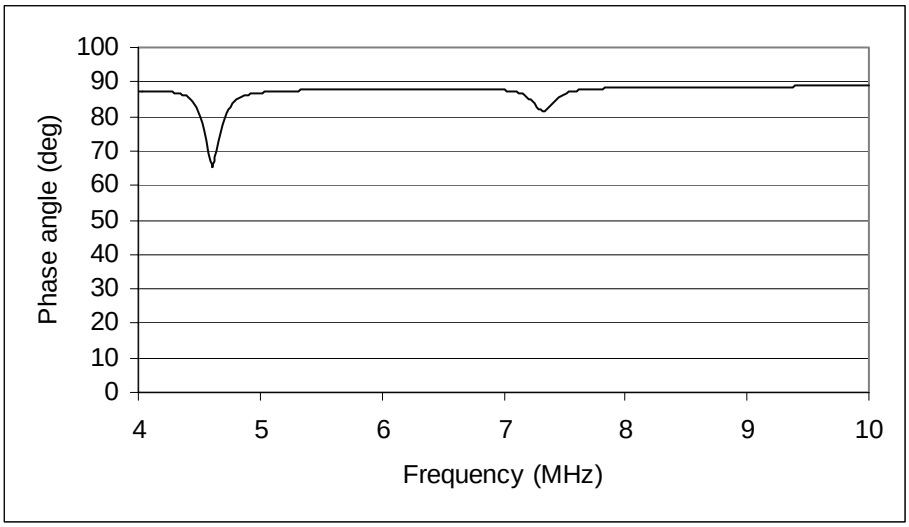

Figure C-50. 07 April 04: Improved sensor 1b

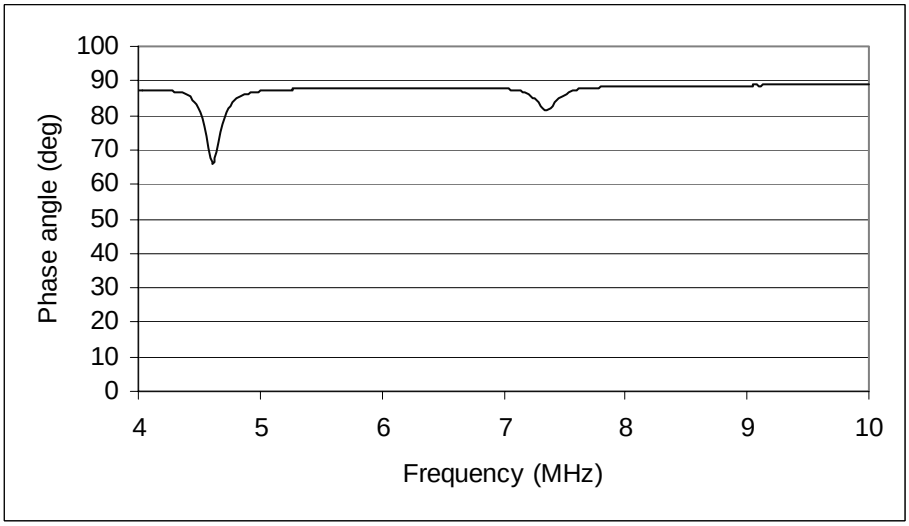

Figure C-51. 15 April 04: Improved sensor 1b

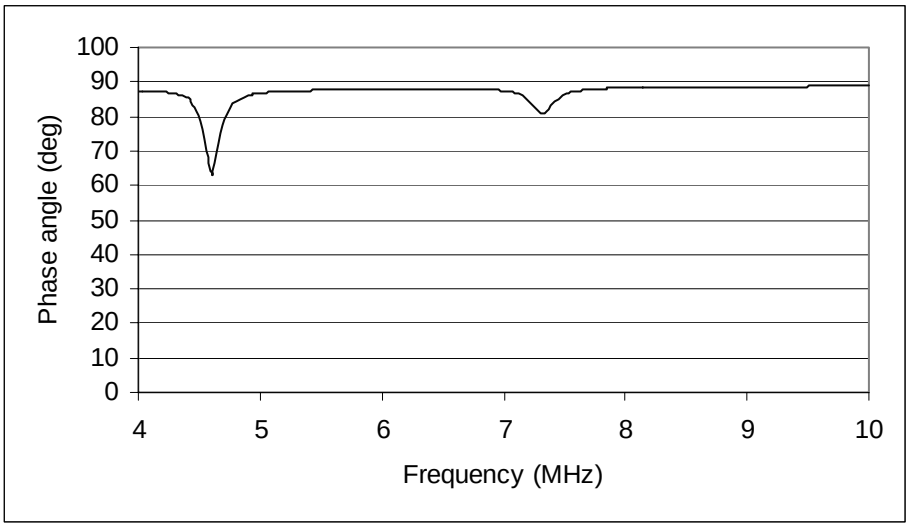

Figure C-52. 20 April 04: Improved sensor 1b

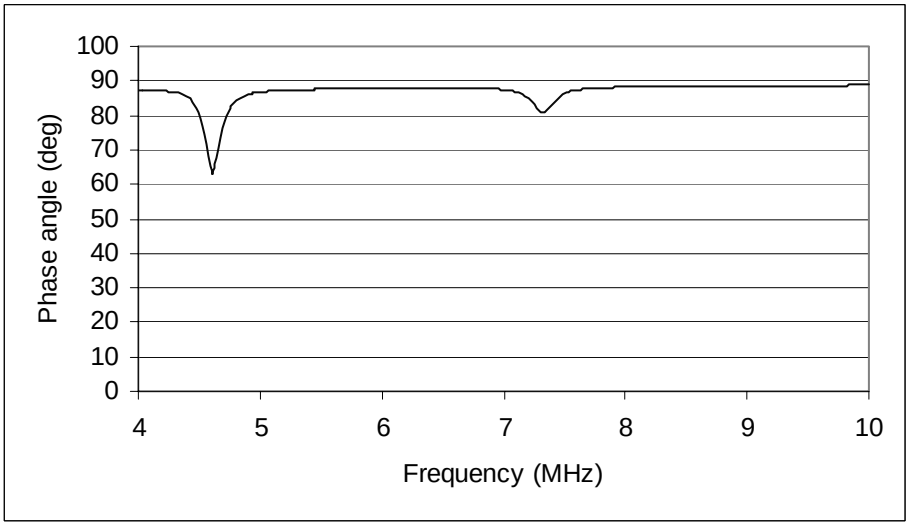

Figure C-53. 22 April 04: Improved sensor 1b

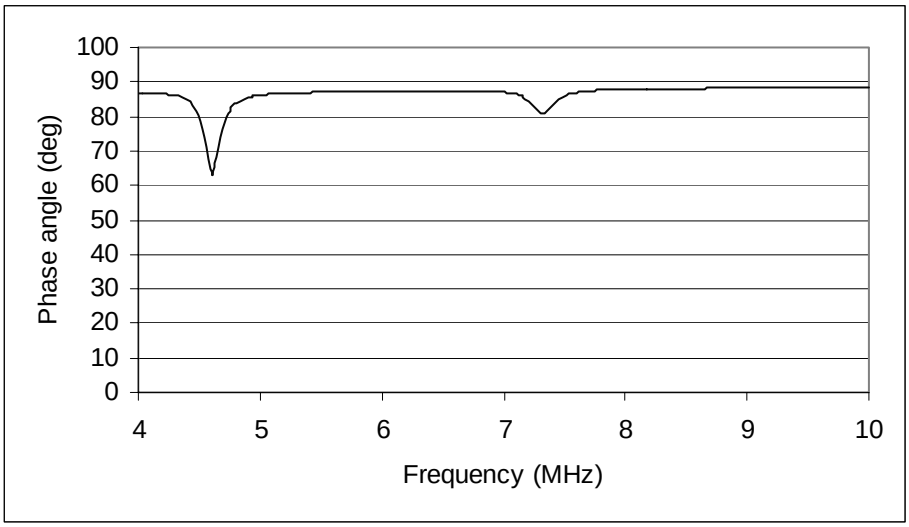

Figure C-54. 27 April 04: Improved sensor 1b

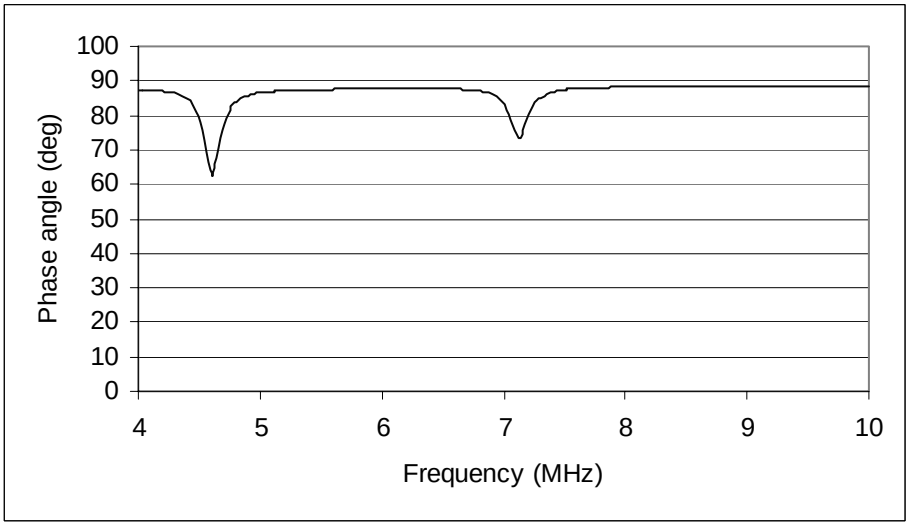

Figure C-55. 05 March 04: Improved sensor 4b

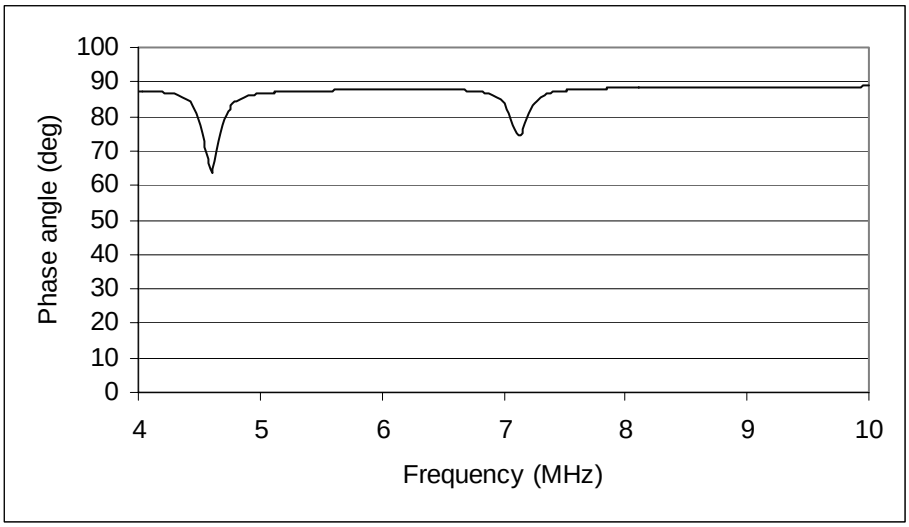

Figure C-56. 08 March 04: Improved sensor 4b

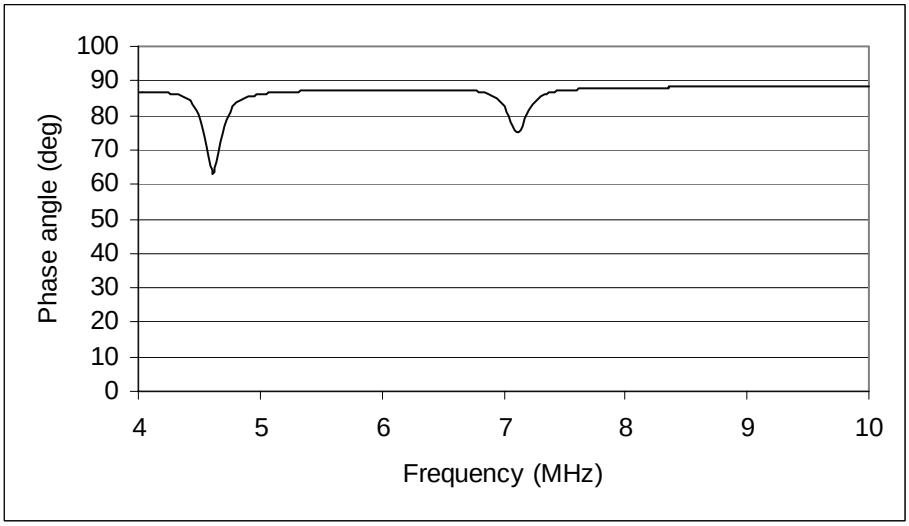

Figure C-57. 09 March 04: improved sensor 4b

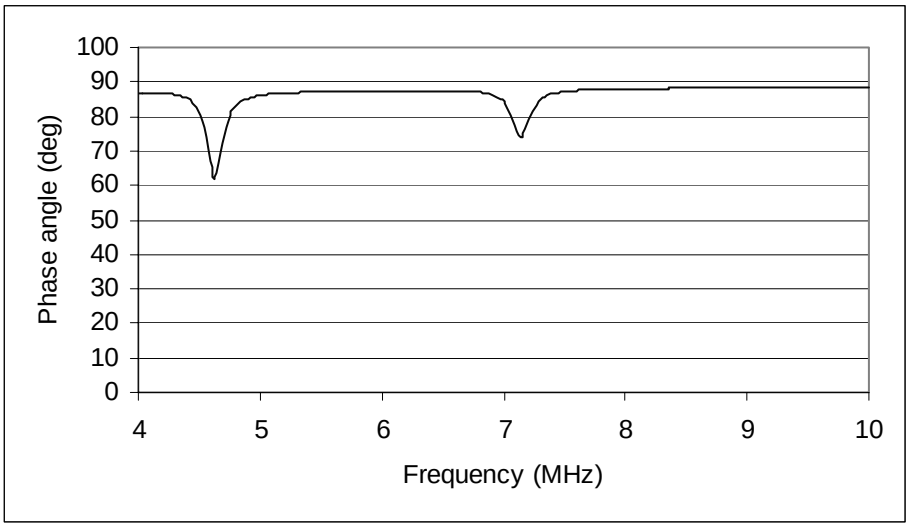

Figure C-58. 11 March 04: Improved sensor 4b

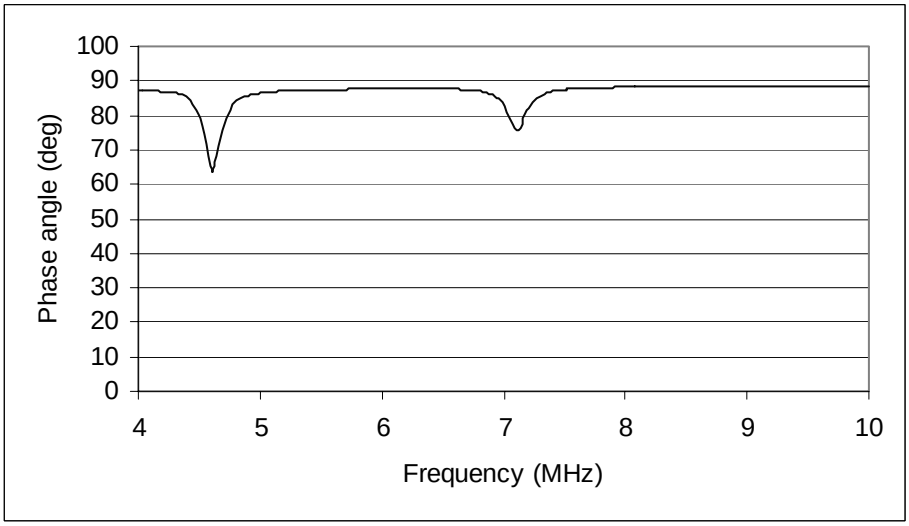

Figure C-59. 12 March 04: Improved sensor 4b

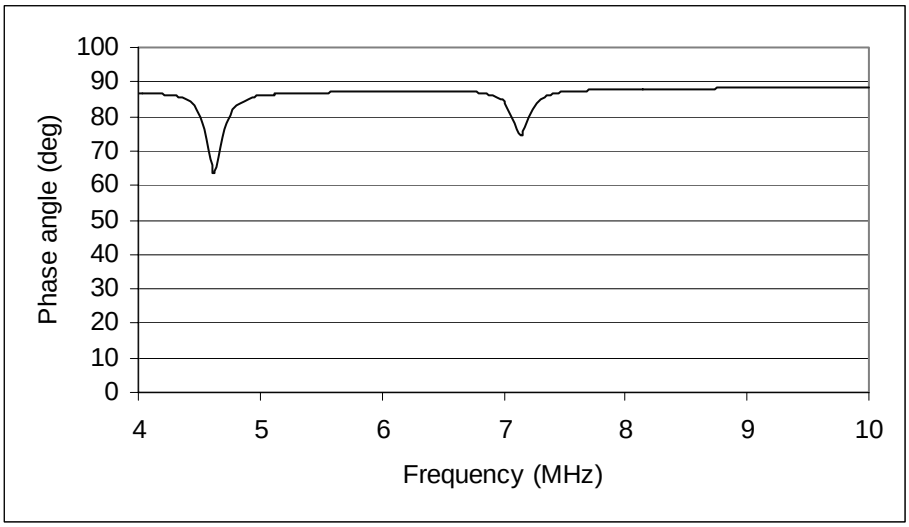

Figure C-60. 22 March 04: Improved sensor 4b

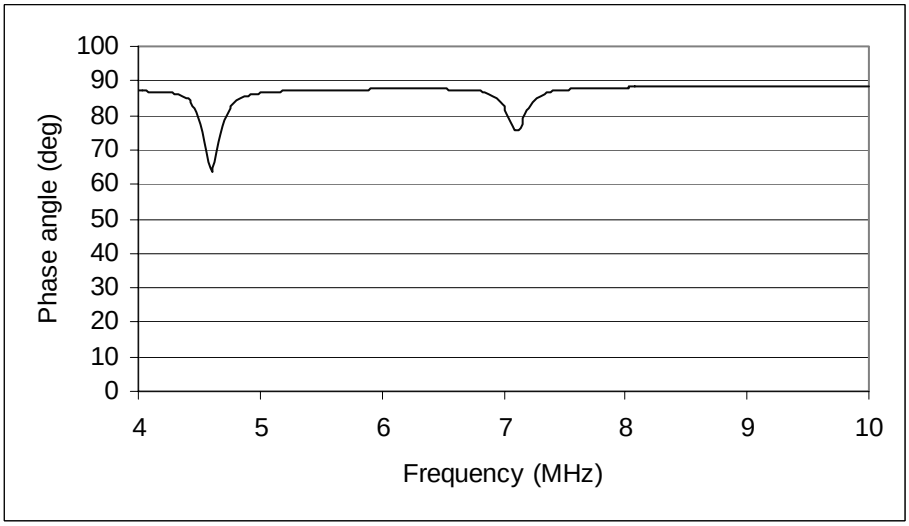

Figure C-61. 23 March 04: Improved sensor 4b

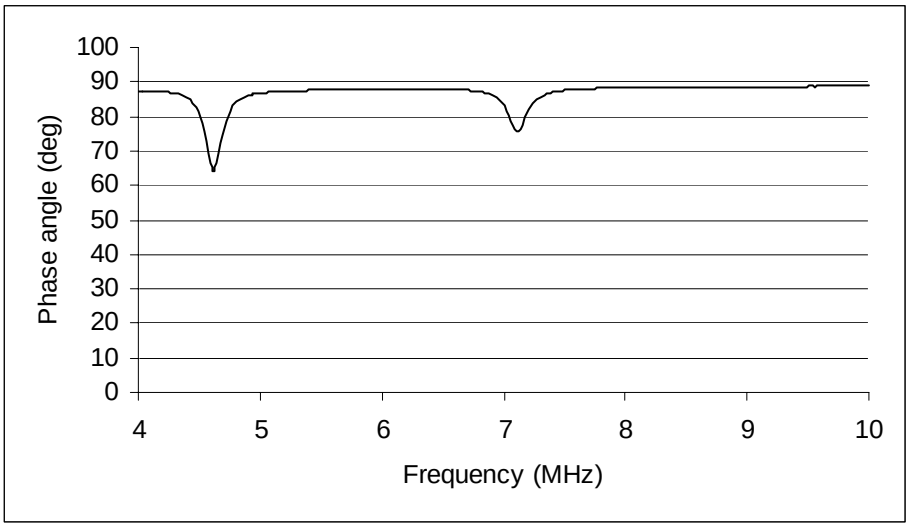

Figure C-62. 24 March 04: Improved sensor 4b

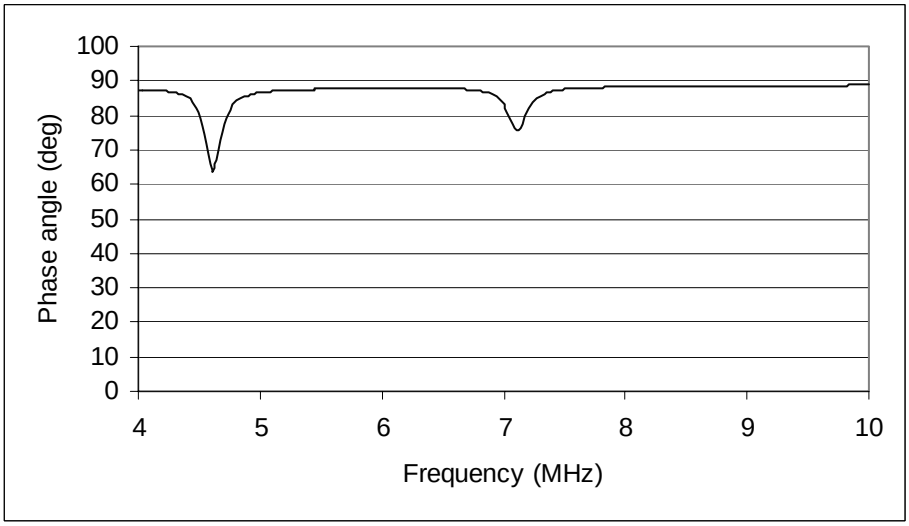

Figure C-63. 25 March 04: Improved sensor 4b

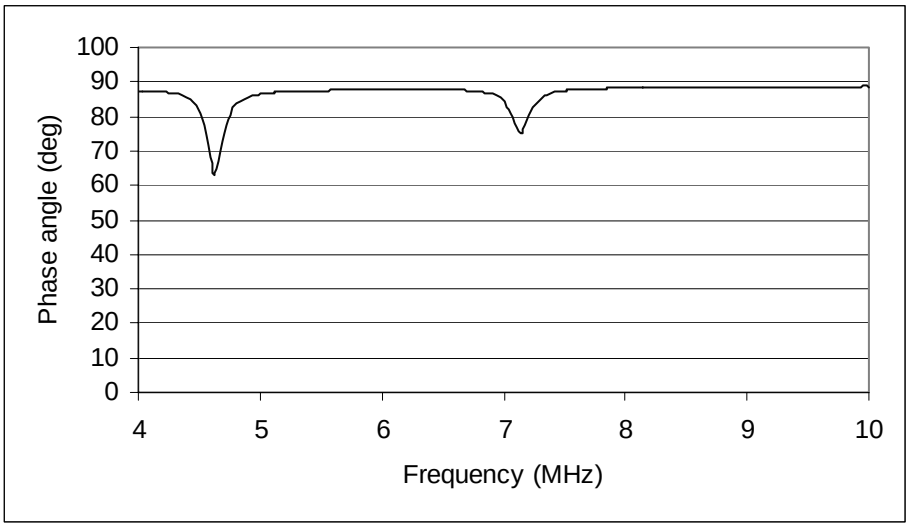

Figure C-64. 26 March 04: Improved sensor 4b

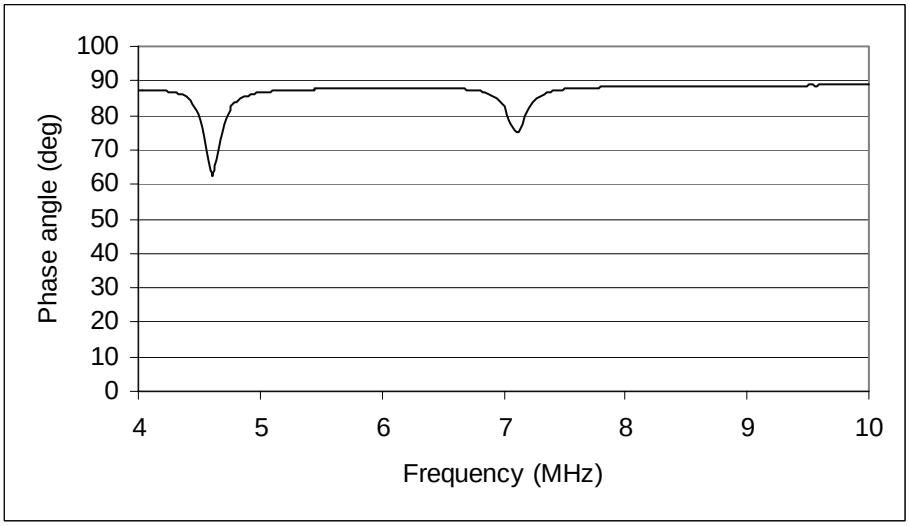

Figure C-65. 30 March 04: Improved sensor 4b

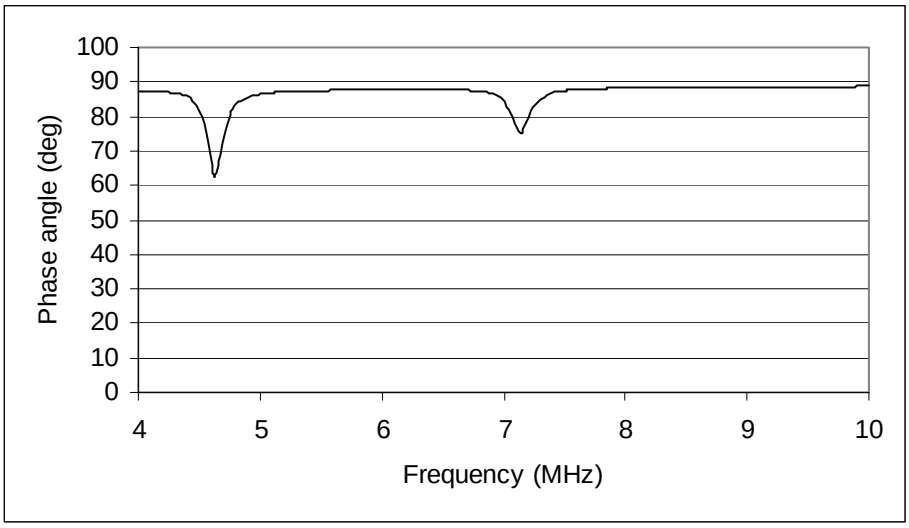

Figure C-66. 01 April 04: Improved sensor 4b

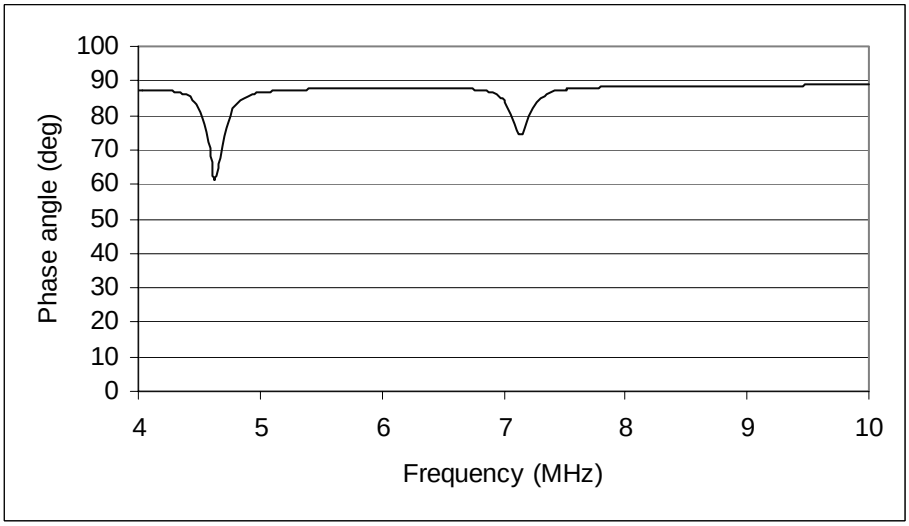

Figure C-67. 06 April 04: Improved sensor 4b

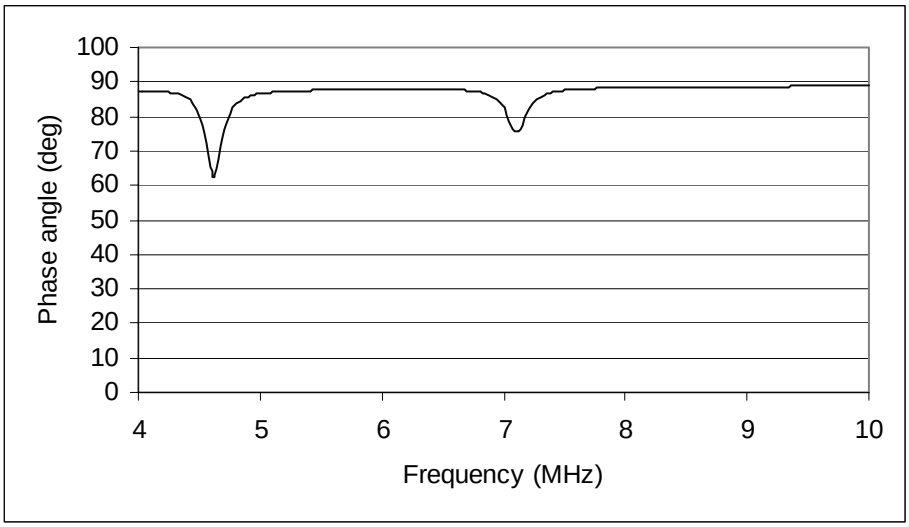

Figure C-68. 07 April 04: Improved sensor 4b

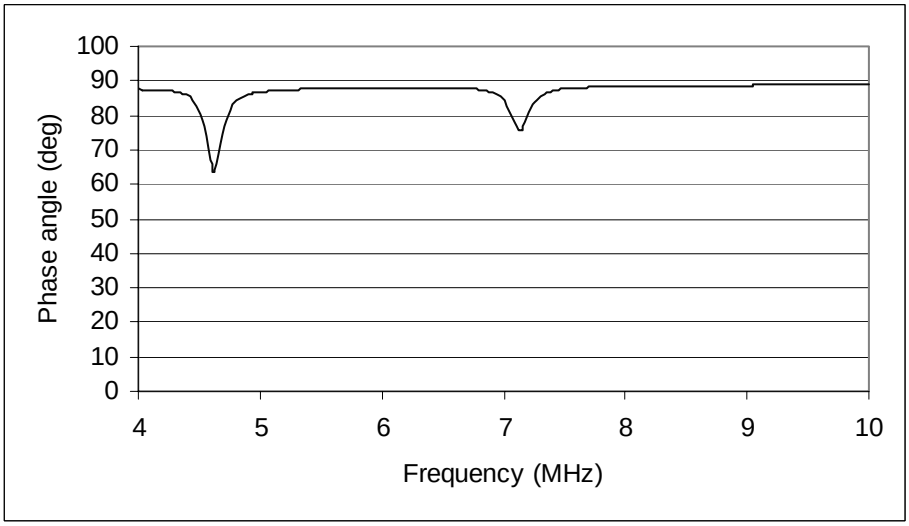

Figure C-69. 15 April 04: Improved sensor 4b

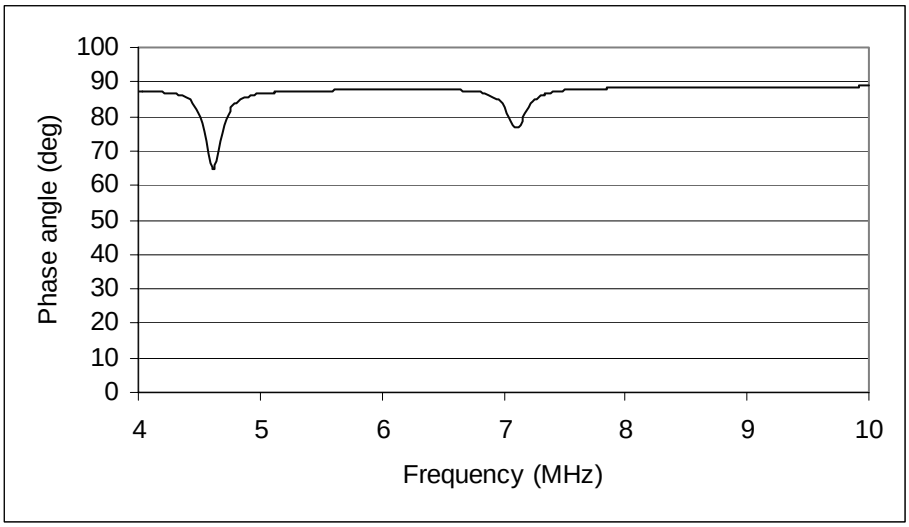

Figure C-70. 20 April 04: Improved sensor 4b

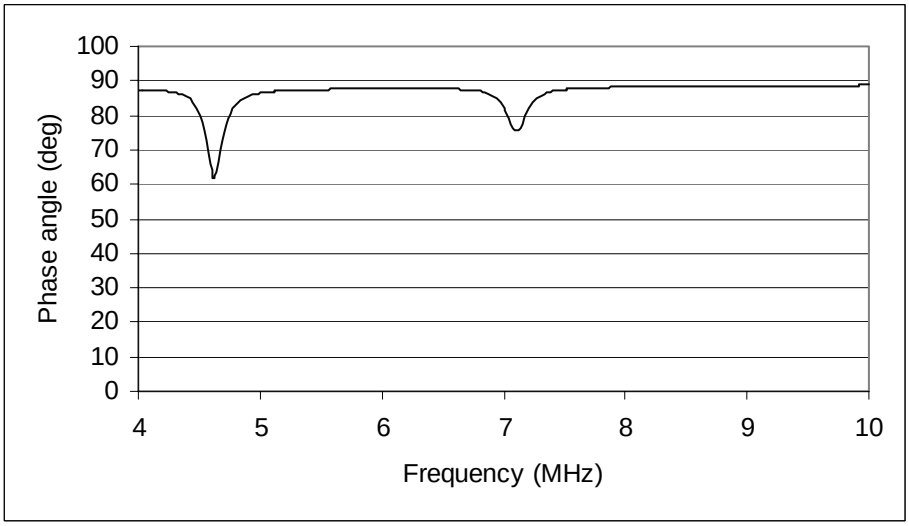

Figure C-71. 22 April 04: Improved sensor 4b

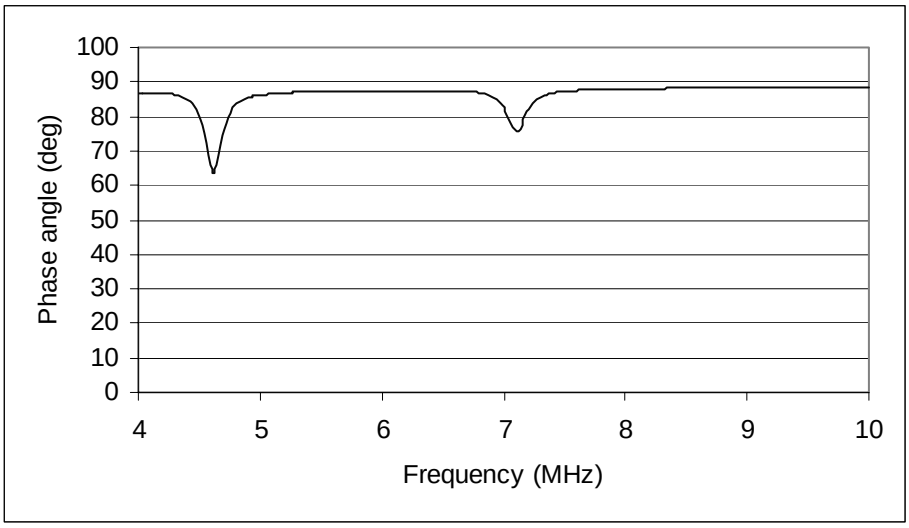

Figure C-72. 27 April 04: Improved sensor 4b

APPENDIX D

Influence of Distance between the Interrogation Coil and the Sensor

D.1 RESULTS O F TRANSMISSION RANGE

The transmission range tests of the sensors were conducted using the Solartron 1260 Impedance/Gain Phase Analyzer. Each sensor was initially interrogated with the interrogation coil placed right on top of the sensor (gap of 0 in.) and then the gap was increased with increments of 0.25 in. until the signal became too weak to distinguish. Results of these reading are presented.

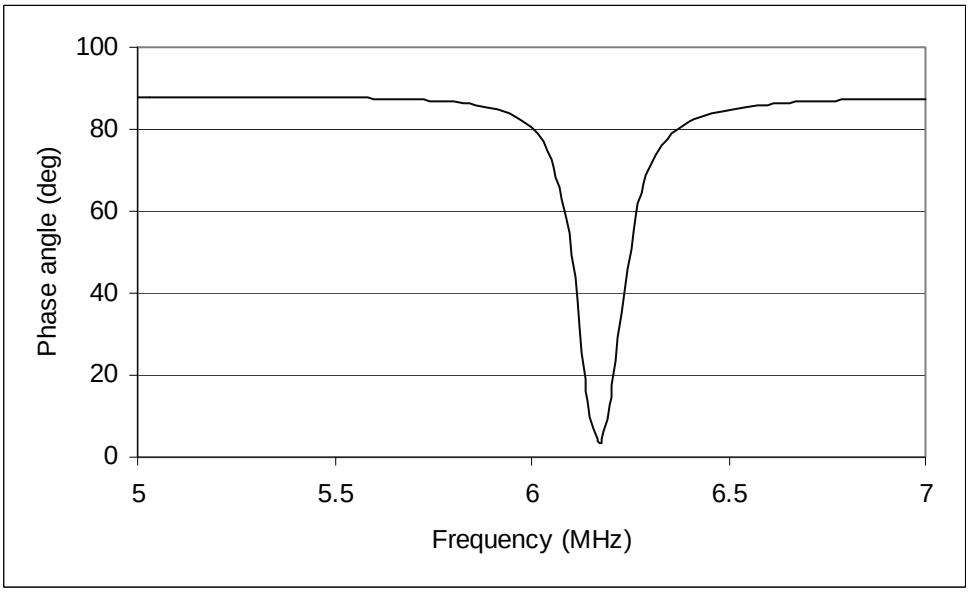

Figure D-1. Basic sensor phase angle response: Gap distance 0.0 in.

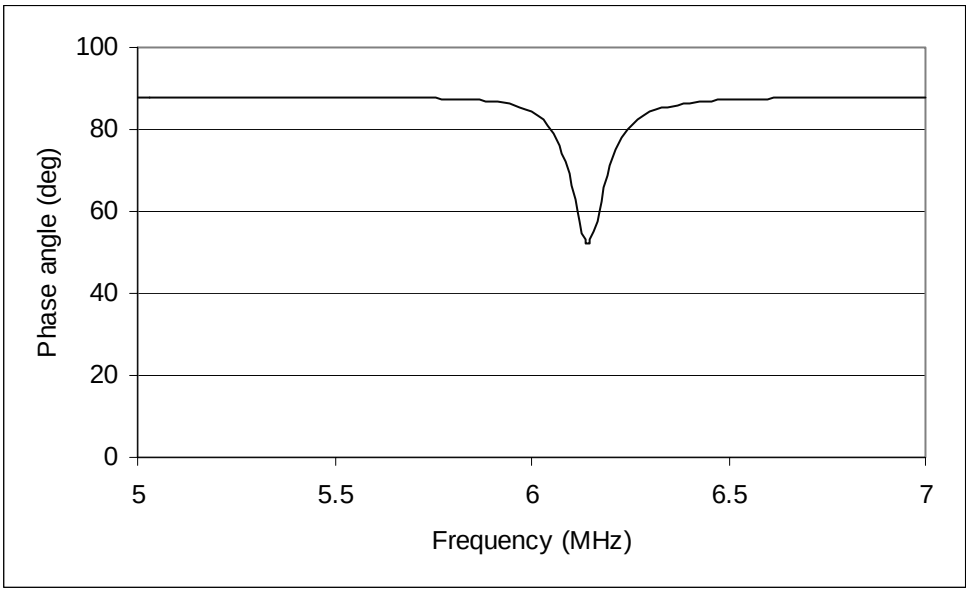

Figure D-2. Basic sensor phase angle response: Gap distance 0.25 in.

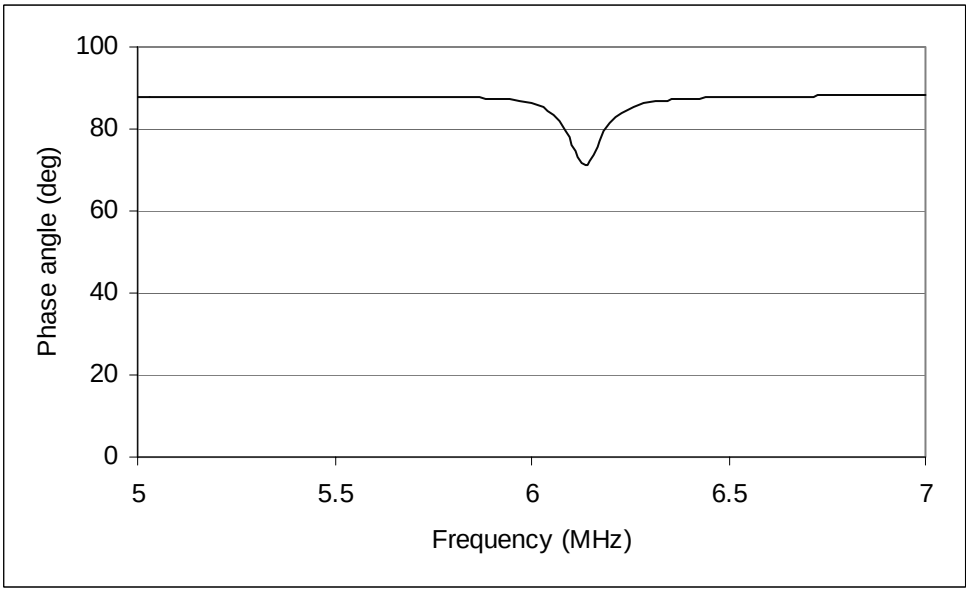

Figure D-3. Basic sensor phase angle response: Gap distance 0.5 in.

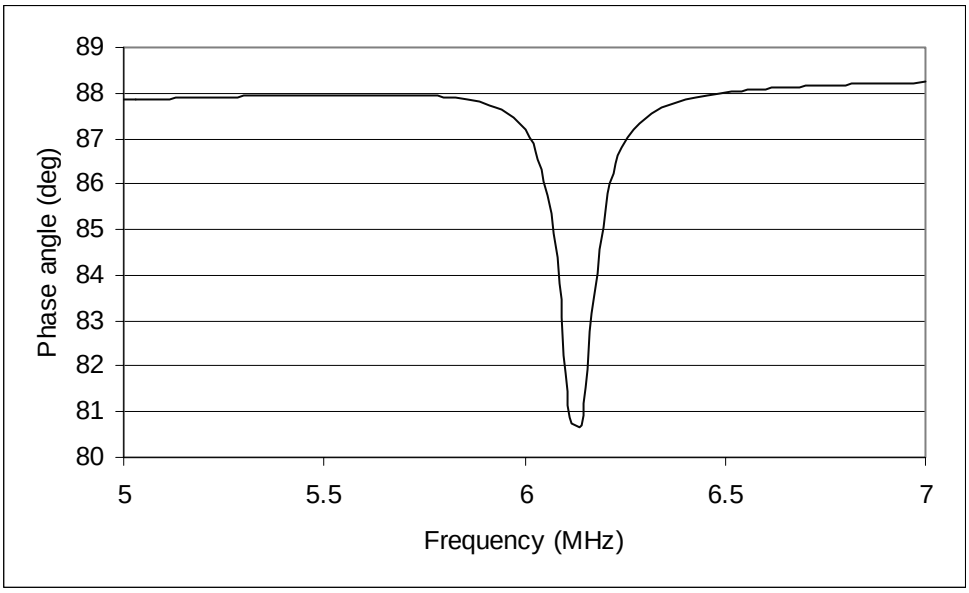

Figure D-4. Basic sensor phase angle response: Gap distance 0.75 in.

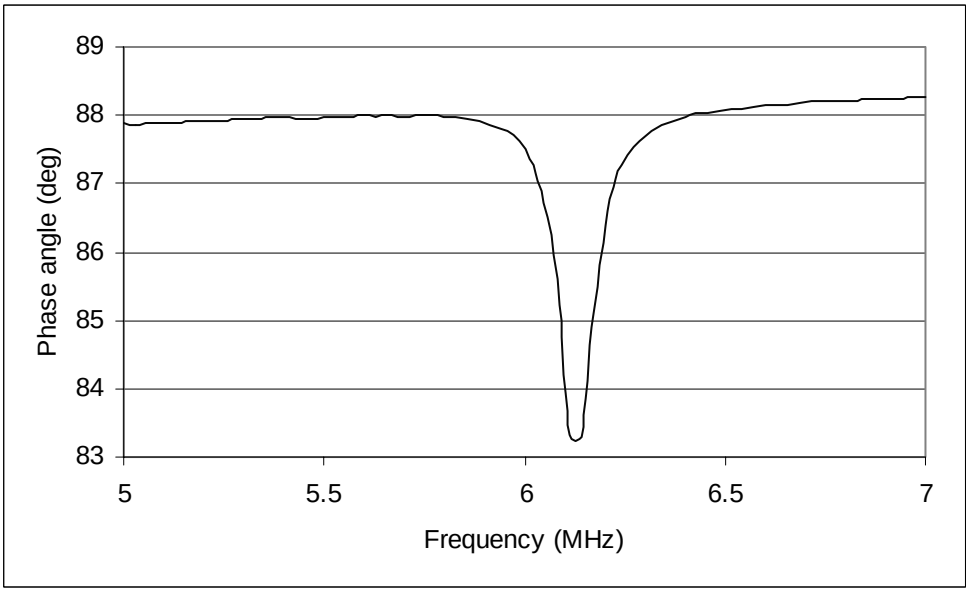

Figure D-5. Basic sensor phase angle response: Gap distance 1.0 in.

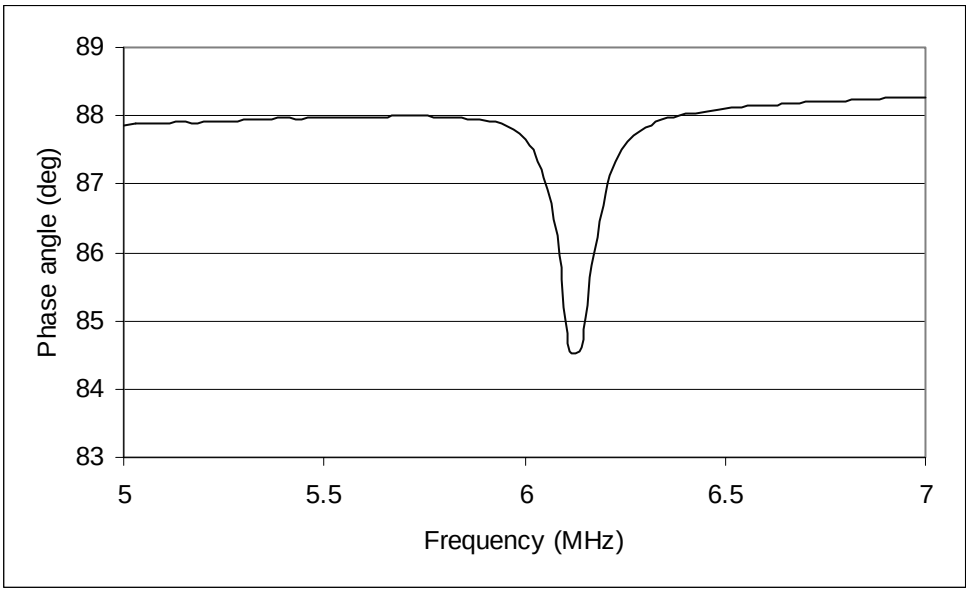

Figure D-6. Basic sensor phase angle response: Gap distance 1.25 in.

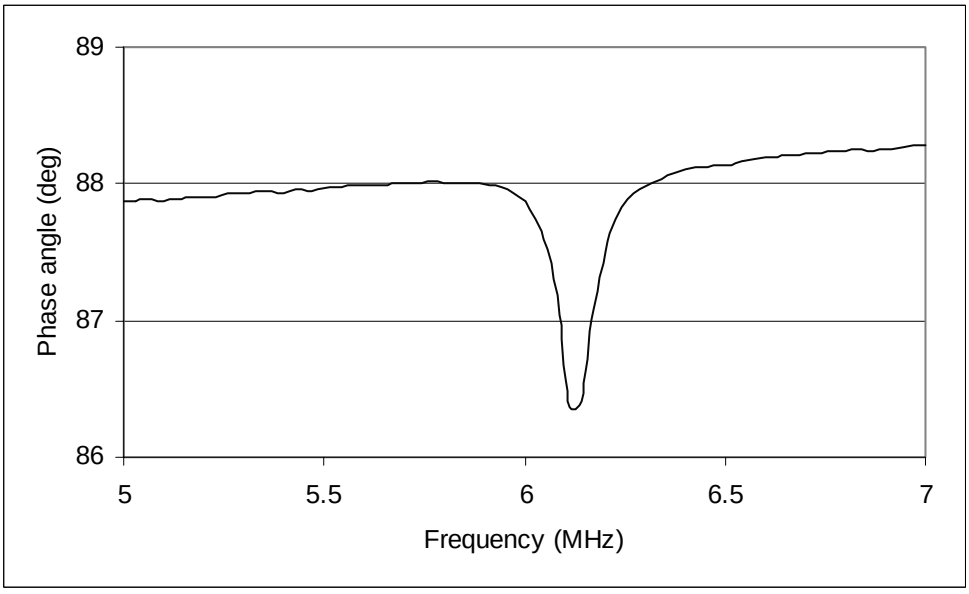

Figure D-7. Basic sensor phase angle response: Gap distance 1.50 in.

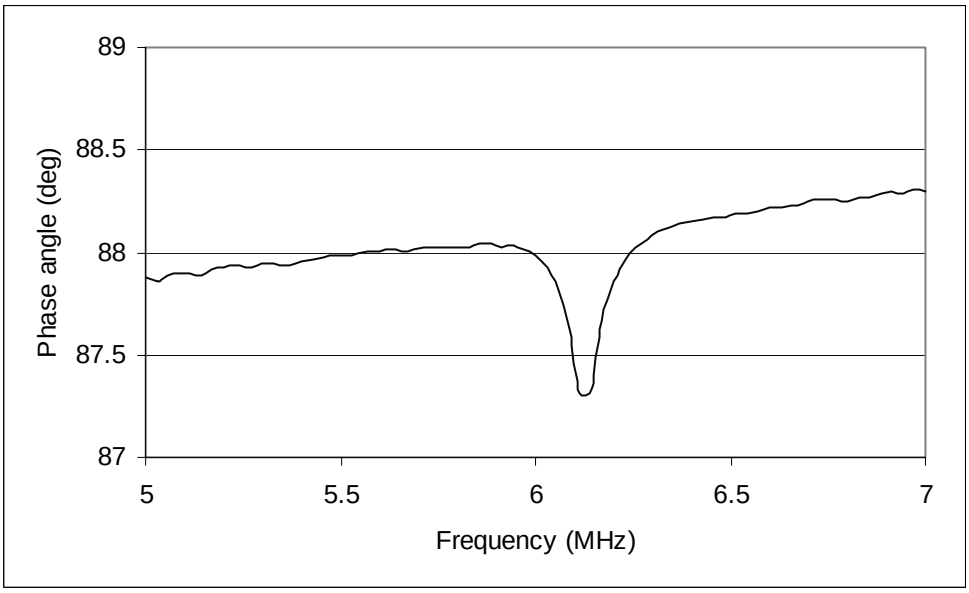

Figure D-8. Basic sensor phase angle response: Gap distance 1.75 in.

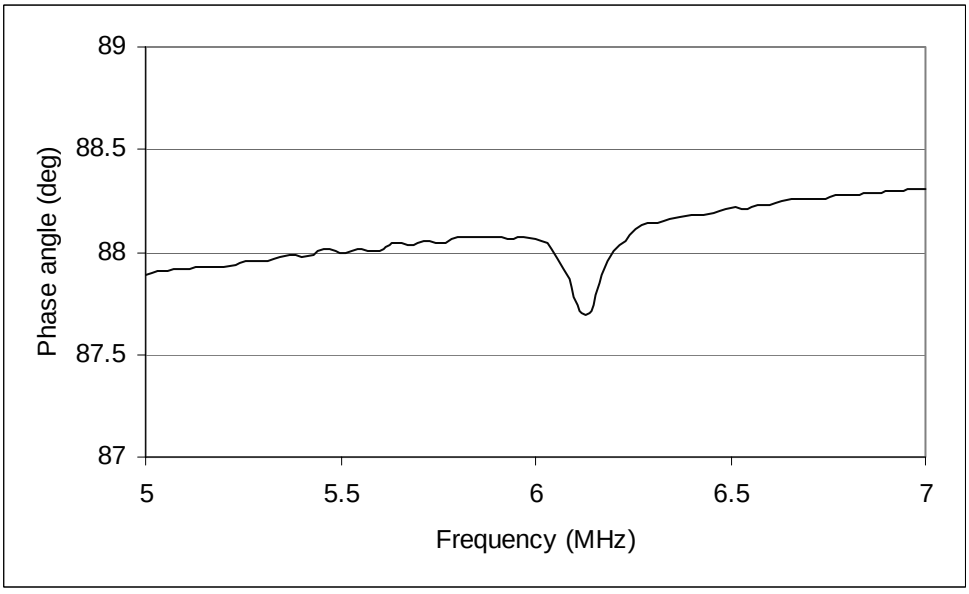

Figure D-9. Basic sensor phase angle response: Gap distance 2.0 in.

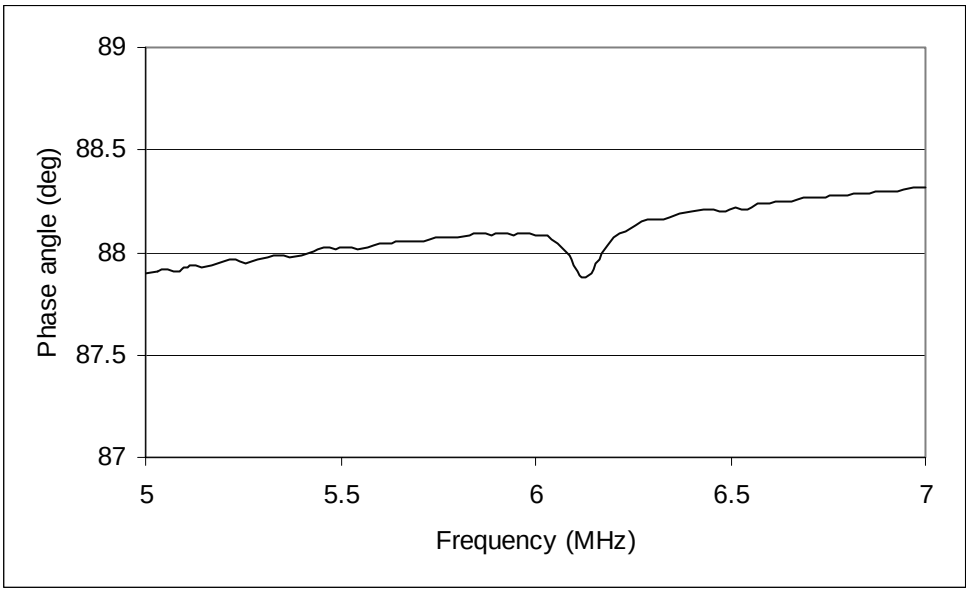

Figure D-10. Basic sensor phase angle response: Gap distance 2.25 in.

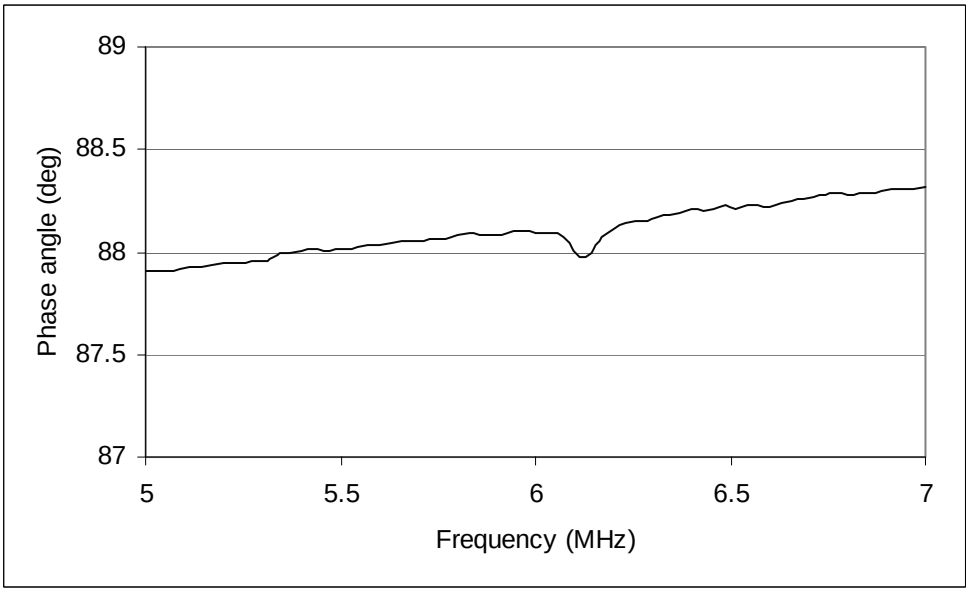

Figure D-11. Basic sensor phase angle response: Gap distance 2.50 in.

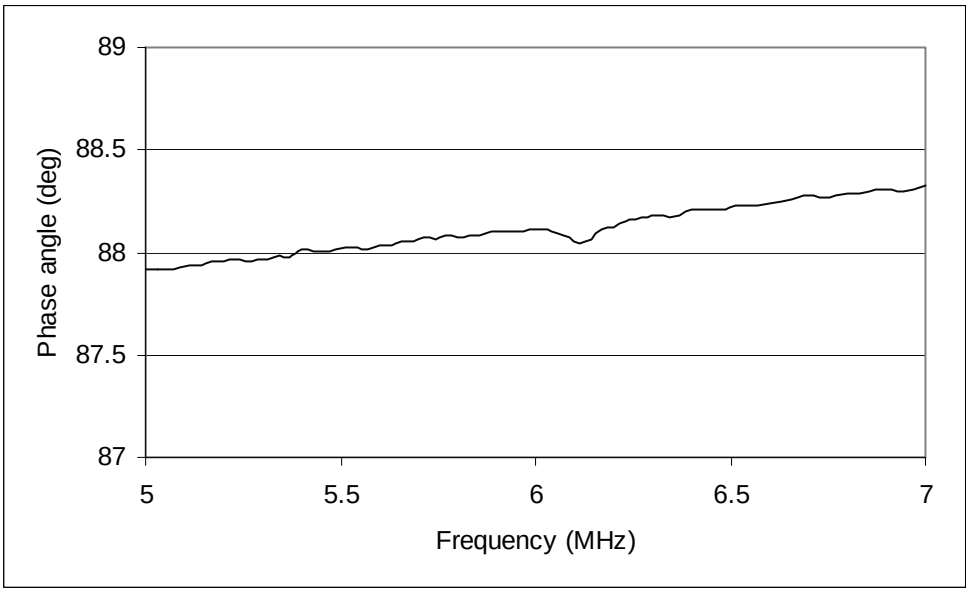

Figure D-12. Basic sensor phase angle response: Gap distance 2.75 in.

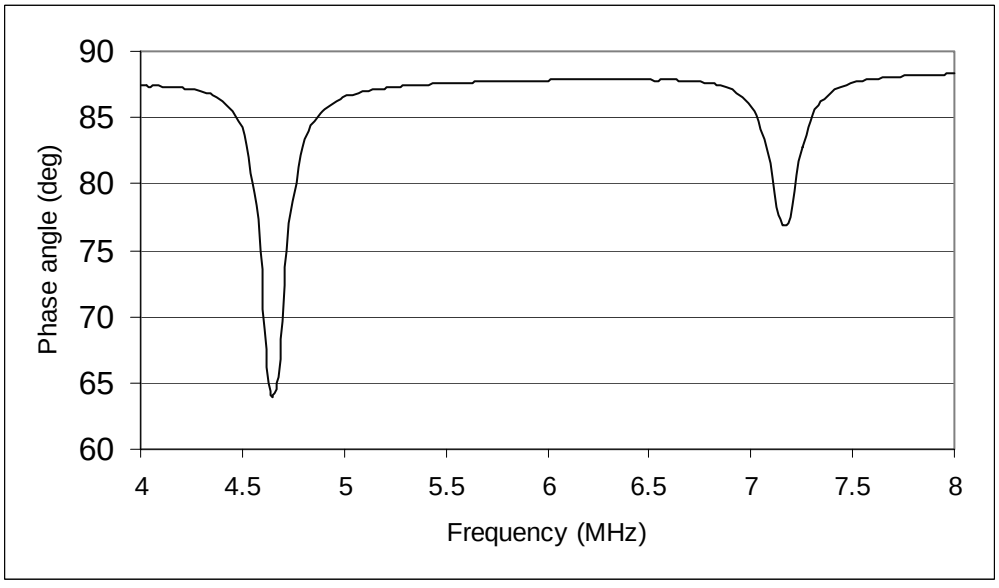

Figure D-13. Improved sensor phase angle response: Gap distance 0.0 in.

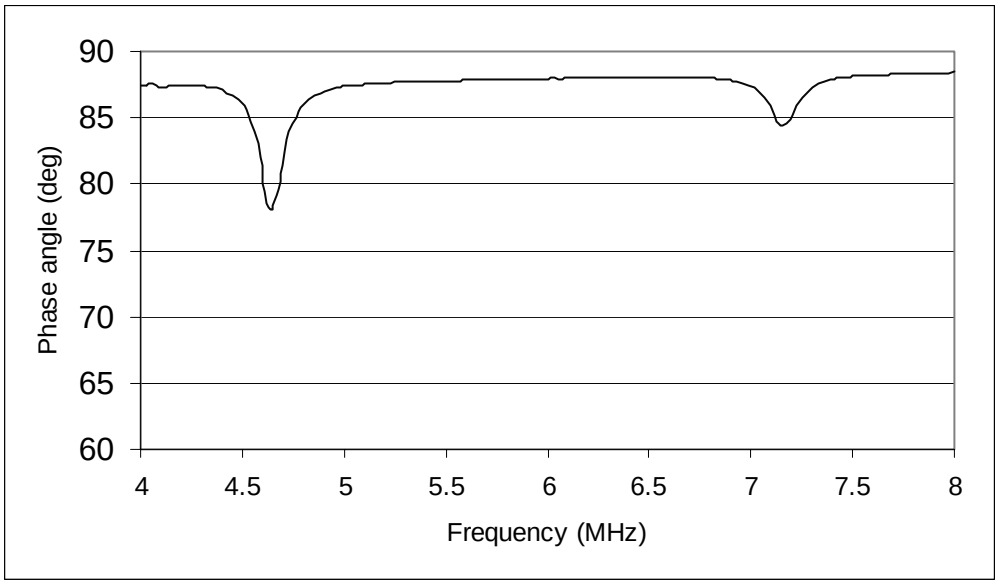

Figure D-14. Improved sensor phase angle response: Gap distance 0.25 in.

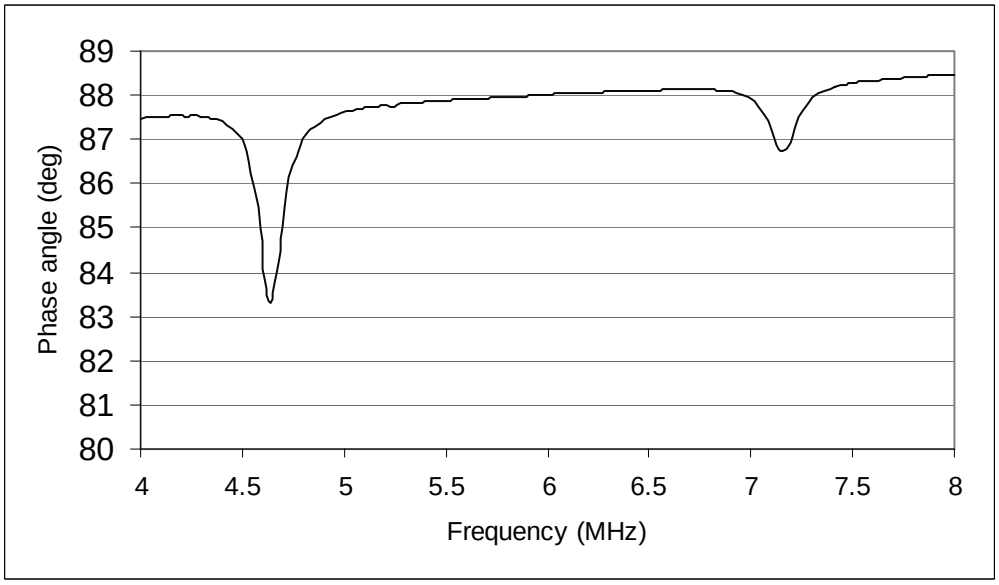

Figure D-15. Improved sensor phase angle response: Gap distance 0.50 in.

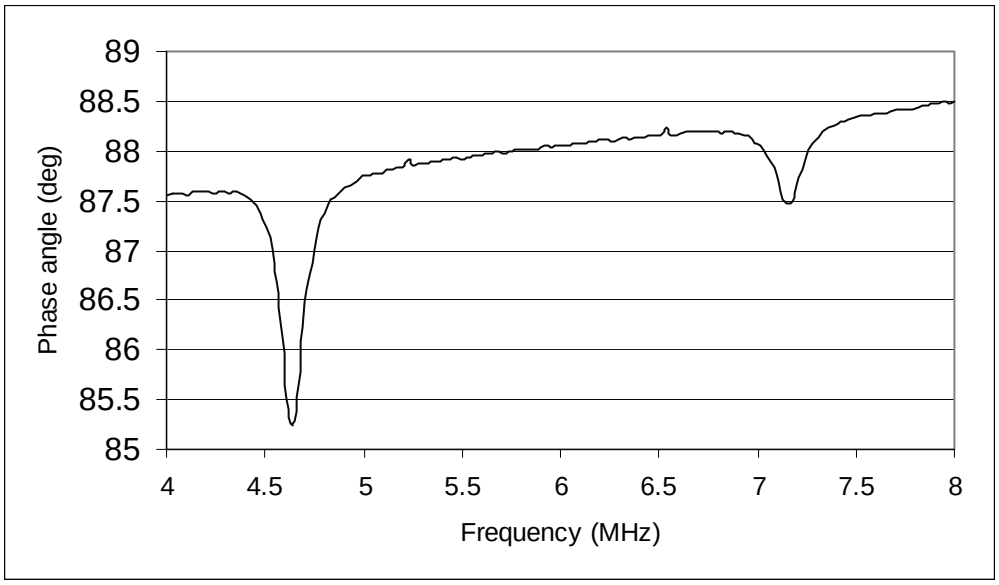

Figure D-16. Improved sensor phase angle response: Gap distance 0.75 in.

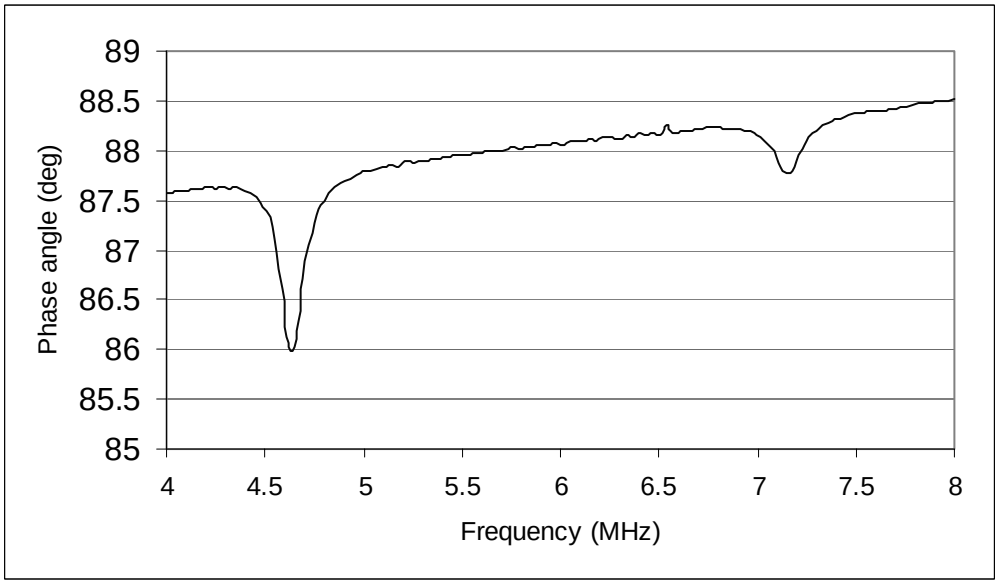

Figure D-17. Improved sensor phase angle response: Gap distance 1.0 in.

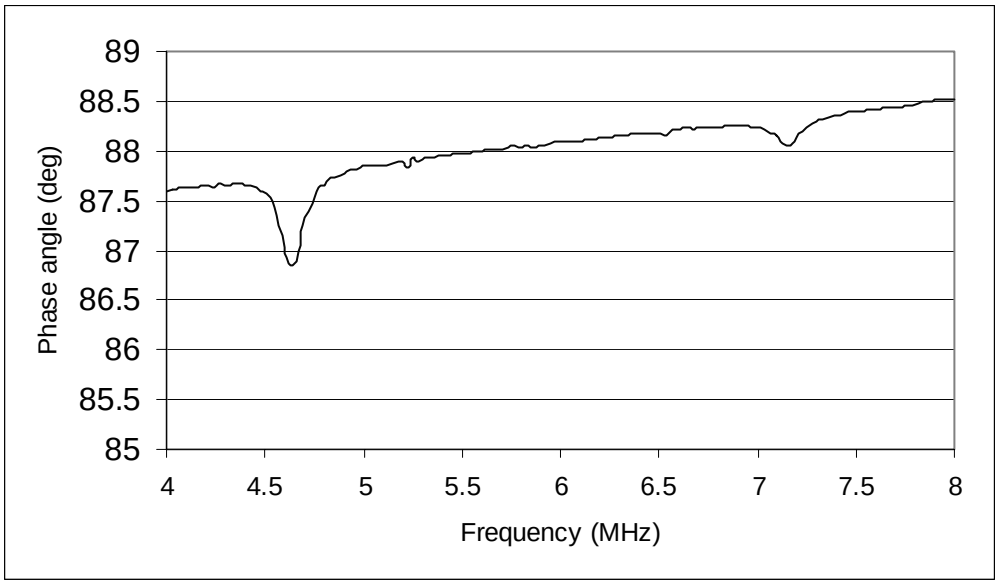

Figure D-18. Improved sensor phase angle response: Gap distance 1.25 in.

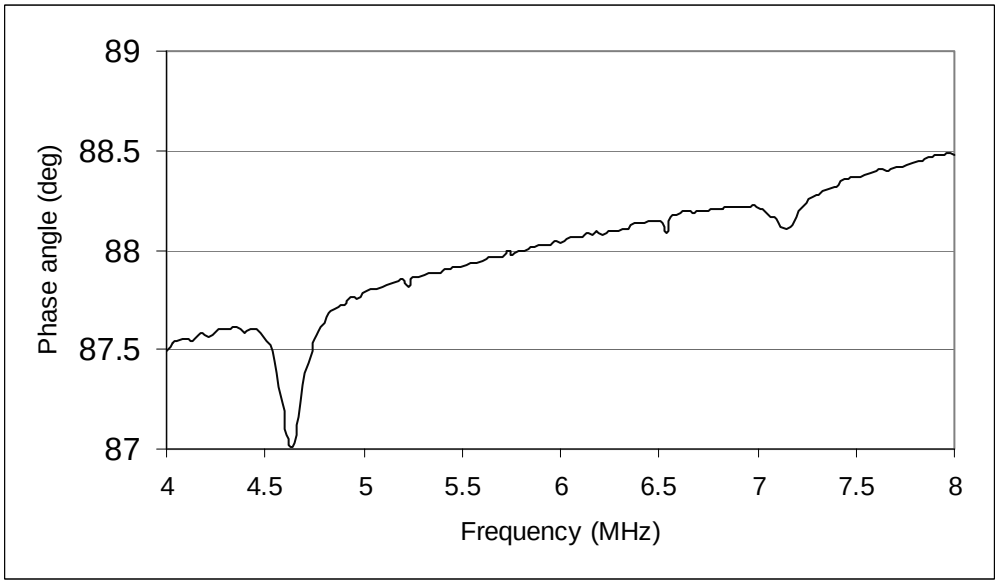

Figure D-19. Improved sensor phase angle response: Gap distance 1.50 in.

APPENDIX E
Influence of Moisture and Chlorides on Transmission Range

E.1 CONCRETE DISCS SUBMERSED ININTO FRESH WATER

One of each type of sensor was embedded with one inch cover in 4 in. concrete cylinders. The cylinders were placed into fresh water and allowed to soak up the moisture. Three interrogations were performed on the sensors: (1) after concrete was allowed to dry cure for one week, (2) after concrete was placed into fresh water for 3 days and (3) after concrete was placed into fresh water for 7 days. The phase angle response is given for each interrogation.

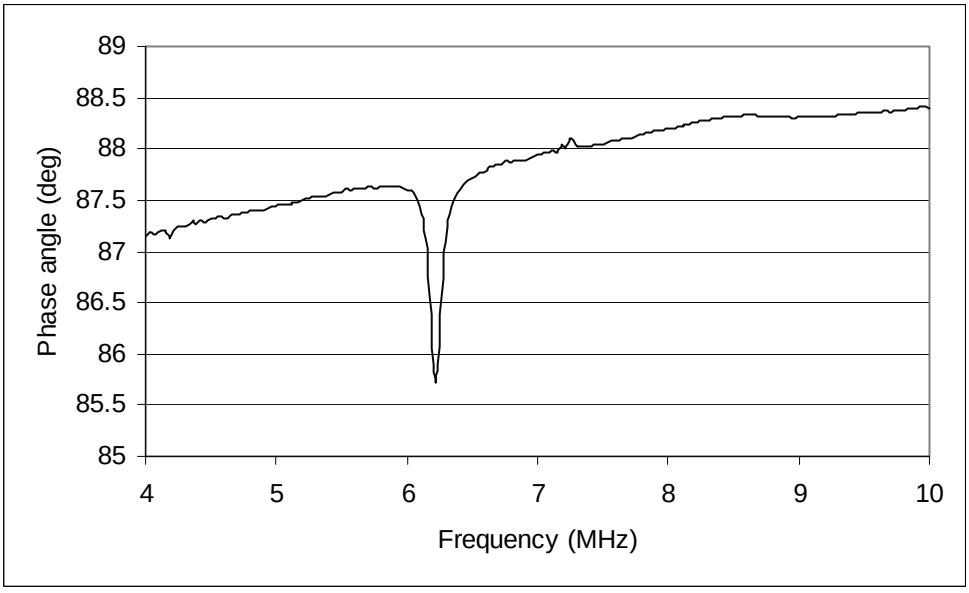

Figure E-1. Basic sensor: after one week curing period

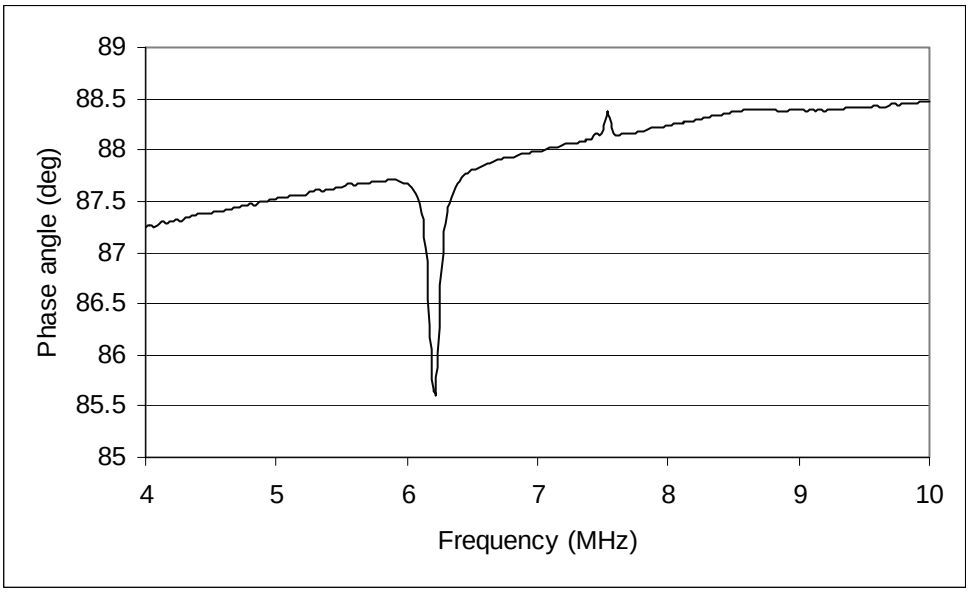

Figure E-2. Basic sensor: concrete exposed to fresh water for 3 days

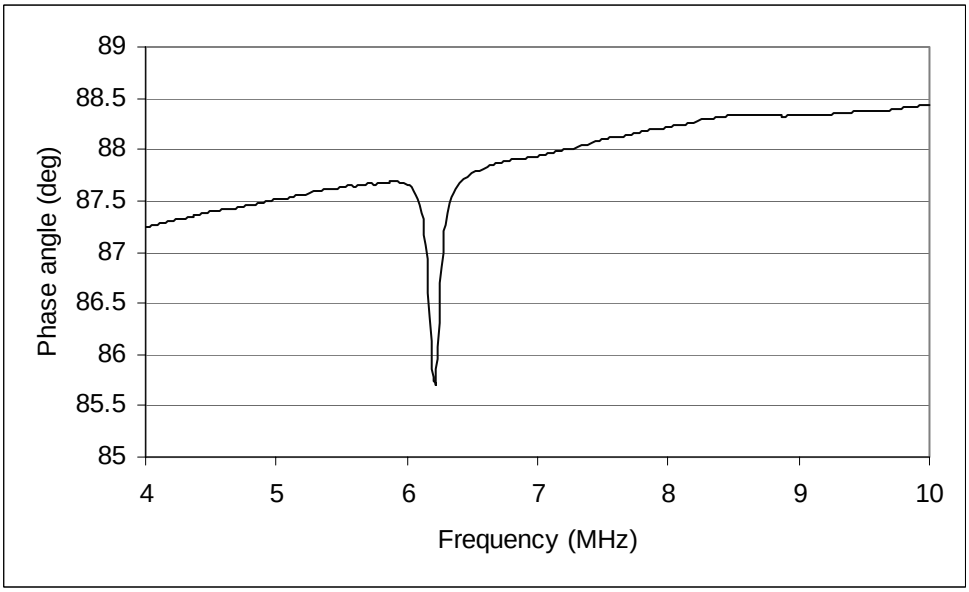

Figure E-3. Basic sensor: concrete exposed to fresh water for 7 days

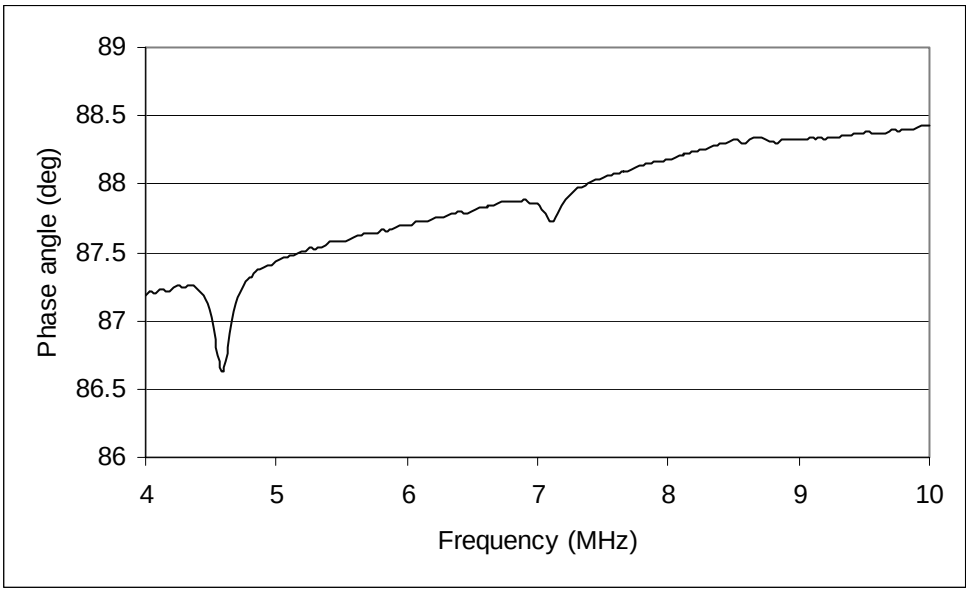

Figure E-4. Improved sensor: after one week curing period

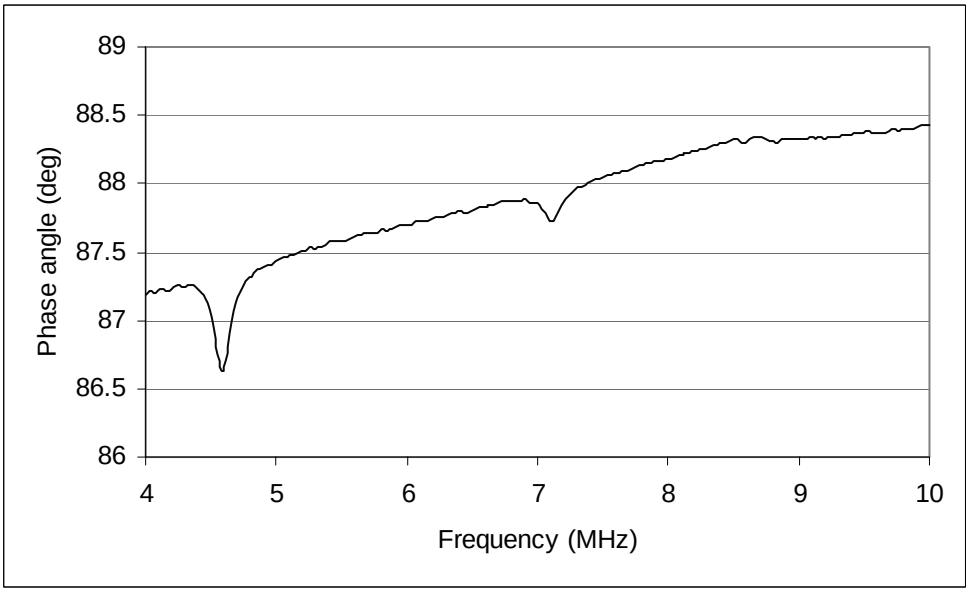

Figure E-5. Improved sensor: concrete exposed to fresh water for 3 days

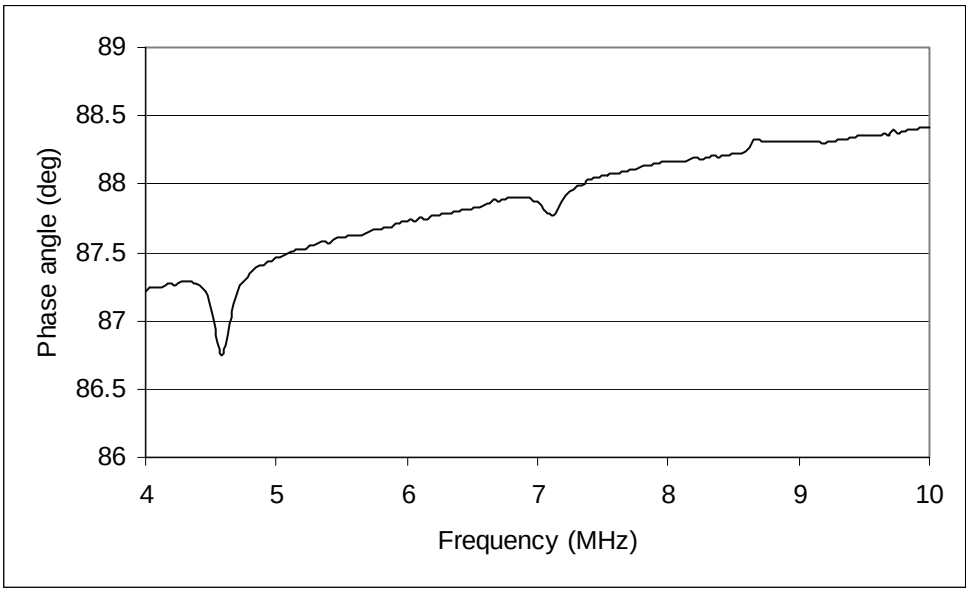

Figure E-6. Improved sensor: concrete exposed to fresh water for 7 days

E.2 CONCRETE DISCS SUBMERSED IN SALT WATER

One of each type of sensor was embedded with one inch cover in 4 in. concrete cylinders. The cylinders were placed into salt water and allowed to soak up the chloride ions. The salt water contained 3.5 % NaCl by weight. Three interrogations were performed on the sensors: (1) after concrete was allowed to dry cure for one week, (2) after concrete was placed into fresh water for 3 days and (3) after concrete was placed into fresh water for 7 days. The phase angle response is given for each interrogation.

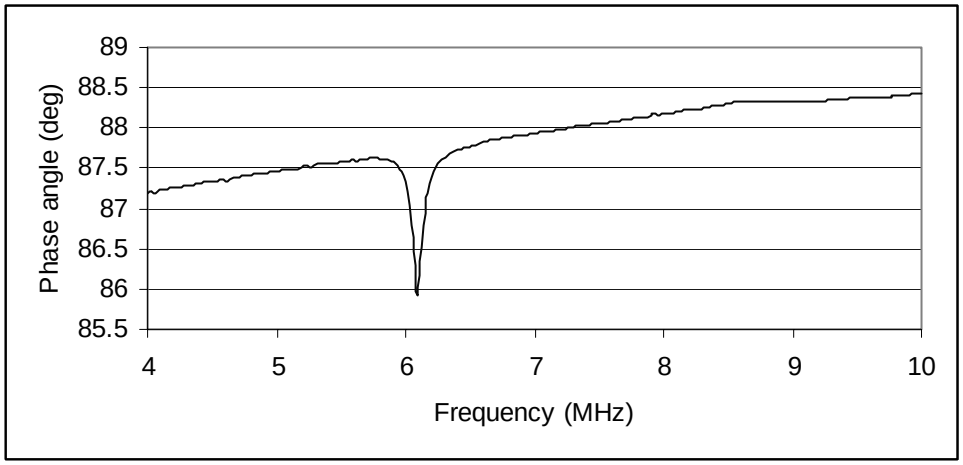

Figure E-7. Basic sensor: after one week of curing

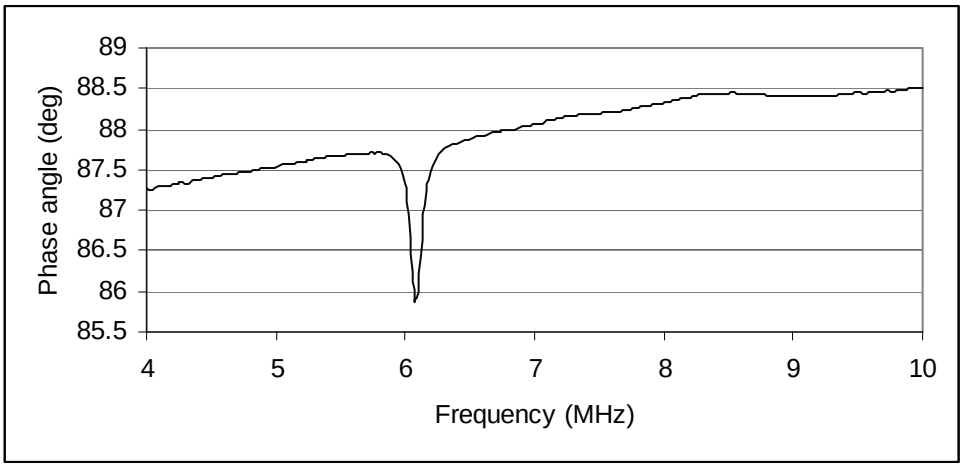

Figure E-8. Basic sensor: concrete exposed to salt water for 3 days

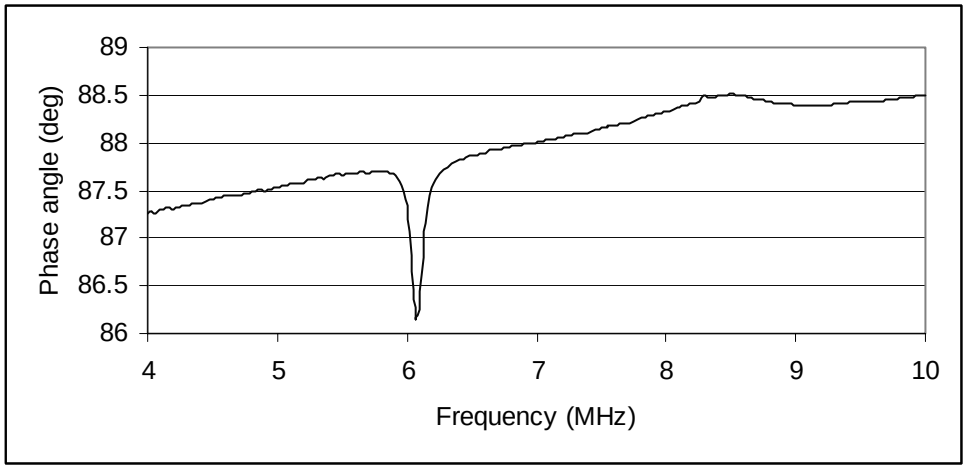

Figure E-9. Basic sensor: concrete exposed to salt water for 7 days

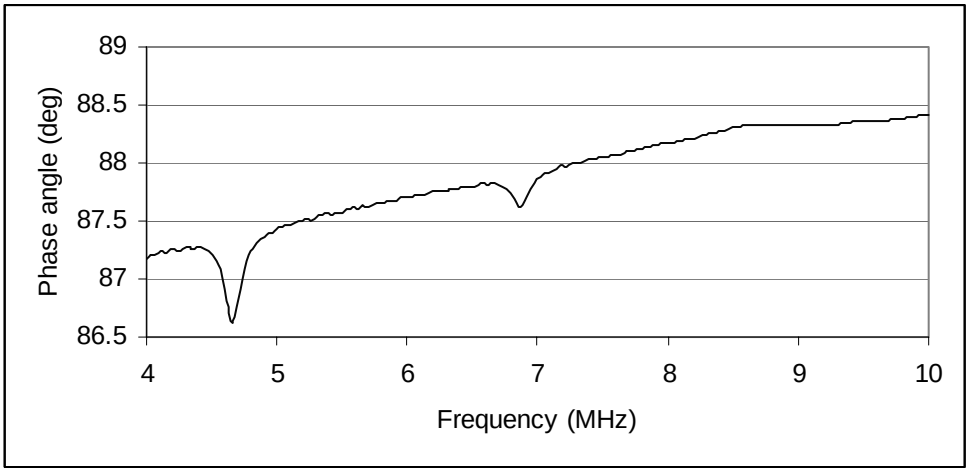

Figure E-10. Improved sensor: after one week of curing

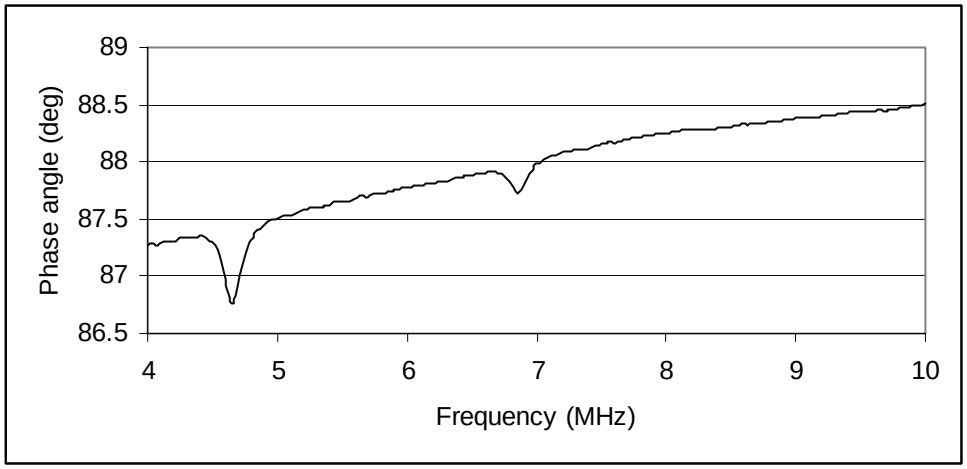

Figure E-11. Improved sensor: concrete exposed to salt water for 3 days

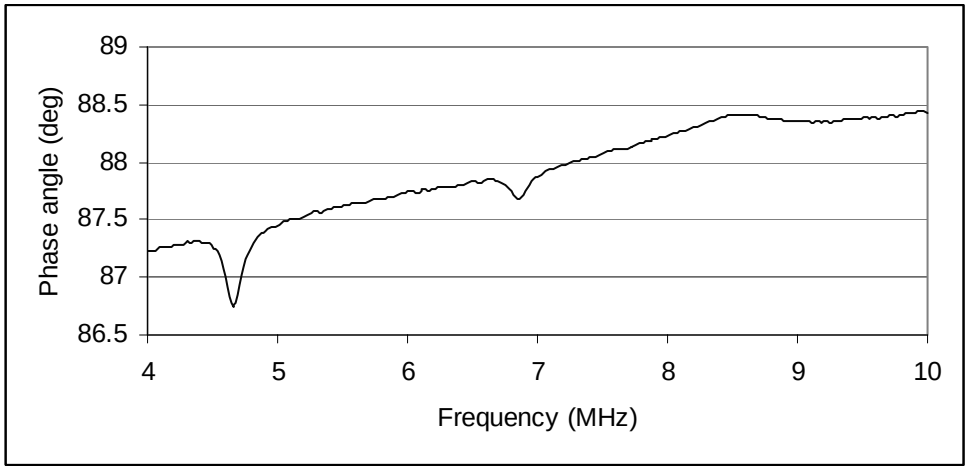

Figure E-12. Improved sensor: concrete exposed to salt water for 7 days

References

1. ACI 224 (1998). “Causes, Evaluation, and Repair of Cracks in Concrete Structures.” Committee 224, American Concrete Institute, Farmington Hills, MI.

2. ACI 318 (2002). “Building Code and Commentary for Structural Concrete (ACI 318-02) and Commentary (ACI 318R-02).” Committee 318, American Concrete Institute, Farmington Hills, MI.

3. ASTM C114-04 (2004). “Standard Test Methods for Chemical Analysis of Hydraulic Cement.” American Society for Testing and Materials, West Conshohocken, PA.

4. ASTM C1152/C1152M (2003). “Standard Test Method for Acid-Soluble Chloride in Mortar and Concrete.” American Society for Testing and Materials, West Conshohocken, PA.

5. ASTM C876 (1999). “Standard Test Method for Half-Cell Potentials of Uncoated Reinforcing Steel in Concrete.” American Society for Testing and Materials, West Conshohocken, PA.

6. ASTM G1 (1999). “Standard Practice for Preparing, Cleaning, and Evaluating Corrosion Test Specimens.” American Society for Testing and Materials, West Conshohocken, PA.

7. ASTM G1 (1999). “Standard Practice for Preparing, Cleaning, and Evaluating Corrosion Test Specimens.” American Society for Testing and Materials, West Conshohocken, PA.

8. C.J. Kitowski, “An investigation of the effect of chloride on reinforcing steel exposed to simulated concrete solutions,” M.S. Thesis, Department of Mechanical Engineering, University of Texas, Austin, TX, 1993.

9. G.H. Koch, M.P. Brongers, N.G. Thompson, J.H. Payer, and Y.P. Virmani, “Corrosion costs and preventative strategies in the United States,” *Supplement to Materials Performance*, U.S. Department of Transportation, Federal Highway Administration, July 1999.

10. Grizzle, Kristi M. (2003). “Development of a Wireless Sensor Used to Monitor Corrosion in Reinforced Concrete Structures.” M.S. Thesis, Dept. of Civil Engineering, University of Texas at Austin.

11. J. Mietz and B. Isecke, “Monitoring of concrete structures with respect to rebar corrosion,” *Construction and Building Materials*, Vol. 10, No. 5, July 1996, pp. 367-373.

12. Jones, Denny A. (1996). Principles and Prevention of Corrosion, 2nd Edition. Prentice Hall, Inc., Upper Saddle River, NJ.

13. L.J. Novak, K.M. Grizzle, S.L. Wood, and D.P. Neikirk, “Development of state sensors for civil engineering structures,” Proceedings of SPIE, Smart Structures and Materials 2003: Smart Systems and Nondestructive Evaluation for Civil Infrastructures, Vol. 5057, 2003, pp. 358-363.

14. M.M. Andringa, “Development of a passive wireless analog resistance sensor,” M.S. Thesis, Department of Electrical and Computer Engineering, University of Texas at Austin, TX, 2003.

15. Novak, Lisa J. (2002). “Development of a Wireless Sensor to Detect Cracks in Welded Steel Connections.” M.S. Thesis, Dept. of Civil Engineering, University of Texas at Austin.

VITA

Jarkko Tuomas Simonen was born on November 21, 1987 in Varkaus, Finland, to Jorma and Liisa Simonen. At the age of ten he and his parents moved to Marietta, GA. There the Author attended public school and got his high school diploma from Walton High School. In the fall of 1997 he enrolled at Auburn University and received a Bachelors of Science in Civil Engineering in 2002. At Auburn he received awards from the office of multicultural affairs for outstanding academic achievements and became a member of the Chi Epsilon honor fraternity. In the fall of 2002 he accepted a position as a research assistant at the University of Texas at Austin and pursued a Master of Science in Engineering specializing in structural engineering. He received his degree in May 2004.

Publications

Jarkko T. Simonen, Matthew M. Andringa, Grizzle M. Kristi, Sharon L. Wood, and Dean P. Neikirk. "Wireless sensors for monitoring corrosion in reinforced concrete structures." Proceedings of SPIE, Smart Structures and Materials 2004: Smart Systems and Nondestructive Evaluation for Civil Infrastructures.

Permanent Address:

2863 Baccurate ct.

Marietta GA, 30062

This thesis was typed by the author.